Tumor-Specific Crosslinking of Glucocorticoid-Induced Tumor Necrosis Factor-Related Receptor as Costimulation for Immunotherapy

Dissertation

zur

Erlangung der naturwissenschaftlichen Doktorwürde
(Dr. sc. nat.)

vorgelegt der

Mathematisch-naturwissenschaftlichen Fakultät

der

Universität Zürich

von

Tanja Susanna Burckhart

aus

Deutschland

Promotionskomitee

Prof. Dr. Christoph Renner (Vorsitz, Leitung der Dissertation)
Prof. Dr. Josef Jiricny
Prof. Dr. Alfred Zippelius
PD Dr. Maries van den Broek

Zürich 2010

Die vorliegende Arbeit wurde von der Mathematisch-naturwissenschaftlichen Fakultät der Universität Zürich auf Antrag von Prof. Dr. Christoph Renner und Prof. Dr. Josef Jiricny als Dissertation angenommen.

Zusammenfassung

Das körpereigene Immunsystem ist nur teilweise in der Lage, Krebszellen zu erkennen und zu vernichten. Krebspatienten besitzen zwar Tumor-spezifische T-Zellen, jedoch wird deren Aktivität durch mehrere Mechanismen gestört. Zum Beispiel werden zytotoxische T-Zellen durch regulatorische T-Zellen (Treg Zellen) inhibiert. Deshalb ist die Aktivierung und Unterstützung von Tumor-spezifischen zytotoxischen T-Zellen eine wichtige Aufgabe in der Immuntherapie. Eine vielversprechende Zielstruktur dafür ist der „Glucocorticoid-Induced Tumor Necrosis Factor-related Receptor“ (GITR), da dieser sowohl auf $CD4^+$ und $CD8^+$ Effektor T-Zellen als auch auf $CD4^+25^+$ Treg Zellen vorkommt. Die Aktivierung des murinen GITR durch den natürlichen Liganden (mGITRL) oder einen agonistischen Antikörper erhöht die Aktivität von Effektor T-Zellen, hemmt die Suppression durch regulatorische T-Zellen und verzögert das Tumorwachstum in diversen Mausmodellen. Die systemische Verabreichung kostimulierender Therapeutika führt jedoch häufig zu globaler Aktivierung von zytotoxischen T-Zellen und kann somit Autoimmunantworten hervorrufen. Zur spezifischen Manipulation von T-Zellen in der unmittelbaren Tumorumgebung haben wir ein neuartiges bispezifisches Fusionsprotein entwickelt, das aus dem murinen GITR Liganden und einem einkettigen Antikörper mit Spezifität für das „Fibroblast Activation Protein“ (FAP) besteht. Eine Tumor-spezifische Anreicherung des Fusionsproteins soll durch Bindung an FAP erreicht werden, da dieses spezifisch auf aktivierten Fibroblasten im Stroma von epithelialen Tumoren und auf Sarkomzellen exprimiert wird.

Das im Rahmen dieser Doktorarbeit produzierte antiFAP-mGITRL Fusionsprotein bildete Dimere und wies eine Affinität von 1.2 µM zu murinem GITR und von 4.5 nM zu murinem FAP auf. Durch die Kultivierung von $CD8^+$ und $CD4^+$ T-Zellen mit dem Fusionsprotein konnte die T-Zell Proliferation sowie die Produktion von IFN-γ und IL-2 gesteigert werden. Eine Verstärkung dieses kostimulatorischen Effekts wurde durch die Präsentation von antiFAP-mGITRL durch FAP^+ Zellen erreicht. Dabei führt membranständiges antiFAP-mGITRL vermutlich zur Vernetzung von mehreren GITR-Molekülen auf der T-Zell Oberfläche, verstärkt dort die Signaltransduktion und resultiert in gesteigerter Kostimulation. *In vitro* Studien zeigten, dass Treg Zellen die Proliferation und Funktion von $CD8^+$ T-Zellen hemmen. Durch die Zugabe unseres antiFAP-mGITRL Fusionsproteins zu einer Kokultur von $CD8^+$ und Treg Zellen konnte die Proliferation sowie die IFN-γ-Produktion von $CD8^+$ T-Zellen wiederhergestellt werden.

Des Weiteren war membranständiges antiFAP-mGITRL 100 Mal effektiver als ungebundenes Fusionsprotein. Zur Übertragung der *in vitro* Ergebnisse in ein syngenes präklinisches Modell wurden tumortragende Mäuse mit antiFAP-mGITRL behandelt. Das Wachstum eines subkutanen Kolonkarzinoms konnte durch immuntherapeutische Behandlung mit antiFAP-mGITRL nicht verlangsamt werden, da die Stromabildung zu gering war. Die antiFAP-mGITRL Therapie eines FAP^+ Osteosarkoms führte hingegen zu gesteigertem Überleben.

Der kostimulatorische Effekt von antiFAP-mGITRL auf T-Zellen sowie die FAP-spezifische Präsentation des Fusionsproteins bilden die Grundlagen einer spezifischen Tumortherapie. Die erwartete Anreicherung von mGITRL im Tumorgewebe soll die zytotoxischen T-Zellen lokal unterstützen und das Risiko einer Autoimmunantwort minimieren. Somit stellt die Behandlung mit antiFAP-mGITRL einen vielversprechenden Ansatz in der Antikörper-basierten Immuntherapie von Tumoren dar.

Abstract

Cancer patients possess tumor-reactive T cells but their function is hampered by many mechanisms. One of these mechanisms involves naturally occurring regulatory T cells (Treg cells) that inhibit effector T cells. Activation or support of the tumor-reactive T cells is therefore a major objective in cancer immunotherapy. Stimulation of glucocorticoid-induced tumor necrosis factor-related receptor (GITR) represents a promising approach since this receptor is expressed on both $CD4^+$ and $CD8^+$ effector T cells as well as on $CD4^+25^+$ Treg cells. Triggering of murine GITR with its natural ligand (GITRL) or anti-GITR agonistic antibodies enhances T cell responses, inhibits Treg-mediated suppression and thereby induces tumor immunity in a variety of murine tumor models. However, systemic administration of costimulatory agents can lead to global T cell activation and autoimmunity. Therefore, we propose to specifically manipulate the T cell compartment in the tumor microenvironment by using a bispecific fusion protein combining mGITRL and a single chain antibody which targets fibroblast activation protein (FAP). Accumulation of antiFAP-mGITRL in the tumor microenvironment can be mediated through binding to FAP, which is specifically expressed on sarcomas and on cancer-associated fibroblasts (CAFs) found in the stroma of epithelial cancers.

The antiFAP-mGITRL fusion protein generated in this study formed dimers and bound to murine GITR with an affinity of 1.2 µM and to murine FAP with an affinity of 4.5 nM. *In vitro* cell assays with murine splenocytes showed that our antiFAP-mGITRL fusion protein can stimulate $CD8^+$ and $CD4^+$ effector T cells as shown by their increased proliferation and production of IFN-γ and IL-2. This costimulatory effect was enhanced when the fusion protein was presented by a FAP-positive cell line mimicking FAP^+ CAFs or FAP^+ tumors. Presumably, the membrane-bound antiFAP-mGITRL allows crosslinking of multiple GITR molecules on the T cells, thus leading to increased signaling and enhanced costimulation. *In vitro*, Treg cells inhibit the expansion and function of $CD8^+$ T cells. Addition of our antiFAP-mGITRL to the Treg:$CD8^+$ T cell coculture could restore proliferation and IFN-γ production of $CD8^+$ T cells. Furthermore, cell membrane-bound antiFAP-mGITRL was 100-fold more effective in overcoming Treg-mediated suppression compared to unbound fusion protein. To translate the *in vitro* results in a preclinical model, we established syngeneic murine cancer models to either target the tumor stroma or the tumor cells directly. Immunotherapeutic antiFAP-mGITRL treatment of a colon carcinoma provoked no delay in tumor growth due to

weak stroma formation. However, therapy of a FAP^+ osteosarcoma led to enhanced survival of mice treated with antiFAP-mGITRL.

The antibody-directed delivery of GITRL opens a new path to positively act on the local T cell environment in the tumor. Targeted delivery and thereby enhanced immunomodulatory effects of antiFAP-mGITRL represent a promising approach in antibody-based tumor immunotherapy.

Table of Contents

Zusammenfassung ..... **I**

Abstract ..... **III**

Table of Contents ..... **V**

Abbreviations ..... **X**

List of Figures ..... **XV**

1 Introduction **1**

1.1 Immunotherapy of tumors 1

1.2 Targets for immunotherapy 2

1.3 Fibroblast activation protein 4

1.4 T lymphocytes in the antitumor response 5

1.5 Regulatory T cells 6

1.6 Costimulation of T cells for tumor therapy 7

1.7 Combination of antibodies and effector molecules for immunotherapy 8

1.8 Glucocorticoid-induced tumor necrosis factor-related receptor and its ligand 10

1.9 Aim of the thesis 12

2 Material and Methods **13**

2.1 Equipment 13

2.2 Reagents and kits 15

2.2.1 Kits 15

2.2.2 Antibodies 15

2.3 Buffer 16

2.4 Primer 18

2.5 Plasmids and bacteria 19

2.5.1 Plasmids 19

2.5.2 Media for bacteria 20

2.5.3 Bacterial strains 20

2.6 Cell culture and media 21

2.6.1 Cell culture media 21

2.6.2 Cell lines 22

2.7 Mice 23

2.8 Software 23

2.9 Bacterial methods 24

2.9.1 Growth of bacteria in suspension 24

2.9.2 Growth of bacteria on agar plates 24

2.9.3 Transformation of competent *E. coli* cells 24

2.9.4 Glycerol stocks of bacteria 24

2.10 Molecular biology techniques 25

2.10.1 Preparation of plasmid DNA from *E. coli* 25

2.10.2 Determination of DNA concentration 25

2.10.3 Agarose gel electrophoresis 25

2.10.4 Amplification of DNA by Polymerase Chain Reaction 26

2.10.5 Digestion of DNA with restriction endonucleases 26

2.10.6 Purification of PCR products and plasmid fragments 27

2.10.7 Ligation of DNA 27

2.10.8 Cloning by recombination of DNA 27

2.10.9 Colony PCR 27

2.10.10 Sequencing 28

2.10.11 Cloning strategies of fusion proteins 28

2.11 Biochemical techniques 30

2.11.1 Dot blot with cell culture supernatant 30

2.11.2 Purification of fusion proteins 31

2.11.3 Purification of mGITRL-Fc 31

2.11.4 SDS Polyacrylamide Gel Electrophoresis 32

2.11.5 Immunochemical detection of proteins by Western blot 32

2.11.6 Determination of protein concentration 32

2.11.7 Concentration and storage of fusion proteins 33

2.11.8 Size Exclusion Chromatography 33

2.11.9 Surface Plasmon Resonance binding assays 33

2.12 Cell culture techniques and immunobiological methods 34

2.12.1 Cultivation of cell lines 34

2.12.2 Large scale cultivation of NS0 cells 34

2.12.3 Cultivation of HEK 293 mGITRL-Fc cells 34

2.12.4 Determination of cell number and viability 35

2.12.5 Transient expression of fusion proteins 35

2.12.6 Stable expression of fusion proteins 35

2.12.7 Flow cytometry analysis 36

2.12.8 Tetramer staining of blood lymphocytes 36

2.12.9 Flow cytometric determination of apparent affinity of fusion proteins to FAP 36

2.12.10 Immunohistochemistry 37

2.12.11 Purification of T cell subsets 37

2.12.12 CFSE labelling of T cells 38

2.12.13 Activation of T cells for FACS analysis 38

2.12.14 Proliferation assays 38

2.12.15 Suppression assays 38

2.12.16 Measurement of cytokine production 39

2.13 Animal experiments 39

2.13.1 *In vivo* tumor growth 39

2.13.2 Treatment protocol of CT26 tumors 39

2.13.3 Treatment protocol of LM8 tumors 40

2.13.4 Preparation of single cell suspension from tumors 40

2.13.5 Preparation of tumors for frozen sections 40

2.14 Statistical analysis 40

3 Results 41

3.1 Production of fusion proteins 41

3.1.1 Cloning of the fusion proteins 41

3.1.2 Production and purification of fusion proteins 42

3.2 Characterization of the fusion proteins 44

3.2.1 Multimerization properties of the fusion proteins 44

3.2.2 Binding of the fusion proteins to the corresponding receptors overexpressed on cell lines 45

3.2.3 Binding of the fusion proteins to GITR on murine T lymphocytes 46

3.2.4 Comparison of binding affinities to murine FAP 49

3.2.5 GITR binding analysis by surface plasmon resonance 50

3.3 Targeting the tumor stroma 53

3.3.1 Purification of T cell subsets 53

3.3.2 Costimulation of $CD4^+$ T cells 54

3.3.3 Costimulation of $CD8^+$ T cells 55

3.3.4 Inhibition of Treg-mediated suppression 56

3.3.5 Therapy of CT26 tumors 59

3.4 Targeting of sarcomas 61

3.4.1 Costimulation of T cells 61

3.4.2 Inhibition of Treg-mediated suppression 63

3.4.3 Characterization of the sarcoma LM8 64

3.4.4 Therapy of LM8 tumors 67

4 Discussion 69

5 Appendix 77

5.1 Amino acid sequence of antiFAP-hGITRL 77

5.2 Amino acid sequence of antiCD33-mGITRL 77

5.3 Amino acid sequence of antiFAP-mGITRL 78

5.4 Amino acid sequence of antiFAP 78

6 References 79

7 Acknowledgements 89

8 Curriculum Vitae 91

Abbreviations

ADCC	antibody-dependent cellular cytotoxicity
APC	antigen presenting cell; flow cytometry: allophycocyanin
APS	ammonium peroxodisulfate
bp	base pair
BSA	bovine serum albumin
CAF	cancer-associated fibroblast
CDC	complement-dependent cytotoxicity
CFSE	5,6-carboxyfluorescein diacetate succinimidyl ester
CHO	Chinese Hamster Ovary
CTL	cytotoxic T lymphocyte
CTLA-4	Cytotoxic T-Lymphocyte Antigen 4
dH_2O	deionized water
DC	dendritic cell
DMEM	Dulbecco's Modified Eagle Medium
DNA	deoxyribonucleic acid
dNTP	deoxyribonucleotide triphosphate
EBNA	Epstein-Barr nuclear antigen
E. coli	*Escherichia coli*
EDTA	ethylenediaminetetraacetic acid
ELISA	Enzyme-linked Immunosorbent Assay
FACS	Fluorescent Activated Cell Sorting

FAP	Fibroblast Activation Protein
FBS	fetal bovine serum
Fc	fragment crystallizable
FITC	fluorescein
Foxp3	forkhead box P3
FSC	forward scatter
g	centrifugation: earth gravity; weight: gram
GITR	Glucocorticoid-Induced Tumor Necrosis Factor Related Protein
GITRL	GITR ligand
h	hour
HEK	Human Embryonic Kidney
HER2	human epidermal growth factor receptor 2
HLA	human leukocyte antigen
HPLC	High Performance Liquid Chromatography
HRP	horseradish peroxidase
H&E	hematoxylin and eosin
IFN	Interferon
IgG	immunoglobulin G
IL	interleukin
i.v.	intravenously
kb	kilo base pair
KD	Measure for the affinity of a ligand/analyte system
kDa	kilodalton

LB	Luria Bertani
M	molar
mAb	monoclonal antibody
MHC	major histocompatibility complex
MPBS	milk powder phosphate-buffered saline
min	minute
NF-κB	nuclear factor kappa-light-chain-enhancer of activated B cells
NK cell	natural killer cell
NKT cell	natural killer T cell
o/n	overnight
PA	parental
PAGE	polyacrylamide gel electrophoresis
PBS	phosphate-buffered saline
PCR	polymerase chain reaction
PD-1	Programmed Death 1
PE	R-phycoerythrin
rpm	rotations per minute
RPMI	Roswell Park Memorial Institute medium
RT	room temperature
RU	response unit
s	second
s.c.	subcutaneously
scFv	single chain variable fragment

SDS	sodium dodecyl sulfate
SDS-PAGE	sodium dodecyl sulfate polyacrylamide gel electrophoresis
SSC	side scatter
TAA	tumor-associated antigen
TAE	TRIS-acetate/EDTA
TCR	T cell receptor
TE	TRIS-EDTA
Teff cell	effector T cell
TEMED	tetramethylen diamine
TGF-β	transforming growth factor β
Th	T helper
TME	tumor microenvironment
TNF	Tumor Necrosis Factor
TRAF	TNF Receptor Associated Factor
Treg cell	naturally-occurring regulatory T cell
TRIS	tris-(hydroxymethyl)-aminomethane
U	unit
UV	ultraviolet
v/v	volume per volume
w/v	weight per volume

Common abbreviations for nucleotides:

nucleotide	1-letter
adenine	A
cytosine	C
guanine	G
thymine	T

Common abbreviations for amino acids:

amino acid	3-letter	1-letter	amino acid	3-letter	1-letter
alanine	Ala	A	leucine	Leu	L
arginine	Arg	R	lysine	Lys	K
asparagine	Asn	N	methionine	Met	M
aspartate	Asp	D	phenylalanine	Phe	F
cysteine	Cys	C	proline	Pro	P
glutamate	Glu	E	serine	Ser	S
glutamine	Gln	Q	threonine	Thr	T
glycine	Gly	G	tryptophan	Trp	W
histidine	His	H	tyrosine	Tyr	Y
isoleucine	Ile	I	valine	Val	V

List of Figures

Figure 1. Schematic presentation of the fusion protein constructs. 41
Figure 2. Visualization of the fusion proteins.. 42
Figure 3. Analysis of multimerization of the fusion proteins by HPLC. 44
Figure 4. Binding analysis of the fusion proteins to their corresponding receptors on stably transfected cell line. 45
Figure 5. Binding analysis of the fusion proteins to primary murine splenocytes 48
Figure 6. Determination of the apparent affinity of the fusion proteins to murine FAP 49
Figure 7. Surface plasmon resonance analysis of the binding to immobilized murine GITR 51
Figure 8. Surface plasmon resonance analysis of the binding to immobilized human GITR 52
Figure 9. Purified T cell subsets 53
Figure 10. antiFAP-mGITRL presented by FAP-positive cells enhances proliferation of $CD4^+$ T cells 55
Figure 11. antiFAP-mGITRL presented by FAP-positive cells costimulates $CD8^+$ T cells 56
Figure 12. antiFAP-mGITRL reduces suppression by Treg cells in a dose-dependent manner 57
Figure 13. antiFAP-mGITRL presented by FAP-positive cells reduces suppression by BALB/c Treg cells 58
Figure 14. mGITRL-Fc delays growth of CT26 tumors. 60
Figure 15. antiFAP-mGITRL presented by FAP-positive cells enhances production of IL-2 and IFN-γ by $CD4^+$ T cells 61
Figure 16. antiFAP-mGITRL presented by FAP-positive cells costimulates $CD8^+$ T cells 62
Figure 17. antiFAP-mGITRL presented by FAP-positive cells reduces suppression by C3H Treg cells 63
Figure 18. LM8 cells from cell culture and from tumor suspension are FAP-positive 64
Figure 19. Detection of FAP on frozen sections of LM8 tumors 66
Figure 20. antiFAP-mGITRL slightly delays tumor growth of LM8 osteosarcoma 67

1 Introduction

1.1 Immunotherapy of tumors

With cancer still being the second most common cause of death in the western world, after cardiovascular diseases, there is a great need for novel treatment options. Most conventional therapy protocols for solid cancers involve surgery combined with radiation or chemotherapy. Success of these treatment strategies is limited by accessibility of the tumor and side effects of the therapy. A major requirement for effective and well-tolerated cancer therapies is the selective delivery of therapeutics to the site of disease. The advances in molecular biology, especially recombinant antibody technology (Hoogenboom, 2005), along with a better understanding of the mechanisms of our immune system provide a strong basis for the development of cancer immunotherapy.

While early reports already postulated that our immune system recognizes modified cells and fights the formation and development of cancer (Burnet, 1970; Ehrlich, 1900; Thomas, 1959), this theory is now accepted as the concept of immune surveillance (Dunn et al., 2004). It can be described by the three Es of cancer immunoediting – elimination, equilibrium and escape: The immune system protects the host from neoplastic disease by recognizing and eliminating these modified cells. However, elimination of the tumor cells is not complete and after a transient equilibrium phase, some transformed cells escape the control of the immune system. Various escape strategies like loss of antigen expression, downregulation of MHC molecules, development of resistance to IFN-γ, generation of an immunosuppressive microenvironment through secretion of cytokines such as TGF-β and IL-10 or mechanisms involving suppressive T cells (regulatory T cells) have been reported to lead to the development of cancer (Smyth et al., 2001). Tumor cell variants with low immunogenicity are selected in the equilibrium phase and eventually grow. Indeed, Robert Schreiber and colleagues showed in 2001 that mice lacking T, B and NKT cells develop chemically-induced carcinoma faster and at a higher rate than wild type mice (Shankaran et al., 2001), thereby validating the concept of cancer immunosurveillance.

Greater understanding of the 3 phases of immunoediting, especially the escape phase, has led to the development of new paths in cancer treatment. The aim is to restore the

immune response against the tumor, e.g. through prophylactic and therapeutic vaccination, adoptive T cell therapy or antibody-based tumor therapy. A dozen of antibodies are already approved for the treatment of a wide variety of cancers and several dozens of antibodies are in phase I to III clinical trials. Furthermore, combination therapy such as monoclonal antibodies (mAb) with high-dose IL-2 or with chemotherapy is common. Most mAb approved by the regulatory authorities to date involve naked Immunoglobulin G (IgG) like Herceptin against metastatic breast cancer, Rituxan for the treatment of non-Hodgkin's lymphoma or Erbitux for metastatic colorectal cancer (Dean-Colomb and Esteva, 2008; Hauptrock and Hess, 2008; Rivera et al., 2008). Additionally, the radiolabeled IgGs Zevalin (Borghaei and Schilder, 2004; Marcus, 2005) and Bexxar (Vose, 2004; Wahl, 2005) are used for the treatment of non-Hodgkin B-cell lymphoma and the antibody drug conjugate Mylotarg (Bross et al., 2001; Linenberger, 2005) is approved for the treatment of acute myeloid leukemia.

1.2 Targets for immunotherapy

Tumor targeting strategies rely on the identification of good quality targets. For highly specific therapy results, restricted expression patterns of these targets are required. Optimal targets should be abundant at the tumor site for accumulation of the therapeutic agent, not be expressed on vital organs to avoid side-effects, not be secreted since the mAb would bind the excess antigen instead of reaching the tumor and, finally, they should be well accessible for circulating agents. The target structures are called tumor-associated antigens (TAAs) and may be unique to an individual tumor or common to a tumor type. Furthermore, some tumor antigens are normal cellular antigens that are highly overexpressed on tumors. TAAs can be classified by their localization either on tumor cells directly or on structures in the tumor microenvironment.

Targeting TAAs on the surface of malignant cells has been proven to be effective and specific in the treatment of certain cancers. The antigen is usually expressed at very high levels on the cancer cells. Nevertheless, a major drawback is the development of resistance to treatment, e.g. through outgrowth of antigen loss mutants (cf. section 1.1). An example for a TAA expressed on the tumor cell surface is human epidermal growth factor receptor 2 (HER2) which is targeted by Trastuzumab that acts through downmodulation of HER2-mediated signaling and increased tumor cell apoptosis (Dean-Colomb and Esteva, 2008; Nahta and Esteva, 2006). Many tumor markers, however, are intracellular proteins and thus not accessible to recognition by antibodies

or immune cells. Peptides derived from these intracellular TAAs are presented on the surface of the tumor cell in the context of the MHC I system. These peptide-MHC complexes are specifically recognized by T lymphocytes through their T cell receptor (TCR). In the presence of costimulatory signals, the activated T cells can then exert their antitumor activity.

An alternative to targets on tumor cells, are TAAs in the tumor microenvironment (TME). These targets have great advantages since TME components are genetically more stable than tumor cells and the TME shares many features among different tumor types. Thus, targeting of these common structures has the potential to cure a greater variety of patients. TME targets can be divided in targets on immune cells and tumor stroma targets.

Tumor-infiltrating immune cells can be manipulated through targeting of structures on antigen presenting cells (APC) that present tumor antigens via their MHC, effector T (Teff) cells with cytotoxic activity and regulatory T cells with suppressive activity. For example, the function of dendritic cells (DCs) can be modulated by vaccination with peptide and stimulating agent (adjuvant, antibody). Thereby, naïve antigen presenting DCs are activated and matured so that they can prime T cells in secondary lymphoid organs. Furthermore, the supply of costimulatory and coinhibitory signals to T cell coreceptors is crucial for the generation and maintenance of immune responses. A more detailed insight into the role of T cells in cancer and options for therapeutic interventions is given in sections 1.4 and 1.6.

The stromal compartment commonly makes 20% to 50% of the mass of epithelial cancers (Welt et al., 1994). It is constituted of blood and lymphoid vessels, the extracellular matrix, mesenchymal cells, fibroblasts and inflammatory cells and molecules. Angiogenesis markers are popular tumor therapy targets. For example, the antibody L19 targets the tumor vasculature by recognizing the extra-domain B of fibronectin which becomes inserted into fibronectin under tissue-remodeling conditions, such as cancer (Zardi et al., 1987). As another approach, structures on cancer-associated fibroblasts (CAF) found in the TME can be targeted for tumor therapy. CAFs are phenotypically and functionally distinct from the fibroblasts present in tissues and have been shown to promote tumor growth in several mouse experiments (Liao et al., 2009; Orimo et al., 2005). Therefore, targeting and inhibiting CAFs has great potential in tumor therapy. An interesting target structure on CAFs is fibroblast activation protein (FAP) which can be targeted by small molecules (Adams et al., 2004) or antibodies (Scott et al., 2003) as described in more detail in the next section.

1.3 Fibroblast activation protein

Fibroblast activation protein (FAP) was first described as the target of mAb F19 which had been generated by immunizing a mouse with cultivated lung fibroblasts (Rettig et al., 1986). FAP is a 95 kDa type II transmembrane protein with serine protease and collagenase activity (Scanlan et al., 1994). Its capacity to degrade type I collagen (Park et al., 1999) explains the implication of FAP in extracellular matrix remodeling.

On one hand, FAP is expressed on tumor cells directly such as sarcomas (Dolznig et al., 2005; Scanlan et al., 1994). On the other hand, FAP is expressed on cancer-associated fibroblasts found in the stroma of about 90% of all human epithelial cancers such as breast, lung or colorectal carcinomas (Garin-Chesa et al., 1990; Rettig et al., 1993; Scanlan et al., 1994) and in the stroma of some melanoma (Huber et al., 2003). This dual expression pattern of FAP allows targeting of a wide variety of cancers. High expression of FAP is restricted to tumors, but some levels of FAP have also been detected in conditions of active stroma remodeling such as wound healing (Garin-Chesa et al., 1990), rheumathoid arthritis (Bauer et al., 2006) or cirrhotic liver (Levy et al., 1999).

High expression of FAP in the tumor microenvironment correlates with poor prognosis (Cohen et al., 2008; Henry et al., 2007) and several animal experiments suggest that FAP promotes tumor growth and metastasis. FAP knockout mice show no overt pathology (Niedermeyer et al., 2000) and have reduced tumorigenesis (Santos et al., 2009). Overexpression of FAP enhances tumor growth (Cheng et al., 2005; Huang et al., 2004) whereas treatment with antibodies (Cheng et al., 2002) or small molecules (Adams et al., 2004) inhibiting the proteolytic activity of FAP attenuates tumor growth in a mouse model. Immunization of mice through administration of a DNA vaccine encoding FAP (Loeffler et al., 2006) or the use FAP-transfected DCs (Lee et al., 2005) did also suppress primary tumor growth as well as metastasis. Without affecting the activity of FAP, long-lasting inhibition of tumor growth and complete regressions could be achieved with an anti-FAP-maytansinoid conjugate in mice, thereby confirming the potential of FAP as a localization target (Ostermann et al., 2008). Successful tumor staining (Brocks et al., 2001; Cheng et al., 2002) with FAP-specific monoclonal antibodies has been reported in murine xenografts and human tumors. Although *in vivo* imaging of human FAP-positive tumors with the humanized ^{131}I-labeled mAb F19 was successful (Scott et al., 2003), no antitumor activity in metastatic colorectal cancer could be achieved (Hofheinz et al., 2003; Scott et al., 2003). To date, there are no anti-human FAP antibodies that also inhibit FAP activity.

1.4 T lymphocytes in the antitumor response

Cytotoxic T cells have been shown to be a major player in the antitumor response. Activation of such tumor-specific T cells is the result of a complex interplay between different components of our immune system (Dunn et al., 2004; Smyth et al., 2001).

One of the first steps in the induction of an immune response is the presentation of epitopes from TAAs in the context of MHC class I and class II complexes. For this, peptides that are shed by tumors or peptides deriving from dying tumor cells are captured by naïve APCs, processed and small fragments are presented via the MHC complex. If tumors deliver danger signals, such as heat shock proteins or IFN-α, the APCs are activated and, in turn, upregulate their costimulatory molecules. The resulting mature APCs migrate to the draining lymph nodes where they stimulate T cells. APCs prime $CD4^+$ T cells via their peptide-MHC II complex and $CD8^+$ T cells via their peptide-MHC I complex and deliver costimulatory signals to both T cell subsets via, e.g. , the B7-CD28 interaction. By these means, T cells are activated in an antigen-specific manner. The TAA-specific T cells differentiate into cytotoxic $CD8^+$ T lymphocytes (CTLs) and $CD4^+$ T helper 1 cells (Th1) that migrate from the lymph node to the tumor. Local APCs further stimulate the T cells directly at the tumor site. The role of Th1 cells is to support the viability and function of CTLs through secretion of IL-2. CTLs kill tumor cells via direct mechanisms through death receptor triggering (Fas-FasL interaction) or release of perforin and granzyme B and through indirect mechanisms via TNF-α. Furthermore, CTLs release pro-inflammatory cytokines such as IFN-γ which inhibits cell proliferation, inhibits angiogenesis, promotes apoptosis, stimulates the adaptive immune system and enhances antigen-processing and presentation, thereby participating in cancer elimination.

Although our immune system provides the tools for an antitumor response, tumors do develop. The principal reason is that the majority of tumor-associated antigens are self-antigens. Indeed, members of the cancer-germ line group (such as MAGE-A4 or NY-ESO-1) or melanoma differentiation antigens (such as MART-1 and tyrosinase) are presented by medullary thymic epithelial cells (Gotter et al., 2004). Therefore, the immune response against these antigens is impaired by either central tolerance where high and intermediate affinity self-reactive T cells are deleted by negative selection in the thymus or by peripheral tolerance through suppressive activity by regulatory T cells. Independently of the type of the tumor antigen, numerous other mechanisms alter the T cell activity in patients. Tolerance of tumors can be induced by secretion of anti-inflammatory cytokines such as TGF-β or IL-10 by the tumor, thereby directly impeding

CTL and Th1 function. Furthermore, tumors don't always deliver danger signals to the environment, thereby failing to activate APCs which in turn induces T cell tolerance instead of T cell activation. Finally, anti-inflammatory cytokines secreted by NKT cells or type 2 macrophages can inhibit both APCs and T cells.

1.5 Regulatory T cells

Immunologic self-tolerance is maintained by regulatory T cells exhibiting suppressive activity. Characterization of these cells has shown that many types of regulatory T cells coexist. Naturally-occurring regulatory T cells originate in the thymus whereas adaptive regulatory T cells such as IL-10/TGF-β secreting Tr1 regulatory T cells or TGF-β/IL-4/IL-10 secreting Th3 helper T cells are induced in the periphery by conversion of $CD4^+25^-$ T cells (Bach, 2003; Roncarolo and Levings, 2000; Weiner, 2001).

Naturally-occurring $CD4^+25^+$ regulatory T cells (Treg cells) constitute 5 to 10% of the peripheral $CD4^+$ T cell subset in the blood. Constitutive high expression of the IL-2 receptor α chain (CD25) has been widely used as a Treg cell marker despite being also present on activated effector T lymphocytes. Treg cells also constitutively express cytotoxic T lymphocyte-associated antigen 4 (CTLA-4, CD152) (Read et al., 2000; Takahashi et al., 2000) and glucocorticoid-induced tumor necrosis factor related receptor (GITR) (McHugh et al., 2002). In mice, intracellular expression of the transcription factor forkhead box P3 (Foxp3) is the most specific marker for this cell population (Fontenot et al., 2003; Hori et al., 2003). $Foxp3^{-/-}$ mice completely lack $CD4^+25^+$ T cells and exhibit lethal lymphoproliferative autoimmune disease but adoptive transfer of Treg cells rescues the mice from the lethal phenotype (Fontenot et al., 2003; Khattri et al., 2003). The regulatory phenotype is maintained by the transcriptional complexes involving Foxp3, NFAT (Nuclear factor of activated T cells), NF-κB and AML1/Runx1 that repress IL-2 and IFN-γ production and upregulate expression of CD25 and CTLA-4 on Treg cells (Bettelli et al., 2005; Sakaguchi et al., 2008; Wu et al., 2006).

Treg cells do not proliferate upon TCR stimulation, however, IL-2 or costimulatory signals can break their anergic state. Treg cells require antigen-specific or polyclonal TCR stimulation to exert their suppressive function. Once activated, they suppress in an antigen-non-specific manner, meaning that they do not only suppress the proliferation and expansion of T cells with the same antigen specificity but also of T cells recognizing other targets. Besides acting on T cells, Treg cells also inhibit the

function of other immune cells. The mechanisms for Treg-mediated immune suppression are not fully elucidated yet and have been reviewed extensively. Effector mechanisms can be divided by those targeting T cells and those inhibiting APCs. Treg cells secrete inhibitory cytokines such as IL-10, TGF-β and IL-35 and thereby inhibit effector T cell function. Another proposed mechanism is IL-2 deprivation of Teff cells, leading to Bim-mediated apoptosis of Teff cells. Furthermore, Teff cells may directly be killed by Treg cells in a granzyme- or perforin-dependent manner. Cell-surface molecules such as Galectin-1 or other yet unknown molecules can induce cell cycle arrest in Teff cells. By inhibiting APCs, Treg cells indirectly prevent the activation of Teff cells. CTLA-4-mediated downregulation of CD80 and CD86 on APCs decreases their costimulatory effect and interaction of LAG-3 with MHC II molecules suppresses DC maturation. Moreover, Treg cells can form stable complexes with APCs, thereby outcompeting the binding to naïve T cells and preventing their priming (Bettini and Vignali, 2009; Rudensky and Campbell, 2006; Sakaguchi et al., 2009; Shevach, 2009). Through these mechanisms, Treg cells are able to sustain peripheral tolerance but they also hamper the immune responses against cancer.

1.6 Costimulation of T cells for tumor therapy

Strong infiltration of $CD4^+25^+Foxp3^+$ T cells in the tumor correlates with poor prognosis in hepatocellular carcinoma (Gao et al., 2007) and ovarian cancer patients (Curiel et al., 2004). In contrast, high $CD8^+$/Treg ratios were reported to be associated with improved survival (Gao et al., 2007; Sato et al., 2005). A promising strategy in tumor therapy is therefore to act on the local balance of effector T cells and Treg cells exclusively in the tumor microenvironment by either supporting the tumor-reactive T cells or inhibiting the suppressive T cell population.

Shimizu et al. have first demonstrated in 1999 that elimination of $CD4^+CD25^+$ T cells elicits potent tumor-specific immune responses to syngeneic tumors *in vivo* and eradicates them. Ever since then, therapeutic strategies are being developed to inhibit Treg cell function, deplete the Treg cell population or prevent their migration to the tumor site. Treg cell recruitment to the tumor has been inhibited by blockade of the Treg-attracting chemokine CCL5 (C-C chemokine ligand 5), thereby leading to delayed tumor growth in a murine pancreatic tumor model (Tan et al., 2009). Alternatively, $CD25^+$ T cells can be depleted in mice by administration of anti-CD25 mAb (clone PC61) but treatment prior to tumor inoculation or up to day 1 afterwards is required to achieve tumor rejection (Onizuka et al., 1999; Shimizu et al., 1999). Since selective

depletion of Treg cells has been proven to be difficult due to unavailability of specific markers, functional inhibition of Treg cells has been investigated. For example, activation of Toll-like receptor 8 (TLR8) in humans (Peng et al., 2005) or stimulation of OX40 on Treg cells in mouse models (Colombo and Piconese, 2007) block Treg-mediated suppression. Besides inhibiting Treg cells, such treatments often also act directly on effector T cells. Indeed, Teff cells are rendered resistant to suppression by Treg cells through the action of costimulatory molecules. Therefore, modulation of effector T cells has been exploited in many therapy models. Therapeutic interventions in cancer models include the supply of mAb or ligands which costimulate T cells (anti-CD28, anti-CD137, anti-OX40, anti-GITR, anti-CD40) or the removal/blockade of coinhibitory signals (anti-CTLA-4, anti-B7-H1, anti-PD-1) as reviewed (Melero et al., 2007; Peggs et al., 2009). Costimulation of CD28 on Teff cells with a CD80-Fc fusion protein delayed tumor growth in a syngeneic mouse model (Liu et al., 2005). Furthermore, blocking CTLA-4 signaling enhanced T cell responses and led to tumor rejection in several mouse models (Leach et al., 1996; Sutmuller et al., 2001; van Elsas et al., 1999). In clinical trials, CTLA-4 blocking antibodies Ipilimumab and Tremelimumab induced durable clinical responses in patients with metastatic melanoma (O'Day et al., 2007; Phan et al., 2003; Ribas et al., 2007). Combination of Ipilimumab with IL-2 led to 22% of partial and complete response in a phase II clinical trial (Maker et al., 2005).

Although tremendous improvements have been made in the field of immunotherapy in the last decade, systemic immune intervention can have severe side effects. A significant innovation has been the introduction of bispecific fusion proteins that specifically deliver the active molecule to the tumor site.

1.7 Combination of antibodies and effector molecules for immunotherapy

Full-length IgGs mediate their antitumor effect by blocking the receptor-ligand interaction (Cetuximab, Bevacizumab), altering cell signaling (Trastuzumab), activating antibody-dependent cellular cytotoxicity (ADCC) or mediating complement-dependent cytotoxicity (CDC) through the Fc domain (Rituximab). However, only few antibodies are approved and the antitumoral effects are not sufficient so that combination with other treatment options, such as chemotherapy, is required. By combining an antibody fragment with a bioactive molecule, it is possible to chose virtually any effector function and deliver therapeutic moieties specifically to the site of disease. Most importantly,

targeted delivery of the often toxic agents to the tumor permits to spare healthy tissue resulting in minimal side effects.

Immunoconjugates combining radionuclides with antibody fragments are powerful tools for both diagnostic (Dancey et al., 2009; Milenic et al., 2004) and therapeutic (Borghaei and Schilder, 2004; Wahl, 2005) applications. Ibritumomab tiuxetan (Borghaei and Schilder, 2004; Marcus, 2005) and Tositumomab (Vose, 2004; Wahl, 2005) are two CD20-specific murine mAbs conjugated with beta-emitting radionuclides (^{90}Y and ^{131}I, respectively) approved for the treatment of non-Hodgkin B-cell lymphoma. However, radioimmunoconjugates bear certain complexities linked to the type and energy of emission, radiolabeling process of the mAb and half-life of the construct.

The only approved antibody-drug conjugate is Mylotarg (Bross et al., 2001; Linenberger, 2005; Sievers and Linenberger, 2001) which combines a humanized CD33-specific mAb with the drug calicheamicin. This complex induces cytotoxic effects, probably due to DNA double strand breaks after internalization of the complex, leading to overall response rates of ~30% in acute myeloid leukemia (Sievers and Linenberger, 2001).

Besides full-length IgGs, other antibody formats have been fused with therapeutic agents. scFv antibody fragments are the format of choice for the delivery of the active molecule to the site of disease. Since scFv immunoconjugates are encoded in a single molecule, production of the fusion protein is easier than an IgG immunoconjugate. Furthermore, the small size of scFv immunoconjugates leads to better tumor uptake than higher molecular weight molecules. An example of such an immunoconjugate is the anti-CD22 scFv fused to truncated Pseudomonas exotoxin A (Kreitman et al., 2009). Although 61% complete remission in hairy cell leukemia patients could be achieved with this antibody-toxin conjugate, severe side effects such as vascular leak syndrome were detected.

Since some drugs are very harmful *in vivo* and selective targeting might not be sufficient to avoid systemic toxicity, the method of antibody-directed enzyme prodrug therapy (ADEPT) was developed. First, an enzyme conjugated to an antibody fragment is administrated and accumulates in the tumor. In a second step, a non-toxic prodrug is given and then specifically activated by the enzyme at the tumor site. Although some clinical response could be obtained with this system, the conjugated enzymes are highly immunogenic if of bacterial or murine origin and make repeated treatment impossible (Bagshawe et al., 2004; Cortez-Retamozo et al., 2004; Napier et al., 2000;

Siemers et al., 1997). To approach this problem, human enzymes have to be tested in a clinical setting.

Use of proinflammatory signals is a promising approach to induce tumor immunity (Fishman and Seigne, 2002). However, untargeted cytokines are highly toxic and can only be applied by isolated limb perfusion (Eggermont et al., 1996). Combination of these cytokines with a targeting component can avoid systemic effects. Proinflammatory cytokines IL-2, IL-12 and TNF-α fused to the L19 scFv recognizing the extradomain B of fibronectin have shown therapeutic effects in preclinical tumor models (Borsi et al., 2003; Carnemolla et al., 2002; Halin et al., 2003) and are currently in clinical development (Rybak et al., 2007). Further fusion proteins investigated in preclinical models include antiCD30-IL-2 (Hirsch et al., 2009), antiErbB2-B7.2 (Gerstmayer et al., 1997) and antiFAP-4-1BBL (Muller et al., 2008).

1.8 Glucocorticoid-induced tumor necrosis factor-related receptor and its ligand

In recent years, great attention has been dedicated to the murine glucocorticoid-induced tumor necrosis factor-related receptor (mGITR). GITR is a 228 amino acids type I transmembrane protein first cloned in 1997 from a murine T cell hybridoma stimulated with the glucocorticoid dexamethasone (Nocentini et al., 1997). Murine GITR is expressed at low levels on naive T cells and is upregulated through TCR stimulation on both $CD4^+$ and $CD8^+$ responder cells (Kanamaru et al., 2004; McHugh et al., 2002; Nocentini et al., 1997; Ronchetti et al., 2004). In contrast, GITR is constitutively expressed at high levels on $CD4^+25^+$ regulatory T cells and further upregulated upon stimulation (Kanamaru et al., 2004; McHugh et al., 2002; Nocentini et al., 1997). The ligand for GITR (GITRL) is a 173 aa type II transmembrane protein and is expressed on macrophages, immature and mature DCs and B cells (Tone et al., 2003).

GITR has been classified as member number 18 of the tumor necrosis factor receptor superfamily and is part of the costimulatory setting of a T cell. GITR triggering leads to NF-κB and MAPK (mitogen-activated protein kinase) activation thus provoking survival and proliferation of T cells (Esparza and Arch, 2005; Ji et al., 2004; Kim et al., 2003; Ronchetti et al., 2004). Indeed, activation of murine splenocytes with soluble (Tone et al., 2003) or membrane-bound GITRL (Cho et al., 2009; Kanamaru et al., 2004; Stephens et al., 2004) or with agonistic anti-GITR antibodies (Nishioka et al., 2008;

Ronchetti et al., 2004; Shimizu et al., 2002), leads to proliferation and to cytokine release by $CD4^+$ and $CD8^+$ effector T cells. Furthermore, *in vitro* addition of GITRL reduces Treg-mediated suppression (Hu et al., 2008; McHugh et al., 2002; Shimizu et al., 2002; Stephens et al., 2004; Valzasina et al., 2005). It has long been a matter of debate if ligation of GITR on regulatory T cells or on effector T cells is responsible for abrogation of Treg-mediated suppression. Preincubation of Treg cells with anti-GITR antibody, before adding the effector T cells, abrogates the suppressive effect (McHugh et al., 2002; Valzasina et al., 2005) thus suggesting a direct effect of GITR triggering on $CD4^+25^+$ Treg cells. However, use of $GITR^{-/-}$ mice has shown that activation of GITR on $CD4^+25^-$ cells and not on Treg cells is responsible for inhibiting suppression (Stephens et al., 2004). It has further been reported that $CD8^+$ and $CD4^+$ T cells are being rendered resistant to suppression through GITR stimulation by GITRL or agonistic anti-GITR mAb DTA-1 in tumor models (Nishikawa et al., 2008; Zhou et al., 2007). Little attention has been dedicated to reverse signaling through GITRL so far. A role in promoting immunosuppression has been proposed, thereby, preventing excessive costimulation through GITR activation, but no conclusive model of GITRL triggering has been established yet (Agostini et al., 2005; Grohmann et al., 2007; Shin et al., 2004; Shin et al., 2002).

The T cell costimulatory properties of GITR activation have been exploited for tumor immunotherapy in mouse models. Tumor growth could be successfully inhibited by activation of GITR with various formats of the natural ligand, e.g. through administration of Fc-mGITRL construct (Hu et al., 2008), mGITRL-transfected cells (Calmels et al., 2005; Cho et al., 2009; Piao et al., 2009) or a DNA vaccine encoding mGITRL and the tumor antigen mERK (mutated extracellular signal-regulated kinase 2) (Nishikawa et al., 2008). Stimulation of GITR with agonistic antibodies alone (clones DTA-1, G3c) (Ko et al., 2005; Nishioka et al., 2008; Ramirez-Montagut et al., 2006), in combination with vaccination against a melanoma differentiation antigen (Cohen et al., 2006) or adoptive transfer of tumor-primed $CD4^+$ T cells (Liu et al., 2009) also enhanced the tumor-specific T cell response and in some cases led to tumor eradication. Success of the anti-GITR treatment was at least in part mediated by enhanced infiltration of $CD8^+$ T cells and a decrease of Treg cell numbers in the tumor (Cho et al., 2009; Ko et al., 2005). While *in vivo* GITR stimulation has been proven to induce or enhance tumor immunity, some autoimmune side effects could be observed. Administration of DTA-1 to BALB/c mice results in moderate titers of anti-parietal autoantibodies occasionally accompanied by mild autoimmune gastritis (Ko et al., 2005; Shimizu et al., 2002). Systemic administration leads to more autoantibody detection than local tumor injection of DTA-1. Autoimmune response in the form of hypopigmentation could be observed in

a study where DNA vaccination in combination with DTA-1 treatment was applied for tumor therapy (Cohen et al., 2006).

1.9 Aim of the thesis

This study exploits the concept of tumor targeting to locally manipulate the T cell compartment. The aim is to activate tumor-specific T cells and thereby elicit an effective anti-cancer immune response resulting in regression of the tumor.

We propose to target the therapeutic agents specifically to the site of disease by using a fusion protein combining the costimulatory molecule GITRL with an antibody fragment targeting FAP. Using the costimulatory properties of GITRL, we aim at expanding and activating $CD4^+$ and $CD8^+$ T cells and diminishing the suppression of $CD8^+$ T cells by Treg cells. Furthermore, presentation of antiFAP-mGITRL by a FAP^+ cell line is expected to enhance this stimulation of T cells and further increase their resistance to Treg-mediated suppression. We hypothesize that membrane-bound antiFAP-mGITRL allows crosslinking of multiple GITR molecules on the T cells, thus leading to increased signaling and enhanced costimulation. The *in vitro* therapeutic efficacy of antiFAP-mGITRL is investigated by treatment of mice carrying a subcutaneous stroma-inducing carcinoma or a FAP^+ sarcoma.

AntiFAP-mGITRL immunotherapy not only has the potential to enhance therapeutic efficacy of GITRL through crosslinking of receptor molecules but also to reduce a harmful autoimmune response.

2 Material and Methods

2.1 Equipment

Agarose Gel Documentation	BioDoc-It Imaging System	UVP, Upland, USA
Autoclave	V-100	Systec, Hünenberg, Switzerland
BIAcore	T100	GE Healthcare/Biacore, Uppsala, Sweden
Blotting apparatus	Trans-Blot SD Semi-Dry Transfer Cell	Bio-Rad, Hercules, USA
Cell counter	CASY Cell Counter Model TT	Roche Innovatis, Bielefeld, Germany
Centrifuges	Centrifuge 5804R Centrifuge 5810R Centrifuge 5415D	Eppendorf, Hamburg, Germany
Electroporation	Gene Pulser II	Bio-Rad, Hercules, USA
Flow cytometers	FACScan FACSCalibur FACSCanto II	BD Biosciences, San Jose, USA
FibraStage cell culture system	FibraStage	New Brunswick Scientific, Edison, USA

HPLC	HP 1100 Series System	Agilent Technologies, Basel, Switzerland
Magnetic-activated cell sorting	MACS Multistand & quadro MACS	Miltenyi Biotec, Bergisch Gladbach, Germany
PCR cycler	T300 Thermocycler	Biometra, Göttingen, Germany
Plate reader	Wallac Victor^2 1420 Multilabel Counter	PerkinElmer, Waltham, USA
Microscope	Polyvar 2	Leica Reichert Jung, Heerbrugg, Switzerland
Shaker system	Multitron 2	Infors HT, Bottmingen, Switzerland
Spectrometer	BioPhotometer	Eppendorf, Hamburg, Germany
Spinner flask & magnetic stirrer	500 ml flat bottom hanging bar spinner flask & BELL-ENNIUM 9 position magnetic stirrer	Bellco, Vineland, USA
Water purification	Milli-Q Gradient System	Millipore, Bedford, USA
Western blot detection unit	ChemiDoc-It Imaging System with BioChemi HR Camera	UVP, Upland, USA

2.2 Reagents and kits

2.2.1 Kits

BCA Protein Assay Kit, Pierce Biotechnology, Rockford, USA

BD OptEIA Set Mouse IFN-γ, BD Biosciences, San Diego, USA

BD OptEIA Set Mouse IL-2, BD Biosciences, San Diego, USA

In-Fusion Dry-Down PCR Cloning Kit, Clontech Laboratories, Mountain View, USA

QIAGEN Plasmid Maxi Kit, QIAGEN, Hilden, Germany

QIAprep Spin Miniprep Kit, QIAGEN, Hilden, Germany

QIAquick Gel Extraction Kit, QIAGEN, Hilden, Germany

Rapid DNA Ligation Kit, Roche Diagnostics, Mannheim, Germany

REDTaq Ready Mix, Sigma-Aldrich, St. Louis, USA

2.2.2 Antibodies

2.2.2.1 Primary antibodies

anti-c-myc (9-E10, Novus Biologicals, Littleton, USA)

mouse monoclonal Penta-His antibody (QIAGEN, Hilden, Germany)

antiHis-biotin (Rockland Immunochemicals, Gilbertsville, PA)

anti-mouse CD4 FITC, anti-mouse CD4 APC, anti-mouse CD8 APC (Miltenyi Biotec, Bergisch Gladbach, Germany),

anti-mouse CD8a FITC, anti-mouse CD8 PerCP (BD Biosciences, San Jose, USA)

anti-mouse CD25 PE, anti-mouse CD4 APC-Alexa750, anti-mouse CD3 PE-Cy7, anti-mouse CD3 (clone 145-2C11) (eBioscience, San Diego, USA)

mouse CD3/CD28 Dynabeads (Invitrogen, Carlsbad, USA)

ESC11 IgG, ESC14 IgG (both recognizing murine and human FAP), vF19 (specific for human FAP) (all produced in-house, manuscript in preparation)

PE-conjugated H-2L^d/AH-1$_{138-147}$ tetramer (SPSYVYHQF) was kindly provided by P. Guillaume and I. Luescher (Ludwig Institute Core Facility, Lausanne, Switzerland)

2.2.2.2 Secondary antibodies

polyclonal goat anti-mouse immunoglobulins/HRP (Dako, Glostrup, Denmark)

anti-human F(ab')$_2$ PE, anti-mouse IgG (H+L) biotin, anti-human (H+L) biotin, streptavidin PE, peroxidase-conjugated anti-bovine IgG (H+L) , AffiniPure F(ab')2 Fragment goat anti-mouse IgG (Jackson ImmunoResearch, Suffolk, UK)

human κ IgG (Sigma-Aldrich, St Louis, USA)

2.3 Buffer

Chemical reagents listed here were purchased from the following manufacturers: Merck (Darmstadt, Germany), Bio-Rad (Hercules, USA), SERV Electrophoresis (Heidelberg, Germany), Invitrogen (Carlsbad, USA), Sigma-Aldrich (St. Louis, USA), Kantonsapotheke (Zürich, Switzerland), Roth (Karlsruhe, Switzerland), Fluka (Buchs, Switzerland), Hänseler (Herisau, Switzerland).

TAE	2 mM	TRIS Ultra
	0.25 mM	Acetic acid
	0.5 mM	EDTA
PBS	150 mM	NaCl
	10 mM	Na_2HPO_4
	1.5 mM	KH_2PO_4
0.1% PBST		PBS
	0.1% (v/v)	Tween20
10%, 2% MPBS		PBS
	10%, 2%	Milk powder

PBS-10% glycerol		PBS
	10% (v/v)	Glycerol
FACS buffer		PBS
	2% (v/v)	FBS, heat-inactivated
	0.03% (w/v)	Sodium azide
	20 mM	EDTA
TE	10 mM	TRIS Ultra
	1 mM	EDTA
		Adjust to pH8
5x SDS loading buffer	0.28 M	TRIS Ultra
	1% (w/v)	SDS
	30% (v/v)	Glycerol
	0.0012% (w/v)	Bromophenol blue
	5.5% (v/v)	β-mercaptoethanol
1.5 M TRIS/SDS pH 8.8	1.5 M	TRIS Ultra
	0.4% (w/v)	SDS
		Adjust to pH8.8
0.5 M TRIS/SDS pH 6.8	0.5 M	TRIS Ultra
	0.4% (w/v)	SDS
		Adjust to pH6.8
12% (v/v) running gel	35% (v/v)	dH_2O
	40% (v/v)	Acrylamide (30%)
	25% (v/v)	1.5 M TRIS/SDS pH 8.8
	0.01% (v/v)	APS
	0.0005% (v/v)	Temed

5% (v/v) stacking gel	61% (v/v)	dH_2O
	13% (v/v)	Acrylamide (30%)
	25% (v/v)	0.5 M TRIS/SDS pH 6.8
	0.01% (v/v)	APS
	0.0007% (v/v)	Temed
SDS running buffer	25 mM	TRIS Ultra
	0.1% (w/v)	SDS
	200 mM	Glycine
Coomassie staining solution	45% (v/v)	Methanol
	10% (v/v)	Acetic acid (99%)
	0.25% (w/v)	Brilliant Blue R
	45% (v/v)	dH_2O
Coomassie destain	45% (v/v)	Methanol
	10% (v/v)	Acetic acid
	45% (v/v)	dH_2O
Western blot transfer buffer	25 mM	TRIS Ultra
	190 mM	Glycine
	20% (v/v)	Methanol
6x DNA loading dye	50% (v/v)	TAE
	50% (v/v)	Glycerol
	0.4% (w/v)	Orange G

2.4 Primer

Primer designation	**Primer sequence (5'-3')**
FAP 5.1	CAGGTACAGCTGAAGCAGTCT
FAP 3.1	ACCACCTCCGGATCCAGCCCGTTTTATTTC

FAP 5.2	CCCATGGGCCAGGTACAGCTGAAGCAG
FAP 3.2	GCCATGGGTGATCCACCACCTCCGGATCCAGC
pEE12_4_fwd	CTTGACACGAAGCTTGCCGCCACCATGAACTGG
pEE12_4_rev	ATGATCAATGAATTCTTAGTGATGGTGATGGTGATGTGA
141106_FWD_BstBI	CTTCGCGACGTACGTTCGAAGCCGCCACCATGAACTGG
141106_REV_EcoRI	TGATTATGATCAATGAATTCTTAGTGATGGTGATGGTGATGTGA
pEE12_4_ext_FWD	GTTCCTTTCCATGGGTCTTTTCTGC
pEE12_4_ext_REV	CAAGTAAAACCTCTACAAATGTGGTATGGC
Seq5_aFAP_end	AGTAGGGAGCTTCCGTACACGTTCG
Seq5_aCD33_end	ACGTTCGGTGGAGGCACCAAGCT

2.5 Plasmids and bacteria

2.5.1 Plasmids

pEAK8	Edge BioSystems, Gaithersburg, USA
pEAK8-antiCD33-antiCD3	pEAK8 with knocked out BamHI restriction site in backbone
pEAK8-antiCD33-mGITRL	with antiCD33 and mGITRL, c-myc- and 6xHis-Tag
pEAK8-antiFAP	with antiFAP scFv, c-myc- and 6xHis-Tag
pEAK8-antiFAP-hGITRL	with antiFAP and hGITRL, c-myc- and 6xHis-Tag
pEAK8-antiFAP-mGITRL	with antiFAP and mGITRL, c-myc- and 6xHis-Tag

pEE12.4	Lonza, Slough, UK
pEE12.4-antiCD33-mGITRL	with antiCD33 and mGITRL, c-myc- and 6xHis-Tag
pEE12.4-antiFAP	with antiFAP scFv, c-myc- and 6xHis-Tag
pEE12.4-antiFAP-hGITRL	with antiFAP and hGITRL, c-myc- and 6xHis-Tag
pEE12.4-antiFAP-mGITRL	with antiFAP and mGITRL, c-myc- and 6xHis-Tag
pEYFP N1 MB36	pEYFP N1 vector (Clontech Laboratories, Mountain View, USA) containing the sequence for the anti-FAP antibody MO36. Provided by K. Pfizenmaier.

2.5.2 Media for bacteria

LB medium	10 g	Tryptone
	5 g	Yeast extract
	5 g	NaCl
	1 l	dH_2O
		heat sterilize medium
LB-Amp	LB medium with 100 µg/mL ampicillin (Sigma, St. Louis, USA) added after sterilization	
LB-Amp plates	LB-Amp with 1.5% (w/v) Difco agar (BD, Sparks, USA) added before sterilization	

2.5.3 Bacterial strains

One shot TOP10 Chemically Competent *E. coli*, Invitrogen, Carlsbad, USA

Fusion-Blue Competent Cells (*E. coli*), Clontech Laboratories, Mountain View, USA

2.6 Cell culture and media

2.6.1 Cell culture media

All cells were cultivated at 37 °C in a 5% CO_2 incubator. Cell culture reagents were purchased from Sigma-Aldrich (St. Louis, USA), SAFC Biosciences (Lenexa, USA), Gibco/Invitrogen (Carlsbad, USA).

D10		Dulbecco's Modified Eagle Medium, with L-glutamine, 4500 mg/l D-Glucose, 110 mg/l Sodium Pyruvate
	10% (v/v)	heat inactivated FBS
	1% (v/v)	Penicillin-Streptomycin (stock solution 5000 units/ml penicillin, 5000 µg/ml streptomycin)
D10 + G418		D10
	200 µg/ml	G418
D10 + Puromycin		D10
	3 µg/ml	Puromycin
D10sel		Dulbecco's Modified Eagle Medium, 4500 mg/l D-Glucose, without L-glutamine, without Sodium Pyruvate
	10% (v/v)	Dialyzed, heat inactivated FBS
	1% (v/v)	Penicillin-Streptomycin
	2% (v/v)	GS supplements (50x)
D5sel		D10sel with only 5% FBS
Dsarcoma		D-MEM/F-12 (1:1)
	10% (v/v)	heat inactivated FBS
	1% (v/v)	Penicillin-Streptomycin

EXC		EX-CELL NS0, serum free, without L-Glutamine
	0.2% (v/v)	SynthChol NS0 Supplement (500x)
	2% (v/v)	GS supplement (50x)
	1% (v/v)	Penicillin-Streptomycin
R10		RPMI 1640 Medium with Glutamax
	10% (v/v)	heat inactivated FBS
	1% (v/v)	Penicillin-Streptomycin
R10 + Puromycin/HTsuppl	1% (v/v)	R10 HT Supplement (100x)
	10 µg/ml	Puromycin
R10 + β-m		R10
	50 uM	β-mercaptoethanol
R10p + Zeocin		R10 with preabsorbed FBS as described in 2.12.1
	200 µg/ml	Zeocin

2.6.2 Cell lines

Name	**Culture medium**	**Description/origin**
NS0	D10	Lonza, Slough, UK
NS0 transfected clones	D10sel 50% D5sel & 50% EXC	Transfections performed as described in section 2.12.6
HEK 293 mGITRL-Fc	R10p + Zeocin	Provided by H. Nishikawa
HEK 293 parental (EBNA)	D10 + G418	Provided by F. Wurm
HEK 293 mFAP	D10 + Puromycin	Produced in-house
CHO parental	R10	Provided by Ludwig Institute for Cancer Research, New York

CHO hCD33	R10 + Puromycin/HT suppl.	CHO cells expressing full length human CD33 antigen (Bauer et al., 2004)
CMS5a parental	R10 + β-m	Provided by H. Nishikawa
CMS5a hGITR	R10 + β-m	CMS5a expressing the extracellular domain of human GITR; provided by H. Nishikawa
CMS5a mGITR	R10 + β-m	CMS5a expressing the extracellular domain of murine GITR; provided by H. Nishikawa
CT26	R10 + β-m	Murine colon carcinoma line; provided by H. Nishikawa
LM8	Dsarcoma	Murine osteosarcoma line; provided by B. Fuchs.

2.7 Mice

6 to 8 weeks female BALB/cHsd1 and 7 weeks old male C3H/Hsd mice were purchased from Harlan Laboratories (Venray, Netherlands). Mice were used within 2 months of delivery.

2.8 Software

BIAcore T100 Evaluation Software V 2.0 (GE Healthcare, Uppsala, Sweden)

CellQuest Pro 4.0.2 (BD Biosciences, San Jose, USA)

FACSdiva (BD Biosciences, San Jose, USA)

FlowJo 7.2.5 (Tree Star, Ashland, USA)

GraphPad Prism V 5.01 for Windows (GraphPad Software, San Diego, USA)

Microsoft Office Excel 2003 (Microsoft, Redmond, USA)

Microsoft Office Word 2003 (Microsoft, Redmond, USA)

SigmaPlot 11.0 (Systat Software, Chicago, USA)

2.9 Bacterial methods

2.9.1 Growth of bacteria in suspension

For small scale cultivation, a 14 ml polypropylene round-bottom tube with 3 ml of LB-Amp medium was inoculated with TOP10 from a glycerol stock. For medium size cultivation, 200 ml of LB-Amp medium was inoculated with a small amount of TG1 from a glycerol stock in a 500 ml Erlenmeyer flask. Bacteria were cultivated o/n at 37 °C in a shaker (200 rpm).

2.9.2 Growth of bacteria on agar plates

50 µl bacterial suspension resulting from freshly transformed *E. coli* cells or from glycerol stock diluted in LB-Amp medium was plated on LB-Amp agar plates. Bacteria were cultivated o/n at 37 °C.

2.9.3 Transformation of competent *E. coli* cells

The mix resulting from a ligation or recombination reaction was added to 1 vial (50 µl) of Fusion-Blue or TOP10 competent *E. coli* cells and incubated 15-30 min on ice. Cells were heat-shocked for 45 s at 42 °C and directly placed one ice for 1 min. 450 µl SOC medium (Invitrogen, Carlsbad, USA) was added followed by shaking for 1 h at 250 rpm at 37 °C. Finally 50 µl were plated on LB-Amp plates.

2.9.4 Glycerol stocks of bacteria

850 µl of o/n bacteria culture was transferred to a 2 ml cryotube and 150 µl of glycerol was added to yield a final glycerol concentration of 15% v/v. After thorough mixing, the tube was stored at -80 °C.

2.10 Molecular biology techniques

2.10.1 Preparation of plasmid DNA from *E. coli*

Small amounts of plasmid DNA required as PCR template were isolated from TOP10 *E. coli* carrying the target plasmid. The DNA was extracted from the bacteria using the QIAprep Spin Miniprep Kit according to the manufacturer's protocol. Molecular biology grade water (Sigma, St. Louis, USA) was used for elution of DNA from the columns.

Large amounts of plasmid DNA required for cloning and for transient and stable transfections of NS0 cells were isolated from TOP10 strains carrying the plasmid. The DNA was extracted using the QIAGEN Plasmid Maxi Kit according to the manufacturer's protocol. Sterile molecular biology grade water (Sigma, St. Louis, USA) was used to redissolve the DNA.

2.10.2 Determination of DNA concentration

Concentration of the prepared plasmid DNA was determined by measuring the absorbance at 260 nm and additionally at 280 nm to account for impurities. For a pure DNA solution, an A_{260nm} of 1 corresponded to a concentration of 50 µg/ml. DNA with a A_{260nm}/A_{280nm} of 1.8-2 was considered as pure.

2.10.3 Agarose gel electrophoresis

For analytical or preparative separation of DNA fragments, 0.7-1% (w/v) agarose (Promega, Madison, USA) gels were prepared with TAE buffer and 10 µg/ml ethidium bromide (Sigma, St. Louis, USA). The samples were mixed with a 6x DNA loading dye. 100 bp and 1 kb DNA ladder (New England BioLabs, Ipswich, USA) were used as size standards at 0.5 µg per lane. A voltage of 80 to 100 V was applied to the gels. After electrophoresis DNA was detected via its fluorescence under UV light and a picture was recorded for documentation purposes.

2.10.4 Amplification of DNA by Polymerase Chain Reaction

Oligonucleotide primers specific for the DNA fragments were designed and purchased from MWG Biotech AG (Ebersberg, Germany) or Microsynth AG (Balgach, Switzerland). All primers are listed in section 2.4.

For amplification of the DNA of interest the Phusion High-Fidelity DNA Polymerase (Finnzymes, Espoo, Finland) was used. 10 mM stock of dNTPs was purchased from Invitrogen (Carlsbad, USA) and GC buffer from the polymerase kit was used.

Reaction conditions were as follows:

Template DNA	10-100 ng
Forward primer	25 pmol
Reverse primer	25 pmol
dNTPs	200 µM
Phusion polymerase	1 U
5x GC buffer	10 µl
dH_2O	adjust volume to 50 µl

Cycling conditions:

Initial denaturation	98 °C	3 min	
Denaturation	98 °C	10 s	
Annealing	69.5 °C	20 s	
Elongation	72 °C	20 s	back to step 2, 30 cycles
Final elongation	72 °C	10 min	

2.10.5 Digestion of DNA with restriction endonucleases

Restriction endonucleases were purchased from New England BioLabs (Ipswich, USA) for digestion of DNA. Reaction buffers, concentration of enzymes and DNA, incubation times and temperatures were chosen according to the manufacturer's instructions. When working with PvuI, the enzyme was heat inactivated for 20 min at 80 °C after digestion.

2.10.6 Purification of PCR products and plasmid fragments

Fragments resulting from digestion or PCR were analyzed by agarose gel electrophoresis. The correct fragment was determined by comparison with the appropriate size standard, excised from the gel and purified using the QIAquick Gel Extraction Kit according to the manufacturer's protocol. Molecular biology grade water was used to elute the DNA from the columns.

2.10.7 Ligation of DNA

The previously digested DNA vector was dephosphorylated prior to the ligation reaction. This was achieved by using 2 U of Shrimp Alkaline Phosphatase (Roche Diagnostics, Mannheim, Germany) for 100 ng of DNA with dephosphorylation buffer provided by the manufacturer. The mix of 11 µl was incubated for 15 min at 37 °C and subsequently for 20 min at 65 °C to inactivate the Alkaline Phosphatase. In parallel, the enzymes from the digested insert were heat inactivated under the same conditions. The DNA was used without further purification and ligation was performed with the Rapid DNA Ligation Kit. In one ligation reaction, 50 ng of insert and 100 ng of plasmid were mixed with DNA dilution buffer from the kit, 20 µl T4 DNA ligation buffer and 10 U T4 DNA Ligase and incubated for 30 min at RT. After the ligation reaction 2-4 µl of the mix was immediately used for transformation of *E. coli* cells.

2.10.8 Cloning by recombination of DNA

The In-Fusion Dry-Down PCR Cloning Kit was used for cloning of the fusion proteins by recombination. 170 ng linearised vector and 60 ng insert resulting from the PCR were mixed at a 1:2 molar ratio in 10 µl dH_2O. This was added to the provided tube containing the ready-to-use reaction powder and incubated for 30 min at 42 °C. Subsequently 40 µl TE buffer was added and 2.5 µl of the mix was used for immediate transformation of competent *E. coli* cells.

2.10.9 Colony PCR

To verify insertion of the insert into the plasmid, a colony PCR reaction was carried out using the REDTaq ReadyMix. A small amount of the colony was mixed with the kit, primers and dH_2O. After the reaction the mix was analyzed on an agarose gel.

Reaction conditions were as follows:

Template	a tip of a colony
Forward primer	10 pmol
Reverse primer	10 pmol
RedTaq Mix	10 µl
dH_2O	adjust volume to 20 µl

Cycling conditions:

Initial denaturation	94 °C	2 min	
Denaturation	94 °C	20 s	
Annealing	60 °C	30 s	
Elongation	72 °C	75 s	back to step 2, 35 cycles
Final elongation	72 °C	7 min	

2.10.10 Sequencing

Successful cloning of all plasmids was confirmed by sequencing of the part of the plasmid containing the fusion proteins as well as the flanking regions. The sequencing reactions were performed by MWG Biotech AG (Ebersberg, Germany) or Microsynth AG (Balgach, Switzerland). The primers used for sequencing are pEE12_4_ext_FWD, Seq5_aFAP_end and Seq5_aCD33_end.

2.10.11 Cloning strategies of fusion proteins

2.10.11.1 Cloning of pEAK8 vectors with fusion proteins

pEAK8-antiCD33-antiCD3 vector (Thiel et al., 2010) was used as starting vector. The vector contains an expression cassette consisting of Kozak-Start-Leader-antiCD33-Linker-antiCD3-c-myc-6xHis-Stop. The BamHI restriction site within the backbone has previously been knocked out and the cassette contains c-myc and 6xHis tags. The fusion proteins are linked by a G4S linker (GGGGS).

Sequences containing a GGGGS (G4S) linker, NcoI restriction site and extracellular human or murine GITR ligand domains (amino acids L49 to S177 for hGITRL and S43 to S173 for mGITRL) flanked on both sides by a BamHI restriction site were sequence optimized and synthesized by GENEART (Regensburg, Germany)

The antiFAP single chain antibody (antiFAP scFv) clone MO36 which recognizes both murine and human FAP (Brocks et al., 2001) was kindly provided by K. Pfizenmaier (Institute of Cell Biology and Immunology, University of Stuttgart, Germany) in the pEYFP N1 MB36 plasmid.

The antiCD33 single chain antibody in the pEAK vector originates from the murine hybridoma M195 secreting an anti-human CD33 IgG (HB-10306, ATCC/ LGC Standards, Molsheim, France).

pEAK8-antiCD33-antiCD3 and the GENEART synthesized constructs Linker-mGITRL and Linker-hGITRL were digested with BamHI, resulting in fragments with sticky ends and removal of Linker-antiCD33 from the vector. Digests were separated by agarose gel electrophoresis, purified by gel extraction and the inserts were ligated into the vector. Successful insertion and correct orientation of the inserts was analyzed by NcoI digestion of purified plasmid DNA of some clones. Hereby produced plasmids pEAK8-antiCD33-mGITRL and pEAK8-antiCD33-hGITRL were digested with NcoI to release the antiCD33-linker insert.

antiFAP sequence was amplified by PCR using primer pairs FAP 5.1 and FAP 3.1 with vector pEYFP N1 MB36 as a template. After gel extraction, the amplified sequence was used as a template for a second round of PCR with primer FAP 5.2 carrying an NcoI restriction site and primer FAP 3.2 introducing the BamHI-Linker-NcoI sequence. Gel purified product was digested with NcoI and ligated into the prepared plasmids, leading to plasmids pEAK8-antiFAP-mGITRL and pEAK8-antiFAP-hGITRL. Successful insertion and correct orientation of the inserts was analyzed by BamHI digestion of plasmid DNA. Production of pEAK8-antiFAP was achieved by digesting pEAK8-antiFAP-mGITRL with BamHI and religating the vector without any insert. Successful cloning was analyzed by BamHI digestion of DNA from resulting clones.

2.10.11.2 Cloning of pEE12.4 plasmid for antiFAP-mGITRL production

The sequence Kozak-Start-Leader-antiFAP-Linker-mGITRL-c-myc-6xHis-Stop was transferred from the vector pEAK8 to pEE12.4 as follows.

Vector pEAK8-antiFAP-mGITRL was digested with XhoI and NotI. Resulting fragments were separated on an agarose gel and the 1569 bp fragment was extracted from the gel. This was used as a template for PCR amplification with primers pEE12_4_fwd (carrying a HindIII restriction site) and pEE12_4_rev (carrying an EcoRI restriction site). The resulting amplified fragment contained the sequence Kozak-Start-Leader-antiFAP-

Linker-mGITRL-c-myc-6xHis-Stop with flanking regions of the pEAK8 vector. The produced insert and the pEE12.4 vector were digested with EcoRI and HindIII, followed by heat inactivation of the enzymes. A short digestion time of 90 min was chosen to achieve partial digestion of the insert since a second HindIII restriction site is present within the antiFAP sequence. Ligation and transformation were performed as described in sections 2.10.7 and 2.9.3. DNA isolated from 10 clones was digested with BamHI to check for presence of pEE12.4 backbone. 2 positive clones were subjected to PCR with the primer pairs pEE12_4_fwd and pEE12_4_rev using Phusion polymerase. Based on electrophoretical separation of the digestion and PCR products, the 2 clones showed the pEE12.4 backbone and correct size of insert.

2.10.11.3 Cloning of pEE12.4 plasmids for antiFAP-hGITRL, antiCD33-mGITRL and antiFAP production

The sequences Kozak-Start-Leader-antiFAP-Linker-hGITRL-c-myc-6xHis-Stop, Kozak-Start-Leader-antiFAP-c-myc-6xHis-Stop and Kozak-Start-Leader-antiCD33-Linker-mGITRL-c-myc-6xHis-Stop were transferred from vector pEAK8 to pEE12.4 by recombination as described below.

The target vector pEE12.4 was digested with EcoRI and BstBI. The inserts from the pEAK8 plasmids were amplified using the primer pair 141106_FWD_BstBI and 141106_REV_EcoRI. These primers contain a BstBI and EcoRI restriction site, respectively, and were designed to share 20 bp of homology at their 5' end with the linearization site of the pEE12.4 backbone. These homologous regions allow for the recombination reaction when insert and linearized vector are incubated together according to the procedure described in section 2.10.8. Successful transfer of the insert was checked by colony PCR with primers pEE12_4_ext_FWD and pEE12_4_ext_REV that bind to the backbone of the pEE12.4 vector close to the polylinker.

2.11 Biochemical techniques

2.11.1 Dot blot with cell culture supernatant

10 µl of cell culture supernatant was transferred to PROTRAN nitrocellulose membrane (0.45 um pore size, Whatman, Dassel, Germany), blocked with 10% MPBS and incubated with anti-c-myc (1:5000 in 2% MPBS) and anti-mouse/HRP (1:1000 in 2%

MPBS). Staining steps were for 1 h at room temperature and were followed by a 10 min washing step in 0.1% PBST. Detection reaction was performed with Amersham ECL Western Blotting Detection Reagent (GE Healthcare, Buckinghamshire, UK).

2.11.2 Purification of fusion proteins

One volume of sterile filtered cell culture supernatant was mixed with one volume of sterile PBS and the mix was incubated with washed TALON Metal Affinity Resin (Clontech Laboratories, Moutain View, USA) at least 2 hours at 4 °C on a roller bed. 2 ml of bead suspension was used per 300 ml of cell culture supernatant. Beads were previously equilibrated by adding 20 volumes of PBS to the bead suspension, centrifugating at 300g and discarding the supernatant. After incubation, the supernatant and bead suspension was poured into a 20 ml Econo-Pac column (Bio-Rad, Hercules, USA) to collect the resin. Flow-through was accelerated with a suction pump at the exit of the column. The flow-through was collected and circulated through the column twice. The column was washed with 200 ml 0.1% PBST and 200 ml PBS. The fusion protein was eluted from the column in 4 fractions of 1ml PBS-150 mM Imidazol (Sigma-Aldrich, St. Louis, USA). The eluate was dialyzed o/n against PBS at 4 °C with a 10 kDa cut-off membrane (SnakeSkin Pleated Dialysis Tubing, Thermo Scientific, Rockford, USA). Proteins were stored at 4 °C for up to one week for further analysis.

2.11.3 Purification of mGITRL-Fc

One volume of sterile filtered cell culture supernatant was mixed with one volume of sterile PBS and the mix was incubated with washed protein A Agarose beads Fast Flow (Millipore, Temecula, USA) at least 2 hours at 4 °C on a roller bed. 1 ml of bead suspension was used per 1000 ml of cell culture supernatant. After incubation, resin was collected in a 20 ml Econo-Pac column washed with 100 ml 0.1% PBST and 100 ml PBS. The fusion protein was eluted from the column in 5 fractions of 900 µl 50 mM glycine pH 2 in tubes containing 100 µl antibody neutralization buffer (1 M TRIS, 1.5 M NaCl, 1 mM EDTA, pH 8). The eluate was dialyzed o/n against PBS at 4 °C with a 10 kDa cut-off membrane. Proteins were stored at 4 °C for up to one week for further analysis.

2.11.4 SDS Polyacrylamide Gel Electrophoresis

20 µl of the eluate was mixed with 5 µl of 5x SDS loading buffer and denatured for 5 min at 95 °C. During electrophoresis, the samples were first focussed in a 5% stacking gel at 40 mA and subsequently separated according to their relative molecular mass in a 12% running gel at 70 mA. Dual Color Precision Plus Protein Standard (Bio-Rad, Hercules, USA) served as size standard and SDS running buffer as described was used. Gels were stained with Coomassie staining solution and destained with Coomassie destain until the protein bands were clearly visible. For documentation, gels were scanned (CanoScan LiDE 70, Canon, Amstelveen, Netherlands).

2.11.5 Immunochemical detection of proteins by Western blot

After electrophoretic separation of the proteins, the unstained gel, two pieces of Extra Thick Blot Paper (Bio-Rad, Hercules, USA) and PROTRAN nitrocellulose membrane (0.45 um pore size) were equilibrated in Western blot transfer buffer. These were assembled on a Trans-Blot SD apparatus and proteins were blotted for 30 min at 12 V per gel. For detection of His-tagged proteins, the membrane was blocked with 10% MPBS for 1 h at RT or o/n at 4 °C. Then, the membrane was incubated with monoclonal mouse PentaHis antibody (1:1000 in 2% MPBS) for 1 h, washed for 10 min with 0.1% PBST and incubated for 1 h with anti-mouse/HRP antibody (1:1000 in 2% MPBS). Control staining were performed with anti-His/anti-mouse/HRP, anti-mouse/HRP alone or peroxidase-conjugated anti-bovine antibody (1:1000 in 2% MPBS). After one washing step for 10 min with 0.1% PBST, detection of the protein was performed using Amersham ECL Western Blotting Detection Reagent. All steps occurred at room temperature.

2.11.6 Determination of protein concentration

Protein concentrations were determined by a colorimetric method using the BCA Protein Assay Kit following the manufacturer's instructions. 10 µl of samples was measured in a 200 µl volume of working reagent. Whenever necessary, the samples were diluted prior to analysis. AffiniPure F(ab')$_2$ Fragment Goat anti-Mouse IgG was used as standard.

2.11.7 Concentration and storage of fusion proteins

The fusion proteins were concentrated with Centriprep centrifugal filter devices Ultracel YM-10 and YM-30 (Millipore, Billerica, USA) depending on the molecular weight of the construct. The volume of the constructs was adjusted to a final concentration of 1 mg/ml in PBS-10% glycerol. The samples were sterile filtered with a syringe (5 ml Omnifix, Braun, Melsungen, Germany) and 0.22 µm disposable filter (Millex-GV, Millipore, Billerica, USA) and stored at -20 °C or -80 °C.

2.11.8 Size Exclusion Chromatography

Purified antiFAP, antiFAP-mGITRL and anti-FAP-hGITRL constructs were analyzed by size exclusion chromatography on a Superose 12 PC 3.2/30 column (GE Healthcare, Uppsala, Sweden) coupled to a HP 1100 Series HPLC System. The column was equilibrated with PBS and calibrated by injection with standards (Sigma, St. Louis, USA) diluted in PBS as follows: 0.4 mg/ml phosphorylase (97 kDa), 0.2 mg/ml bovine serum albumin (66 kDa), 0.2 mg/ml ovalbumin (45 kDa) and 0.2 mg/ml cytochrome c (12 kDa). The constructs were diluted in PBS to 0.2 mg/ml and 10 µl were applied to the column at a flow rate of 50 µl/min. All injections were performed at least twice.

2.11.9 Surface Plasmon Resonance binding assays

Binding assays were performed with a BIAcore T100 (GE Healthcare, Uppsala, Sweden) at 25 °C. A CM5 sensor chip (GE Healthcare, Uppsala, Sweden) was activated with NHS/EDC for 7 min at a flow rate of 5 µl/min. Recombinant human GITR-Fc (R&D Systems, Minneapolis, USA) (10 µg/ml) was immobilized in 10 mM sodium acetate buffer (pH 5.0) on the chip by amine coupling, resulting in 770 RUs after ethanolamine treatment (7 min). Recombinant murine GITR-Fc (R&D Systems, Minneapolis, USA) (10 µg/ml) was coated on a separate flow cell in the same buffer, resulting in 480 RUs. For the binding assays the analytes were dialysed against HBS-EP buffer (10 mM HEPES pH7.4, 150 mM NaCl, 3 mM EDTA and 0.005% surfactant P20, GE Healthcare, Uppsala, Sweden) and dilutions thereof were injected over the chip at a flow rate of 30 µl/min for 10 min. Each series of dilutions was measured twice. Washing was done by injecting 10 mM Glycine-HCl pH 2.2 twice for 60 s.

Kinetic data were analysed with BIAcore T100 Evaluation Software V 2.0. Double-referenced association and dissociation phase data on human GITR were globally fit to

a simple 1:1 interaction model. Affinity on murine GITR was calculated by fitting of the 1:1 Langmuir binding model to the steady-state plateaus.

2.12 Cell culture techniques and immunobiological methods

2.12.1 Cultivation of cell lines

All cells were cultured at 37 °C and 5% CO_2 in media described in section 2.6.1. Most adherent cell lines were detached from cell culture flasks by incubation with PBS-1 mM EDTA. LM8 cells were detached by 5 min incubation with Trypsin-EDTA solution (Gibco/Invitrogen, Carlsbad, USA) and cultivation medium was then added for neutralization of trypsin. All cells were flushed off the flask with a pipette, centrifugated for 5 min at 1500 rpm, resuspended in cultivation medium and 5 to 10% was reseeded in T flasks.

2.12.2 Large scale cultivation of NS0 cells

Stable NS0 clones were either grown in T300 cell culture flasks (inoculation of 60 x 10^6 cells in 300 ml medium) or FibraStage bottles (inoculation of 200 x 10^6 in 500 ml medium). Cultivation medium (50% D5sel and 50% EXC) was replaced every 5 days. Inoculation parameters for the FibraStage were top_hold 30 s, up 2 mm/s, bottom_hold 0 s, down 2 mm/s and cultivation parameters were top_hold 20 s, up 1.5 mm/s, bottom_hold 60 s, down 1.5 mm/s.

2.12.3 Cultivation of HEK 293 mGITRL-Fc cells

FBS was preabsorbed prior to cultivation of HEK 293 mGITRL-Fc cells to remove bovine IgG. 2 ml protein G Agarose beads Fast Flow (Millipore, Temecula, USA) were washed with 50 ml PBS, centrifugated at 300g and supernatant was discarded. 50 ml of heat-inactivated FBS was incubated o/n at 4 °C with 1 ml of washed beads on a roller bed. Beads were collected in an Econo-Pac column and flow-through was used for preparation of the cell culture medium. Bovine IgGs were eluted from the column with 5 bed volumes of 50 mM glycine pH 2. Column was equilibrated with 20 bed volumes of PBS for preabsorption of next FBS sample.

HEK 293 mGITRL-Fc cells were cultivated in R10p + Zeocin medium and treated as described in section 2.12.1.

2.12.4 Determination of cell number and viability

Cell number, size distribution and viability of cell lines and murine splenocytes were determined with the help of CASY Cell Counter + Analyzer System Model TT (Roche Innovatis, Bielefeld, Germany). 50 µl of sample cell suspension was mixed with 10 ml of CASYton solution and analyzed with the cell counter. The method is based on Electrical Current Exclusion which measures the volume and viability of the cell in a dye-free setting.

2.12.5 Transient expression of fusion proteins

Correct cloning of the fusion proteins was assessed by transient transfection of HEK 293 EBNA cells. 8 µg DNA and Fugene6 (Roche, Mannheim, Germany) at a ratio reagent:DNA of 3:1 were incubated for 1 hour in 800 µl DMEM at room temperature and subsequently added to a 50% confluent T75 cell culture flask in D10 medium without FBS. The following day 10% FBS (v/v) was added to the culture. The supernatant was harvested after 3 to 5 days, filtrated and analyzed. Presence of construct in the supernatant was assessed by flow cytometry as described in section 2.12.7.

2.12.6 Stable expression of fusion proteins

Stably transfected NS0 cell lines were generated by electroporation according to the protocol provided by Lonza. Briefly, 40 µg sterile DNA was digested for 4 hours with PvuI at 37 °C in a final volume of 100 µl and the enzyme was subsequently heat inactivated (20 min, 80 °C). 1 x 10^7 NS0 cells were resuspended in 700 µl DMEM in an electroporation cuvette (4 mm gap cuvette, BTX Harvard Apparatus, Holliston, USA), DNA was added and a single pulse of 250 V, 400 µF was delivered. Cells were plated at serial dilutions in D10 in flat bottom 96-well plates. The next day D10sel medium was added. Four to six weeks later the supernatants were screened by dot blot. Positive clones were transferred to a 24-well plate in 1 ml D10sel. In a weekly fashion, the clones were tested for fusion protein expression and positive clones were transferred first into a 6-well plate and subsequently into T75 cell culture flasks.

2.12.7 Flow cytometry analysis

Supernatants of transient expression or purified fusion proteins from stable expression were characterized by flow cytometry. All constructs were tested for binding on the following target cell lines: HEK 293 parental, HEK 293 mFAP, CHO parental, CHO hCD33, CMS5a parental, CMS5a mGITR and CMS5a hGITR. Purified construct was also tested for binding to naïve and activated murine splenocytes. 1 x 10^6 cells/well were stained with supernatant (100 ul, undiluted) or purified protein (10 µg/ml in 200 µl FACS buffer). Detection was performed with Penta-His (1:200) and anti-mouse Fcγ PE (1:200) for HEK 293 and CHO cell lines and with Penta-His (1:200), anti-mouse IgG (H+L) biotin (1:200) and streptavidin PE (1:200) for CMS5a cell lines and splenocytes. Incubations were performed in 200 µl staining volume (unless otherwise specified) for 30 min at 4 °C and were separated by two washing steps with FACS buffer. Murine splenocytes were co-stained with anti-mouse CD3 PE-Cy7, CD4 APC-Alexa750 and CD8-PerCP.

LM8 cells from cultivation in tissue culture flasks and freshly digested LM8 tumor cell suspension were stained with the fusion proteins as described above. Detection was performed with antiHis-biotin (1:100) and streptavidin PE (1:200). Control staining was performed with ESC11 IgG (10 µg/ml), vF19 (10 µg/ml) and anti-human $F(ab')_2$ PE.

Flow cytometry analysis was performed using FACScan and FACSCanto II cytometers with FACSdiva software.

2.12.8 Tetramer staining of blood lymphocytes

Blood samples from BALB/c mice were stored in FACS buffer until tetramer staining. Samples were stained with 12 µg/ml PE-labeled H-2L^d/AH-1$_{138\text{-}147}$ tetramer for 10 min at 37 °C before additional incubation with CD8a FITC antibody for 15 min at 4 °C. After erythrocyte lysis with 1 ml BD FACS Lysing Solution (BD Biosciences, San Diego, USA), 1 x 10^4 $CD8^+$ T cells were measured on a FACScan cytometer and percentage of tetramer-positive cells among $CD8^+$ T cells was determined.

2.12.9 Flow cytometric determination of apparent affinity of fusion proteins to FAP

For affinity studies, antiFAP-hGITRL, antiFAP-mGITRL and antiFAP fusion proteins were serially diluted with FACS buffer. Fusion protein at various concentrations was

incubated with 3 x 10^5 HEK 293 mFAP cells. Detection was performed with Penta-His (1:100), anti-mouse IgG (H+L) biotin (1:100) and streptavidin PE (1:200). All incubation steps were performed for 1 h at 4 °C in a 100 µl final volume. For each dilution, fluorescence intensity of 1 x 10^4 cells was measured with a FACScan supported by CELLQUEST software. Mean fluorescence intensity of the live population of each sample was converted to percentage of maximum binding for each fusion protein and plotted against fusion protein concentration. For determination of apparent affinity of antiFAP to FAP, half maximal binding concentration (KDapp) was calculated with the help of a regression line connecting the 2 measurements closest to 50% of maximal binding. All experiments were done 3 times with different batches of antibodies.

2.12.10 Immunohistochemistry

6 µm frozen sections of tumors were fixed for 10 min in cold acetone, washed in PBS and blocked 10 min with PBS-1% FBS. The sections were then incubated with 10 µg/ml ESC11, ESC14 or human κ IgG isotype control for 1 h at RT and subsequently with anti-human (H+L) biotin (1:80) in PBS with 2% normal mouse serum (Jackson ImmunoResearch, Suffolk, UK) for 45 min. Incubation for 30 min with VECTASTAIN ABC reagent (Vector Laboratories, Burlingame, CA) supplemented with 2% normal mouse serum was followed by staining with ImmPACT DAB substrate solution (Vector Laboratories, Burlingame, CA) for 10 min. After rinsing with tap water, sections were counterstained with Mayer's Haematoxylin solution (Sigma-Aldrich, St. Louis, USA), washed and bedded in glycerin-gelatin (Kantonsapotheke, Zürich, Switzerland). Separate tumor sections were stained with hematoxylin and eosin according to standard procedure. All slides were examined with a Polyvar 2 microscope.

2.12.11 Purification of T cell subsets

Spleens from naïve BALB/c or C3H mice were crushed, filtered and depleted of erythrocytes by ACK lysis (ACK Lysing Buffer, Invitrogen, Carlsbad, USA). T cell subsets were purified using MACS microbeads (Miltenyi Biotec, Bergisch Gladbach, Germany) according to the manufacturer's protocol. Positive selection was performed with anti-mouse CD8 microbeads. $CD4^+25^+$ regulatory T cells and $CD4^+25^-$ effector T cells were separated with the $CD4^+25^+$ Regulatory T Cell Isolation Kit. Purity of the resulting populations was analyzed by flow cytometry (anti-mouse CD4 FITC, CD8a FITC, CD25 PE).

2.12.12 CFSE labelling of T cells

Target $CD8^+$ or $CD4^+25^-$ cells were labelled with 2.5 µM 5,6-carboxyfluorescein diacetate succinimidyl ester (CFSE, Molecular Probes, Eugene, USA) in PBS for 6 min in the dark at 37 °C. Cells were subsequently washed three times with 10 ml D10 medium. Cell assays were performed in D10 medium in a 200 µl final volume in 96-well flat bottom cell culture plates.

2.12.13 Activation of T cells for FACS analysis

Fresh mouse BALB/c splenocytes were stimulated for 2 days with antiCD3/CD28 microbeads (ratio 5:1). 8 x 10^6 cells per well were cultivated in 5 ml R10 in 6-well-plates. On day 2, the beads were removed magnetically before antibody staining.

2.12.14 Proliferation assays

In BALB/c proliferation assays, 1 x 10^5 target $CD8^+$ or $CD4^+25^-$ cells were incubated with parental or mFAP transfected HEK 293 cells (2 x 10^4) in the presence of a suboptimal dose of 1 µg/ml soluble anti-mouse CD3. AntiFAP-mGITRL or antiFAP fusion protein was added at the indicated concentrations. CFSE dilution was assessed by flow cytometry on day 3 using a FACScan cytometer. All assays were performed at least twice in 6 replicates per sample. For analysis, the divison index of CFSE-positive cells was calculated with FlowJo. The division index is the average number of cell divisions of the total population, thereby including both dividing and non-dividing cells.

Proliferation assays with C3H splenocytes were performed as described for BALB/c splenocytes with the exception of $CD8^+$ T cells that were stimulated with 0.01 µg/ml soluble anti-mouse CD3 since this was determined as the dosis required for suboptimal TCR stimulation. Prior to FACS analysis, C3H samples were stained with anti-mouse CD4 APC or CD8a APC for clear identification of the different populations. All C3H proliferation assays were all performed three times in 2 to 6 replicates per sample.

2.12.15 Suppression assays

In suppression assays, BALB/c or C3H $CD8^+$ T cells (1 x 10^5) were cocultured with different ratios of $CD4^+25^+$ cells (1:1, 3:1, 9:1) in the presence of 2 x 10^4 parental or mFAP transfected HEK 293 cells. Splenocytes from BALB/c mice were stimulated with

2 x 10^4 mouse CD3/CD28 Dynabeads and cells from C3H mice were stimulated with 0.1 µg/ml soluble anti-mouse CD3. AntiFAP-mGITRL or antiFAP fusion protein was added at different concentrations (0.01 – 10 µg/ml). CFSE dilution of $CD8^+$ T cells was measured by flow cytometry after 3 days. C3H samples were co-stained with anti-mouse CD8 APC before flow cytometric measurements. All assays were performed at least twice in triplicates. For analysis the average number of cell divisions (divison index) of CFSE-positive cells was calculated with FlowJo. The percent suppression was calculated by the equation ((1-(division index $CD8^+$ & $CD4^+CD25^+$)/(division index $CD8^+$)) x100.

2.12.16 Measurement of cytokine production

Cell culture supernatants from day 3 were analysed for IL-2 and IFN-γ levels by ELISA. The assays were performed using BD OptEIA Set Mouse IL-2 and BD OptEIA Set Mouse IFN-γ kits according to the manufacturer's protocol.

2.13 Animal experiments

2.13.1 *In vivo* tumor growth

Mice were inoculated subcutaneously in the flank with tumor cells resuspended in 100 µl PBS. Tumor growth was monitored daily or every other day by caliper measurement and tumor volume was determined by (length x $width^2$)/2. Body weight was monitored weekly. For therapy, mice were injected intravenously in the tail vein for five consecutive days with 100 µg fusion protein in 100 µl PBS-10% glycerol. The mice were euthanized when the tumor reached a diameter of 15 mm. All animal experiments were carried out under a project license granted by the Veterinäramt des Kantons Zürich (98/2008).

2.13.2 Treatment protocol of CT26 tumors

6 female BALB/c mice per group were inoculated s.c. with 1 x 10^5 CT26 cells. When diameter of the tumors reached 2 to 3 mm (between day 8 and 17), mice were treated with the fusion proteins on 5 consecutive days (PBS, mGITRL-Fc, antiCD33-mGITRL, antiFAP-mGITRL). For analysis of AH-1 specific $CD8^+$ T cells, blood samples were

collected through tail vein puncture on day 3 after tumor inoculation and day 8 or 9 after treatment start.

2.13.3 Treatment protocol of LM8 tumors

12 to 14 male C3H mice per group were inoculated s.c. with 2 x 10^6 LM8 cells. On day 3, all mice showed palpable tumors of 1 to 2 mm in diameter. Mice received daily injections of fusion protein (PBS, antiFAP, antiCD33-mGITRL, antiFAP-mGITRL) from day 3 to 7.

2.13.4 Preparation of single cell suspension from tumors

In a separate experiment, a LM8 tumor of 5 mm in diameter was removed from one mouse and dissociated mechanically with a scalpel. A single cell suspension was obtained by enzymatic digestion in HBSS medium (Gibco/Invitrogen, Carlsbad, USA) containing 0.01% DNase I, 0.01% hyaluronidase, and 0.1% collagenase IA (all obtained from Sigma-Aldrich, St. Louis, USA). After 2 h incubation at 37 °C the suspension was filtered through a 70 µm cell strainer (BD Biosciences, San Jose, CA).

2.13.5 Preparation of tumors for frozen sections

LM8 tumors with 5 mm diameter were removed for histological analysis and immunostaining. Tumors were embedded in Tissue-Tek O.C.T. compound (Sakura Finetek, Zoeterwoude, Netherlands), frozen in liquid nitrogen and stored at -80 °C until sectioned.

2.14 Statistical analysis

Student's unpaired *t*-test was used for statistical analysis of proliferation experiments. Log rank test was used for analysis of Kaplan-Meier survival curves.

3 Results

3.1 Production of fusion proteins

3.1.1 Cloning of the fusion proteins

The fusion proteins containing the N-terminal antiFAP single chain antibody and murine or human GITRL at the C-terminus were constructed as shown schematically in Figure 1. The recombinant antiFAP scFv antibody fragment was connected to the extracellular domain of murine GITRL (amino acids 43-173) by a 5 amino acid long GGGGS linker. The control constructs included antiFAP, antiFAP-hGITRL (amino acids 49 to 177 of human GITRL) and antiCD33-mGITRL. For purification and detection purposes, c-myc and hexahistidine tags were added at the C-terminal end. The amino acid sequences of the fusion proteins are provided in section 5. The mGITRL-Fc fusion protein, produced with HEK 293 mGITRL-Fc cells provided by H. Nishikawa, consists of the extracellular domain of mGITRL cloned at the N-terminus of a murine IgG_2 Fc fragment including the hinge region.

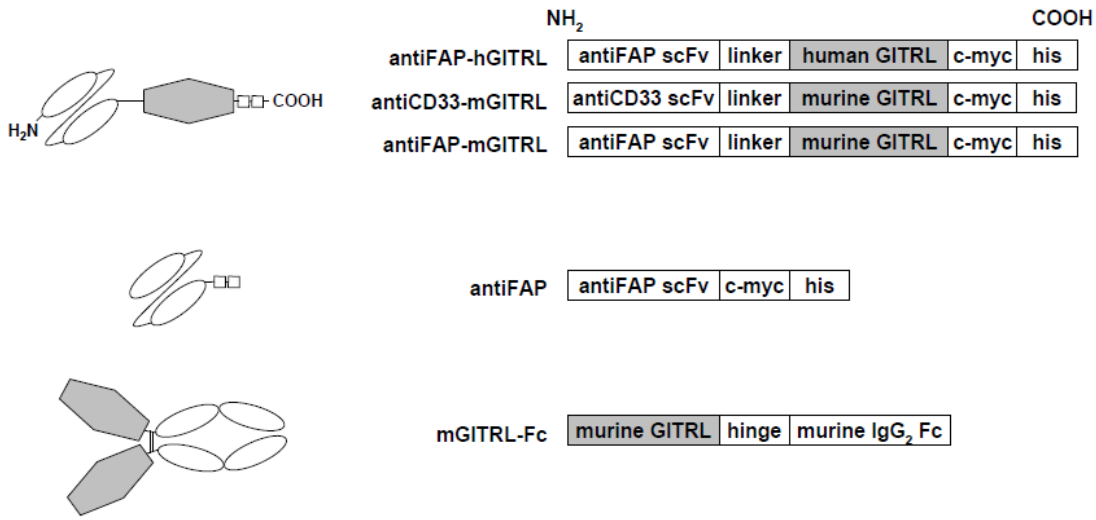

Figure 1. Schematic presentation of the fusion protein constructs.

3.1.2 Production and purification of fusion proteins

For production of the fusion proteins, we generated stably transfected NS0 cell lines with the sequences for antiFAP-hGITRL, antiCD33-mGITRL, antiFAP-mGITRL and antiFAP. The resulting clones were analyzed for production of the fusion proteins by dot blot and the best producer for each fusion protein was expanded. The fusion proteins antiFAP-hGITRL, antiCD33-mGITRL, antiFAP-mGITRL and antiFAP were obtained from the supernatant of NS0 cells cultivated with the FibraStage system or in T300 cell culture flasks. Routine yields of fusion protein were 10 to 25 mg/l of cell culture supernatant, depending on clone productivity. The mGITRL-Fc fusion protein was purified from the supernatant of stably transfected HEK 293 cells cultivated in T300 cell culture flasks. The yield of the mGITRL-Fc fusion protein produced in the HEK 293 system was considerably lower than the yield of the other fusion proteins produced with the NS0 cells. The mGITRL-Fc transfected HEK 293 cells produced up to 0.5 mg/l fusion protein in T300 cell culture flasks.

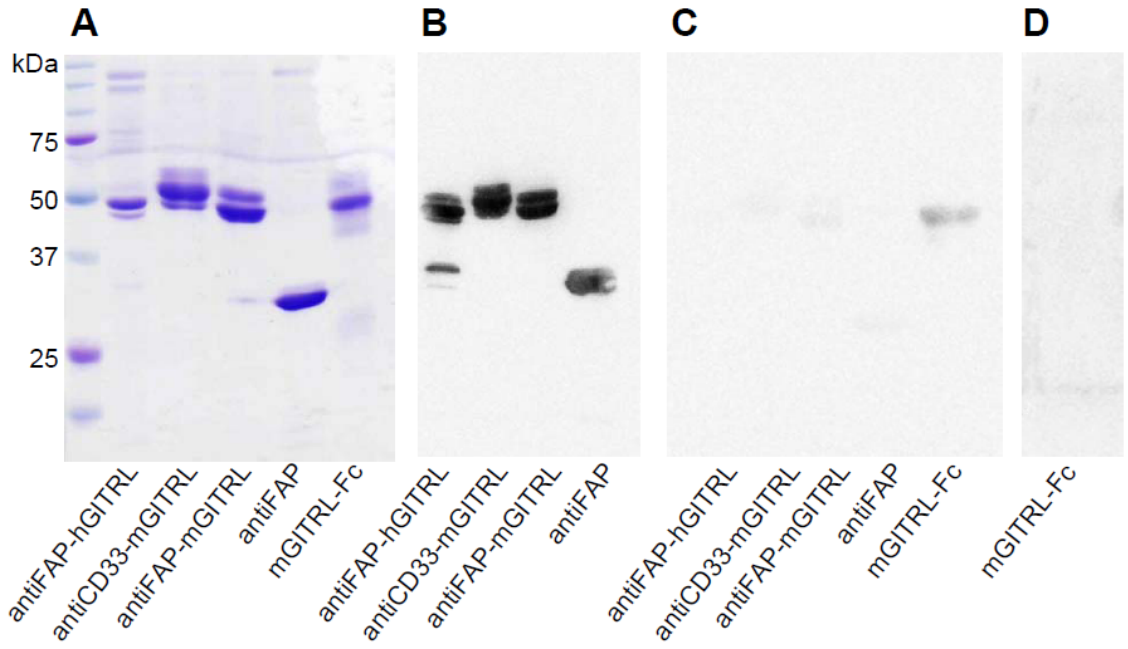

Figure 2. Visualization of the fusion proteins. The 5 fusion proteins were produced in stably transfected NS0 or HEK 293 cells and purified as described. Purified proteins were treated with reducing buffer, separated by SDS-PAGE and either visualized by Coomassie staining (A) or after transfer to nitrocellulose membrane by Western blot analysis with anti-His/anti-mouse (B), anti-mouse (C) or anti-bovine (D) antibody.

The purity of each fusion protein was greater than 90% as determined by Coomassie-stained reducing SDS-PAGE analysis (Figure 2A). The observed bands at a molecular weight of 50 kDa for the antiFAP-hGITRL, antiCD33-mGITRL, antiFAP-mGITRL and mGITRL-Fc fusion proteins correlate well with the calculated molecular mass of the

monomeric units of 45.2 kDa, 45.2 kDa, 45.8 kDa and 40.3 kDa respectively. The observed multiple bands of these fusion proteins were stained positively in Western blot (Figure 2B) and are possibly due to secondary modifications such as glycosylation of the GITRL domain (Hu et al., 2008; Wyzgol et al., 2009). Western blot detection of antiFAP-hGITRL with anti-His and anti-mouse/HRP revealed an additional band under 37 kDa, indicating minor degradation of the fusion protein. The antiFAP single chain antibody was detected at the predicted molecular mass of 30 kDa.

The mGITRL-Fc fusion protein does not contain a His-tag and was therefore purified with protein A beads recognizing the Fc domain. Since protein A beads also bind to bovine IgGs present in the FBS, an IgG removal step is required to obtain pure fusion protein after purification. Therefore, prior to cultivation of mGITRL-transfected HEK 293 cells, we removed the bovine IgGs from the FBS with protein G beads that have a high affinity to bovine IgGs. The mGITRL-Fc fusion protein and bovine IgGs from the FBS have a similar molecular mass, therefore their bands in SDS-PAGE overlap. To check the purity of mGITRL-Fc fusion protein produced in medium with preabsorbed FBS, we performed a Western blot analysis with the purified protein. Our mGITRL-Fc fusion protein could be detected with anti-mouse antibody (Figure 2C). No bovine antibody was detected in the mGITRL-Fc band (Figure 2D), thereby confirming successful purification of the fusion protein without contaminating bovine IgGs.

3.2 Characterization of the fusion proteins

3.2.1 Multimerization properties of the fusion proteins

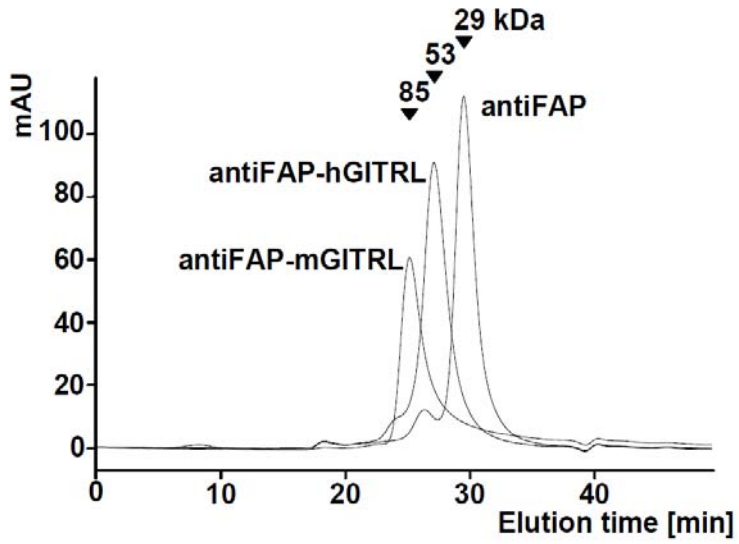

Figure 3. Analysis of multimerization of the fusion proteins by HPLC. The elution profile of the fusion proteins from a Superose 12 PC 3.2/30 column is displayed. The molecular weight of the 3 main peaks was calculated (arrowheads).

The multimerization state of the antiFAP-hGITRL, antiFAP-mGITRL and antiFAP fusion proteins was analyzed by size exclusion chromatography. Purified fusion protein samples were loaded on a Superose 12 PC 3.2/30 column and the molecular masses were calculated according to the retention time on the column (Figure 3). AntiFAP eluted in a main symmetric peak at a calculated molecular mass of 29 kDa corresponding to protein monomers and a small peak of homodimers at 67 kDa. AntiFAP-hGITRL eluted at a molecular weight of 53 kDa with a small shoulder at 120 kDa corresponding to monomers with a small amount of trimers. AntiFAP-mGITRL shows an asymmetric peak with a maximum at 85 kDa indicating the dimeric assembly of antiFAP-mGITRL with only minor amounts of monomers. Thus, the three fusion proteins have different multimerization properties.

3.2.2 Binding of the fusion proteins to the corresponding receptors overexpressed on cell lines

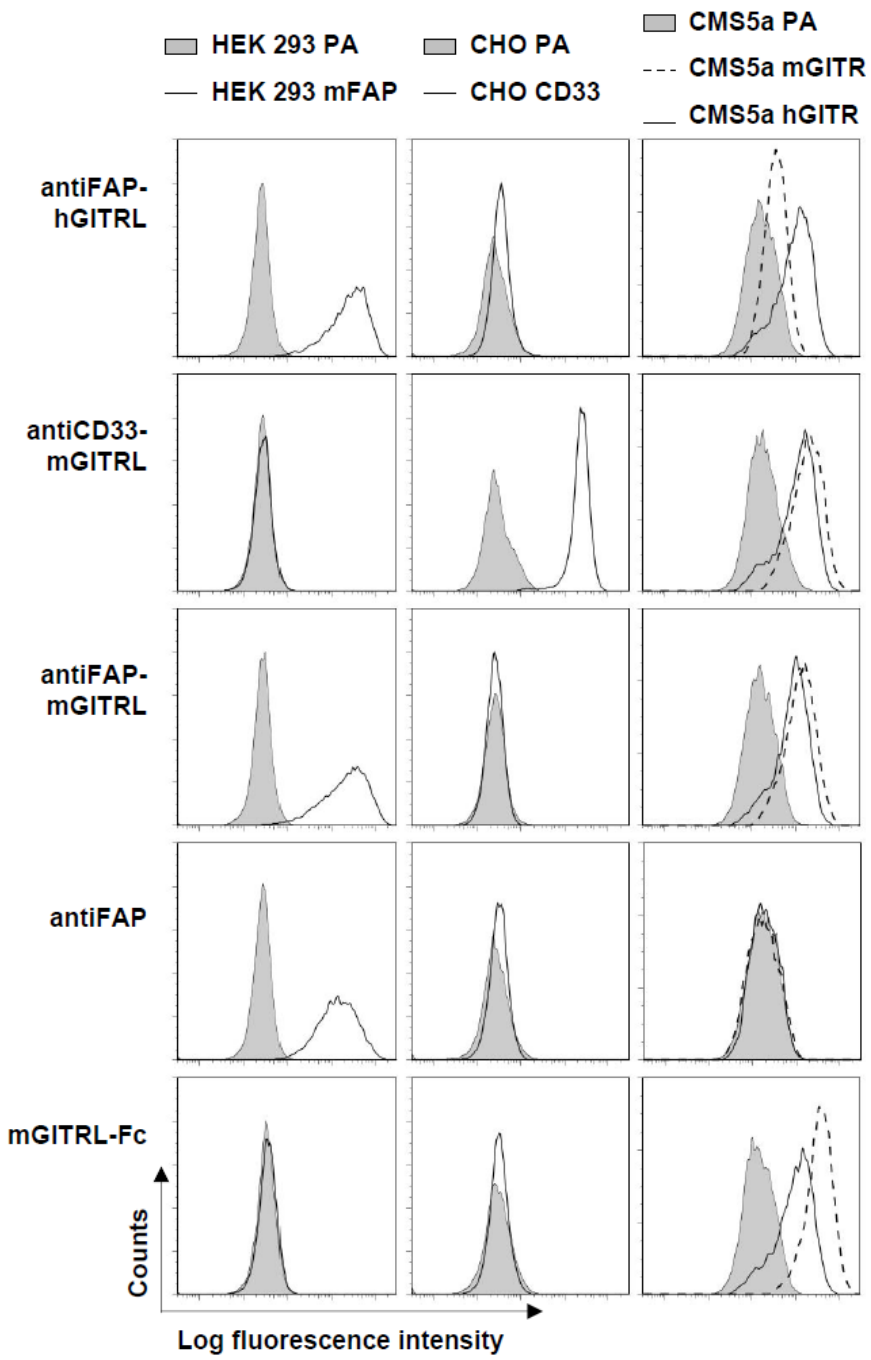

Figure 4. Binding analysis of the fusion proteins to their corresponding receptors on stably transfected cell lines. Purified fusion proteins were incubated with HEK 293 (column 1) parental (grey filled) or mFAP-transfected (black), CHO (column 2) parental (grey filled) or CD33-transfected (black) and CMS5a (column 3) parental (grey filled), mGITR-transfected (dashed) or hGITR-transfected (black) cells and analyzed by flow cytometry.

After biochemical characterization of the fusion proteins, we first verified their capacity to bind their cognate receptor by flow cytometry. For that purpose, cell lines overexpressing murine FAP, human CD33, murine GITR or human GITR and parental

cell lines were stained with the fusion proteins. The antiFAP-hGITRL, antiFAP-mGITRL and antiFAP fusion proteins selectively bound to mFAP-expressing HEK 293 cells whereas, as expected, antiCD33-mGITRL and mGITRL-Fc did not recognize FAP (Figure 4, column 1). None of the fusion proteins bound to the parental HEK 293 cells. AntiCD33-mGITRL bound to CD33-transfected CHO cells whereas no binding was observed on parental CHO cells (Figure 4, column 2). All other fusion proteins showed no binding to any of the two CHO cell lines. The antiFAP single chain antibody did not bind to mGITR- or hGITR-transfected CMS5a cells (Figure 4, column 3). AntiFAP-hGITRL, antiCD33-mGITRL, antiFAP-mGITRL and mGITRL-Fc all recognized the human and murine isoform of GITR. However, the human GITRL domain showed a stronger binding to human GITR than to murine GITR. Binding of mGITRL-Fc to mGITR-transfected CMS5a cells was better than to hGITR-transfected CMS5a cells.

3.2.3 Binding of the fusion proteins to GITR on murine T lymphocytes

We further analyzed binding of the fusion proteins to naturally GITR-expressing target cells. Splenocytes from BALB/c mice were isolated, stained with the fusion proteins and binding was measured by flow cytometry (Figure 5).

The antiFAP-mGITRL, antiCD33-mGITRL and mGITRL-Fc fusion proteins all bound to murine GITR on both $CD4^+$ and $CD8^+$ T cell subsets. Geometric mean of fluorescence intensity (Gmean) after staining with antiFAP-mGITRL fusion protein was 151 on naïve $CD4^+$ and 45 on $CD8^+$T cells compared to 26 and 16, respectively, for the naïve cells stained with the detection system alone. Binding of antiCD33-mGITRL to naïve T cells resulted in Gmean values of 162 and 46 for $CD4^+$ and $CD8^+$ T cells, respectively. Thus, our fusion proteins were able to detect the higher GITR expression on naïve $CD4^+$ T cells than on naïve $CD8^+$ T cells (Kanamaru et al., 2004).

Naïve $CD4^+$ T cells, but not naïve $CD8^+$ T cells, stained with the mGITRL-containing constructs showed an asymmetric peak. This is possibly due to the $CD4^+25^+$ Treg cells within the $CD4^+$ population since Treg cells constitutively express high levels of GITR (Kanamaru et al., 2004; McHugh et al., 2002; Nocentini et al., 1997).

Activated $CD8^+$ and $CD4^+$ T cells show maximal GITR expression 48h after stimulation (Ronchetti et al., 2004; Suvas et al., 2005). We, therefore, stimulated BALB/c splenocytes with anti-CD3/CD28 microbeads for 48h and then analyzed the binding of our fusion proteins to GITR. The antiFAP-mGITRL, antiCD33-mGITRL and mGITRL-Fc fusion proteins all showed enhanced binding to activated T cells compared to naïve T

cells. Binding of these fusion proteins to activated $CD4^+$ T cells increased 2.3-fold compared to naïve $CD4^+$ T cells. The Gmean of antiFAP-mGITRL was 345 for activated $CD4^+$ T cells compared to 151 for naïve cells. Gmean values of 360 and 162 for antiCD33-mGITRL and 1154 and 495 for mGITRL-Fc were measured for activated and naïve $CD4^+$ T cells, respectively. The binding of the fusion proteins to activated $CD8^+$ T cells increased nearly 4-fold, as shown by the Gmean values on activated $CD8^+$ T cells of 186 for antiFAP-mGITRL, 179 for antiCD33-mGITRL and 675 for mGITRL-Fc compared to 45, 46, and 183, respectively, for naïve $CD8^+$ T cells.

AntiFAP and antiFAP-hGITRL did not bind to mGITR on either naïve or activated T cells. In contrast to the staining with mGITR-transfected CMS5a cells, the antiFAP-hGITRL did not show any crossreactivity with the naturally mGITR-expressing cells.

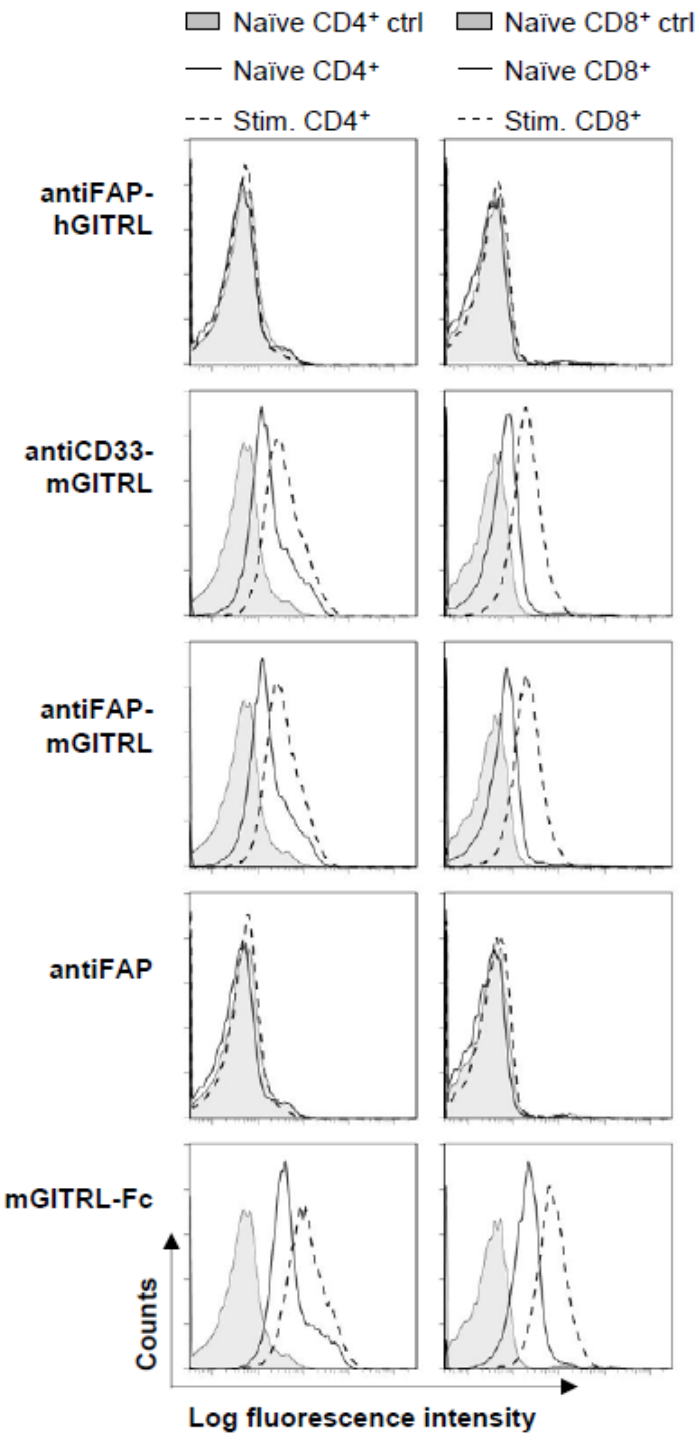

Figure 5. Binding analysis of the fusion proteins to primary murine splenocytes. Fresh BALB/c splenocytes were activated for 48h with anti-CD3/CD28 microbeads, stained with the purified fusion proteins and analyzed by flow cytometry. Columns 1 and 2 show naïve (black) and stimulated (dashed) $CD4^+$ and $CD8^+$ gated T lymphocytes, respectively. As control (ctrl), naïve T cells stained with the detection system alone are shown (filled grey).

3.2.4 Comparison of binding affinities to murine FAP

We previously showed that the antiFAP-hGITRL, antiFAP-mGITRL and antiFAP fusion proteins specifically recognize mFAP on stably transfected cells (Figure 4), thereby confirming that the antiFAP domain of the fusion proteins is functional. In a next step, we quantified the binding of the scFv to murine FAP. The apparent affinities (KDapp) of the constructs were measured on mFAP-transfected HEK 293 cells by analyzing the binding of serial dilutions of the fusion proteins (Figure 6). Half maximum fluorescence intensity was used to calculate the apparent affinity to murine FAP. For all fusion proteins, KDapp values in the low nanomolar range were determined. AntiFAP-hGITRL and antiFAP showed KDapp values to mFAP of 35 ± 21 nM and 29 ± 11 nM, respectively, thus displaying no significant differences in binding affinities. However, antiFAP-mGITRL showed a better apparent affinity of 4.5 ± 3.1 nM.

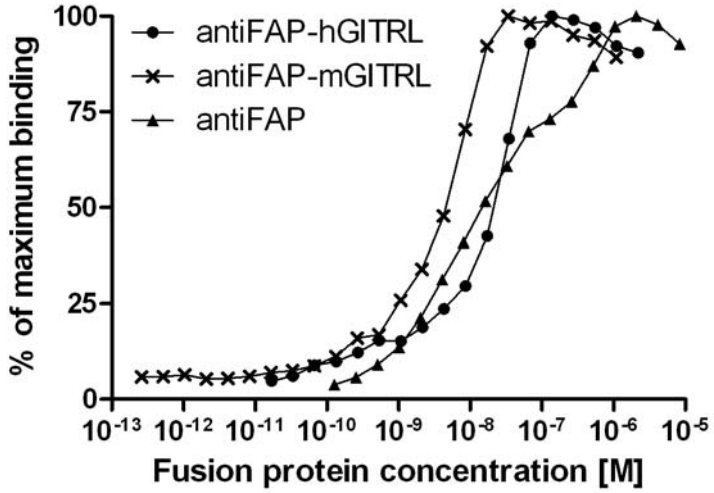

Figure 6. Determination of the apparent affinity of the fusion proteins to murine FAP. mFAP-transfected HEK 293 cells were incubated with serial dilutions of fusion protein (circle: antiFAP-hGITRL, cross: antiFAP-mGITRL, triangle: antiFAP) and stained for flow cytometry analysis. Mean fluorescence intensity of live cells was converted to percentage of maximal binding and plotted against fusion protein concentration. Apparent affinity is calculated from half maximum binding. One representative experiment of three is shown.

3.2.5 GITR binding analysis by surface plasmon resonance

We next compared the binding affinities of the fusion proteins to recombinant murine GITR. This interaction was assessed by surface plasmon resonance (SPR) on a CMS5 chip coated with recombinant murine GITR-Fc protein (Figure 7). The KD values were calculated by fitting of the 1:1 Langmuir binding model to the steady-state plateaus reached after injection of the fusion proteins. The antiFAP-mGITRL fusion protein bound mGITR with a KD of 1190 ± 242 nM, antiCD33-mGITRL bound with a KD of 1710 ± 105 nM and mGITRL-Fc bound with a KD of 1790 ± 136 nM. AntiFAP-hGITRL, antiFAP and hGITRL-Fc did not bind to murine GITR.

To compare the affinities of the human and murine GITR/GITRL systems, we also measured the binding to recombinant human GITR (Figure 8). The KD values were calculated by fitting of the double-referenced association and dissociation data by a simple 1:1 interaction model. AntiFAP-hGITRL bound to hGITR with a KD of 14 ± 2 nM and hGITRL-Fc bound with a KD of 10 ± 2 nM. AntiFAP-mGITRL, antiFAP and mGITRL-Fc fusion proteins did not bind to human GITR.

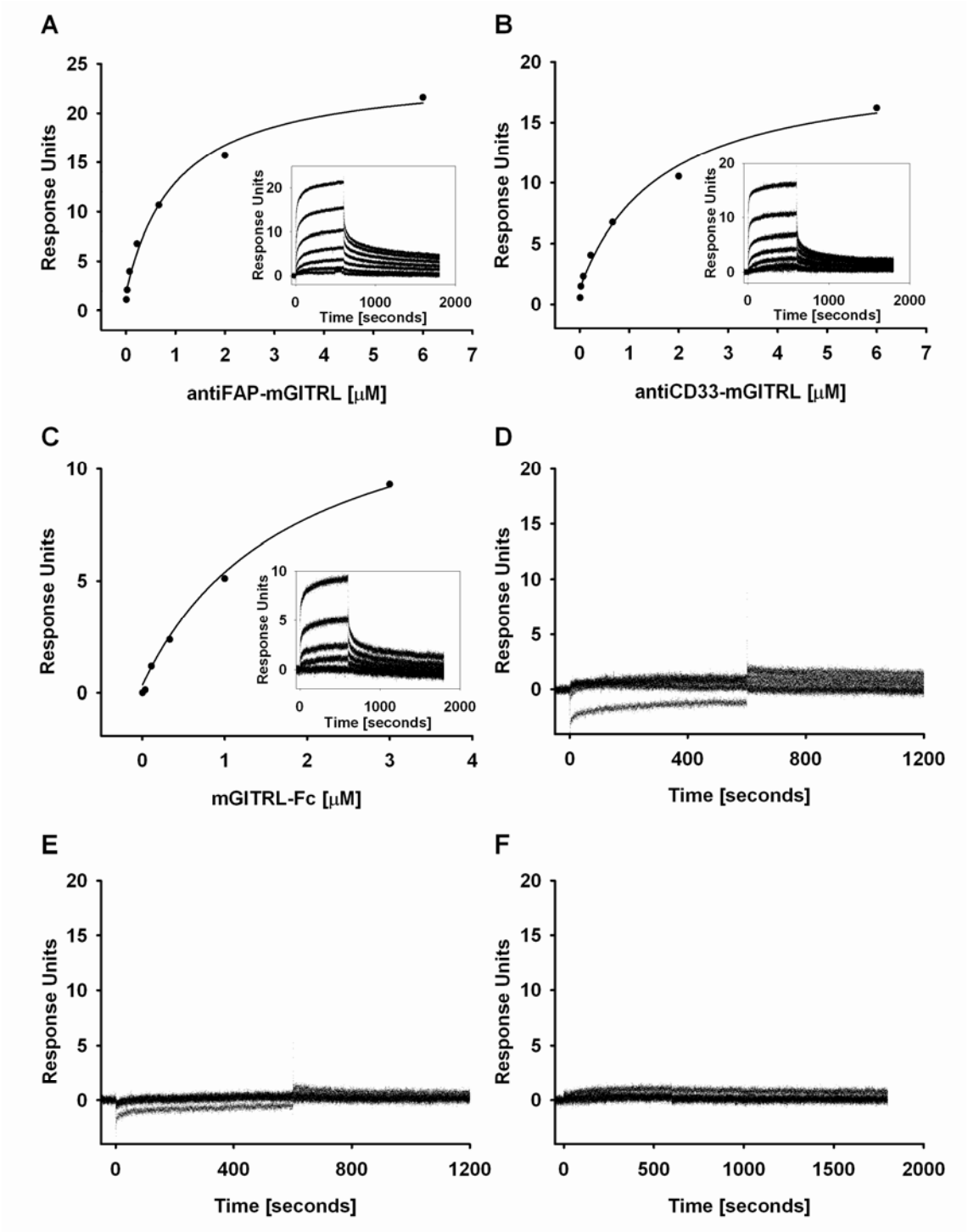

Figure 7. Surface plasmon resonance analysis of the binding to immobilized murine GITR. Sensograms of injections of serial dilutions of antiFAP-mGITRL (A, inset), antiCD33-mGITRL (B, inset), mGITRL-Fc (C, inset), antiFAP-hGITRL (D), antiFAP (E) and hGITRL-Fc (F) are shown. The outer graph from A, B, C shows the nonlinear 1:1 Langmuir fitting of the steady-state binding data.

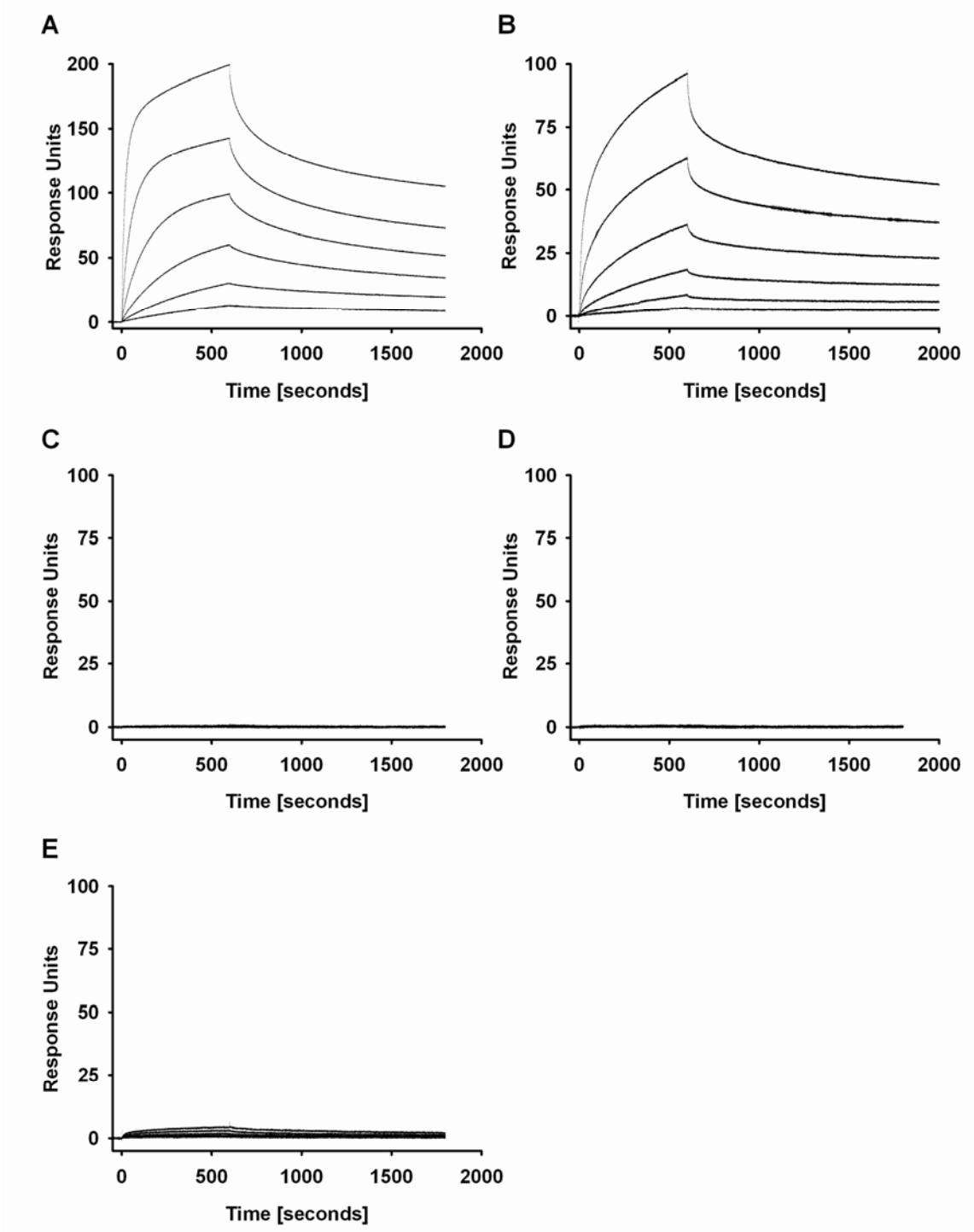

Figure 8. Surface plasmon resonance analysis of the binding to immobilized human GITR. Sensograms of injections of serial dilutions of antiFAP-hGITRL (A), hGITRL-Fc (B), antiFAP-mGITRL (C), antiFAP (D) and mGITRL-Fc (E) are shown.

3.3 Targeting the tumor stroma

3.3.1 Purification of T cell subsets

To analyze the costimulatory effect of the fusion proteins on different murine T cell subsets, we separated regulatory and effector T cells using MACS microbeads. Positive selection with anti-mouse CD8 microbeads typically resulted in a 95% pure $CD8^+$ population (Figure 9A). The $CD4^+25^+$ Regulatory T Cell Isolation Kit routinely yielded a 90% pure $CD4^+25^-$ population and an 85-95% pure $CD4^+25^+$ population as determined by flow cytometry (Figure 9B, C).

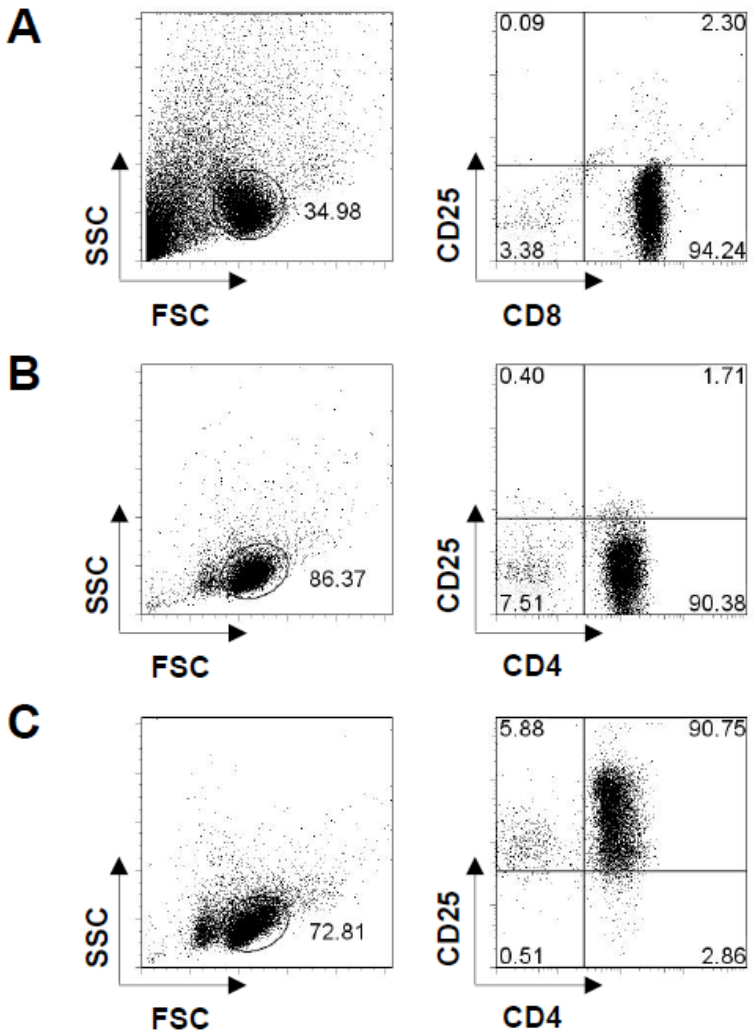

Figure 9. Purified T cell subsets. Freshly isolated BALB/c splenocytes were separated into $CD8^+$ (A), $CD4^+25^-$ (B) and $CD4^+25^+$ (C) T cell subsets using MACS microbeads. Purity of the populations was controlled by flow cytometry analysis. The dotplots (right column) show the phenotype of the live population gated in the forward/side scatter dotplot (left column). Numbers in the dotplots refer to the percentage of cells within the respective gate.

3.3.2 Costimulation of CD4$^+$ T cells

The costimulatory activity of the fusion proteins on murine CD4$^+$25$^-$ T cells was assessed by measuring the proliferation upon TCR stimulation with 1 µg/ml soluble anti-CD3 antibody. This suboptimal TCR stimulus allowed to monitor the costimulatory effect of GITR activation since the costimulatory effect would be less pronounced at higher anti-CD3 concentrations. Proliferation of CD4$^+$ T cells was analyzed after 3 days and the average number of divisions of the total T cell population (division index) was calculated with FlowJo as described (Figure 10A). The resulting division index of lower than 1 is due to the fact that a suboptimal TCR stimulus was used and that not all cells within the T cell population responded to this weak stimulus. We further added fusion protein and FAP-negative or FAP-positive HEK 293 cells to the T cell culture to assess the influence of costimulation on the T cells. Addition of 1 µg/ml soluble antiFAP-mGITRL to CD4$^+$25$^-$ cells led to the same proliferative activity as with the antiFAP control construct. However, presentation of antiFAP-mGITRL in a membrane-bound form (1 µg/ml antiFAP-mGITRL with mFAP-transfected HEK 293 cells) increased proliferation of CD4$^+$25$^-$ T cells by 43%. In contrast to the lower concentration, 10 µg/ml of antiFAP-mGITRL in the presence of HEK 293 parental cells led to a 39% increase in T cell proliferation compared to cultivation in the presence of antiFAP. Presentation of 10 µg/ml antiFAP-mGITRL by FAP-positive HEK 239 cells did not further increase proliferation compared to fusion protein in the presence of parental HEK 293 cells. It is of note that the proliferation of CD4$^+$ T cells was equal for FAP-presented antiFAP-mGITRL at both concentrations tested. This indicates that in a setting where the fusion protein is being presented to the T cells by mFAP transfected HEK 293 cells, lower fusion protein concentrations are sufficient to efficiently costimulate CD4$^+$ T cells.

The activation and function of CD4$^+$25$^-$ cells was assessed by measuring cytokine secretion. IFN-γ and IL-2 in the supernatant from the proliferation assay was quantified by ELISA. Parental or mFAP-transfected HEK 293 cells cultivated alone produced no IL-2 or IFN-γ (data not shown). Secretion of IFN-γ by CD4$^+$ T cells was not enhanced by costimulation with any concentration of unbound antiFAP-mGITRL in the presence of HEK 293 parental cells compared to cultivation in the presence of antiFAP (Figure 10B). However, presentation of antiFAP-mGITRL by mFAP expressing cells increased IFN-γ production to 1952 pg/ml compared to 639 pg/ml for cultivation with antiFAP (at 1 µg/ml). The same 3-fold increase was also observed at 10 µg/ml fusion protein. Thus a substantial increase in IFN-γ production could not be triggered through antiFAP-mGITRL in the presence of parental HEK 293 cells at the tested concentrations. In contrast, secretion of IL-2 was enhanced by soluble fusion protein (Figure 10C).

Unbound antiFAP-mGITRL in the presence of parental HEK 293 cells increased IL-2 production 2.3-fold at 1 µg/ml and 2.7-fold at 10 µg/ml compared to control cultivation in the presence of antiFAP. Presence of HEK 293 mFAP cells instead of parental cells led to a 2.9-fold increase at 1 µg/ml and a 3.2-fold increase at 10 µg/ml compared to cultivation with antiFAP. Thus, the presence of HEK 293 mFAP cells further enhanced IL-2 production by $CD4^+$ T cells even at low fusion protein concentrations.

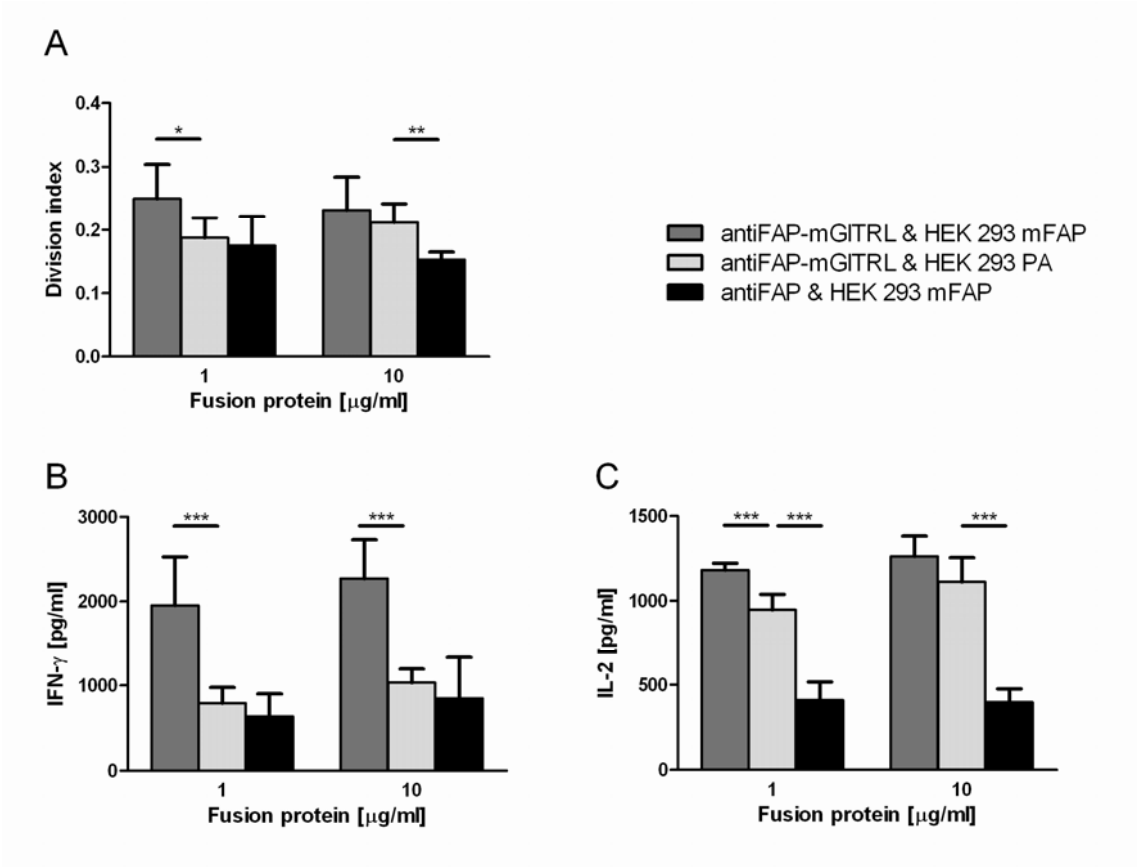

Figure 10. antiFAP-mGITRL presented by FAP-positive cells enhances proliferation of $CD4^+$ T cells. 1 x 10^5 freshly isolated BALB/c $CD4^+25^-$ T cells were stimulated with 1 µg/ml soluble anti-CD3 antibody and various concentrations of antiFAP-mGITRL or control construct. 2 x 10^4 mFAP-positive (HEK 293 mFAP) or parental cells (HEK 293 PA) were added for presentation of the fusion protein. Proliferation of T cells was assessed by measuring CFSE-dilution on day 3 and calculating the average number of cell divisions (division index) with FlowJo (A). IFN-γ (B) and IL-2 (C) production was quantified by ELISA. *:p<0.05, **:p<0.01, ***:p<0.001

3.3.3 Costimulation of $CD8^+$ T cells

The influence of FAP targeting on the activation of $CD8^+$ T cells was analyzed by proliferation assays. Proliferation of $CD8^+$ T cells was measured in the presence of a suboptimal dosis of 1 µg/ml soluble anti-CD3 antibody and the fusion proteins (Figure 11A). Presentation of antiFAP-mGITRL by HEK 293 mFAP cells enhanced proliferation of $CD8^+$ T cells compared to antiFAP-mGITRL with parental HEK 293 cells or

compared to antiFAP control construct, as the division indexes were 0.37, 0.20 and 0.11, respectively (at 1 µg/ml fusion protein). In contrast to $CD4^+$ T cells, $CD8^+$ T cells produced minimal amounts of IFN-γ upon stimulation with soluble anti-CD3 (Figure 11B). Unbound antiFAP-mGITRL as costimulatory signal triggered significant IFN-γ secretion in the presence of HEK 293 parental cells. Moreover, the presence of HEK 293 mFAP cells led to a further 3.8-fold increase of IFN-γ concentration in the supernatant at 1 µg/ml antiFAP-mGITRL compared to unbound fusion protein. At 10 µg/ml antiFAP-mGITRL, the increase was 2.6-fold compared to cultivation in the presence of parental HEK 293 mFAP cells. Maximal IFN-γ secretion reached comparable levels at both 1 and 10 µg/ml of targeted fusion protein. Overall costimulatory effect on proliferation of $CD8^+$ T cells was stronger than on $CD4^+$ T cells.

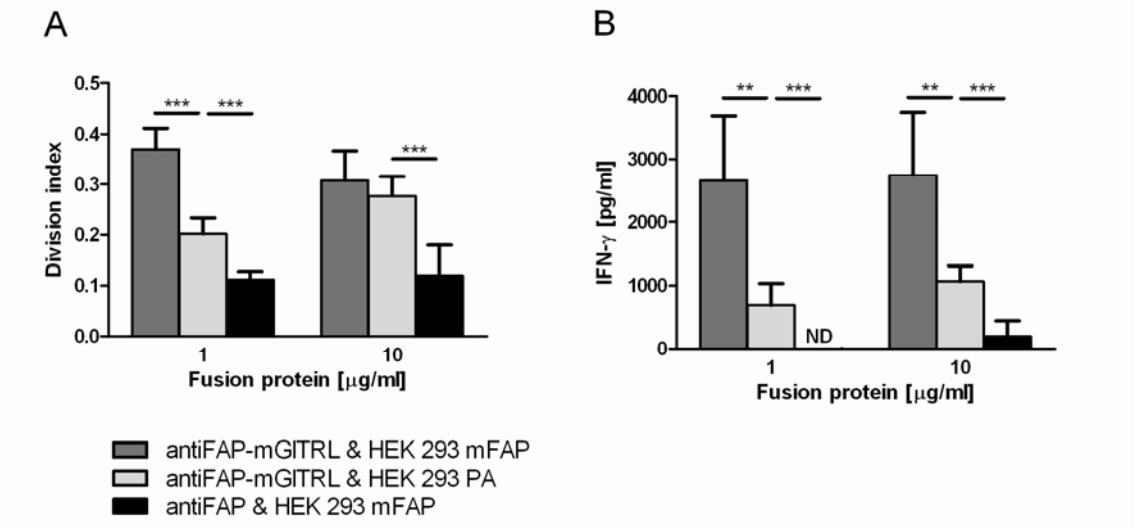

Figure 11. antiFAP-mGITRL presented by FAP-positive cells costimulates $CD8^+$ T cells. 1 x 10^5 purified BALB/c $CD8^+$ T cells were incubated with 1 µg/ml soluble anti-CD3 antibody, various concentrations of antiFAP-mGITRL or control construct and HEK 293 mFAP or HEK 293 PA cells (2 x 10^4). Costimulatory effect of the fusion protein was measured by CFSE-dilution (A) and IFN-γ production (B) on day 3. **:p<0.01, ***:p<0.001

3.3.4 Inhibition of Treg-mediated suppression

GITRL has not only been described to costimulate $CD8^+$ and $CD4^+$ effector T cells, but also to reduce the inhibitory effect of Treg cells on effector T cells. We therefore cocultivated $CD4^+25^+$ Treg cells with $CD8^+$ effector T cells at a ratio of 1:1 in the presence of mFAP-expressing or parental HEK 293 cells and varying concentrations of fusion protein to measure the influence of antiFAP-mGITRL on Treg-mediated suppression (Figure 12). Since the overall stimulation by soluble antiCD3 antibody was quite weak, the suppression assays were performed with anti-CD3/CD28 beads that allowed good monitoring of the suppressive capacity of Treg cells. Basal suppression

by Treg cells was 62% and, as expected, antiFAP control construct did not reverse suppressive Treg cell activity (Figure 12, black bars). Soluble antiFAP-mGITRL in the presence of parental HEK 293 cells, showed a dose-dependent effect on reduction of suppressive activity of Treg cells (Figure 12, light grey bars). Indeed, 0.01 µg/ml of soluble antiFAP-mGITRL in the presence of parental HEK 293 cells did not alleviate suppression but at 0.1 µg/ml suppression of $CD8^+$ T cells was reduced to 48%. At 1 µg/ml antiFAP-mGITRL, inhibition of suppression nearly reached its maximum. Inhibition of suppression was strongly enhanced by antiFAP-mGITRL in the presence of mFAP HEK 293 cells (Figure 12, dark grey bars). 0.01 µg/ml antiFAP-mGITRL presented by HEK 293 mFAP cells already reduced suppression to 42%. Suppression could be lowered up to 32% but not completely abrogated at higher fusion protein concentrations. 0.01 µg/ml antiFAP-mGITRL presented by FAP-positive cells was nearly as effective in overcoming Treg-mediated suppression as the 100-fold higher dose of 1 µg/ml unbound antiFAP-mGITRL (42% to 38%, p=0.039).

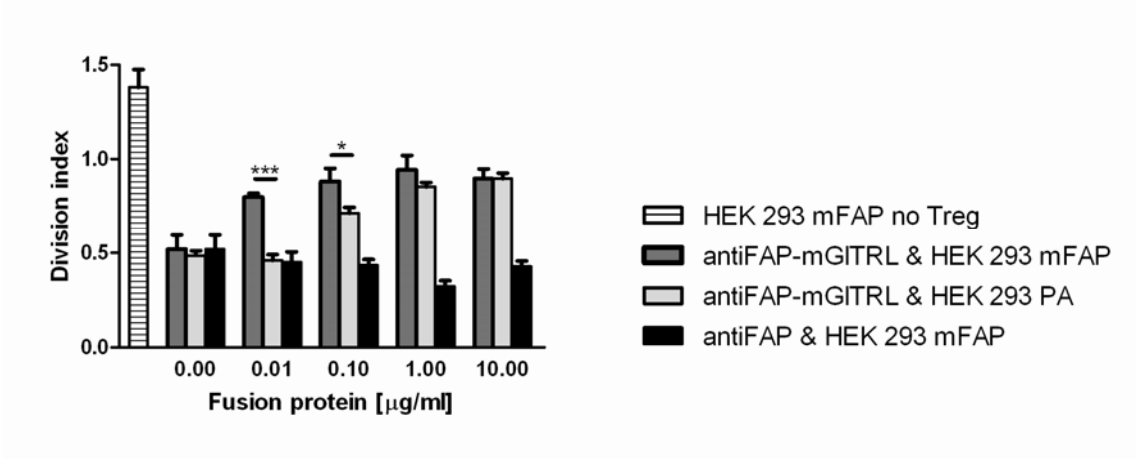

Figure 12. antiFAP-mGITRL reduces suppression by Treg cells in a dose-dependent manner. 1 x 10^5 BALB/c $CD8^+$ T cells were cocultivated with 1 x 10^5 $CD4^+25^+$ Treg cells in the presence of 2 x 10^4 anti-CD3/CD28 microbeads and antiFAP-mGITRL or antiFAP for 3 days. HEK 293 mFAP or parental cells were added for presentation of the fusion protein. In a dose-response assay, different concentrations of fusion protein were used and proliferation of Teff cells was measured by CFSE-dilution. *:p<0.05, ***:p<0.001

The influence of Treg:Teff ratio on suppressive activity was tested at 0.1 and 1 µg/ml of fusion protein (Figure 13). Without GITRL stimulus, at a 1:1 Treg:Teff ratio Treg cells suppressed the proliferation of $CD8^+$ T cells by 77% (p<0.0001), 35% at a 1:3 ratio (p=0.003) and 14% at a 1:9 ratio (Figure 13A). At 0.1 µg/ml, antiFAP-mGITRL was potent in relieving suppression by Treg cells, thereby being significantly more effective in the presence of mFAP HEK 293 cells than parental HEK 293 cells (Figure 13A, dark grey vs. light grey bars). At a 1:3 ratio, antiFAP-mGITRL in the presence of parental HEK 293 cells partially inhibited the suppressive effect whereas the fusion protein

presented by mFAP HEK 293 cells could completely restore $CD8^+$ Teff cell proliferation compared to unsuppressed $CD8^+$ T cells (p=0.236). 1 µg/ml antiFAP-mGITRL restored proliferation to the same extent for both bound and unbound fusion protein at all Treg:Teff ratios (Figure 13C, dark grey vs. light grey bars). Similar effects were seen in the secretion of IFN-γ by $CD8^+$ T cells (Figure 13B, D). 0.1 µg/ml antiFAP-mGITRL in the presence of parental HEK 293 cells could increase IFN-γ production of $CD8^+$ T cells compared to cells cultivated with antiFAP (Figure 13B, light grey vs. black bars). This effect was enhanced by the use of FAP-positive cells. At a 1:9 Teff:Treg ratio, where inhibition of proliferation and IFN-γ secretion was only minor, the presence of mFAP HEK 293 cells with antiFAP-mGITRL increased IFN-γ secretion by $CD8^+$ T cells to levels even above the usual production seen for anti-CD3/CD28 stimulated non suppressed $CD8^+$ T cells. Stimulation of Treg:Teff cocultures with 1 µg/ml antiFAP-mGITRL partially restored IFN-γ production but no difference could be observed between bound and unbound fusion protein (Figure 13D).

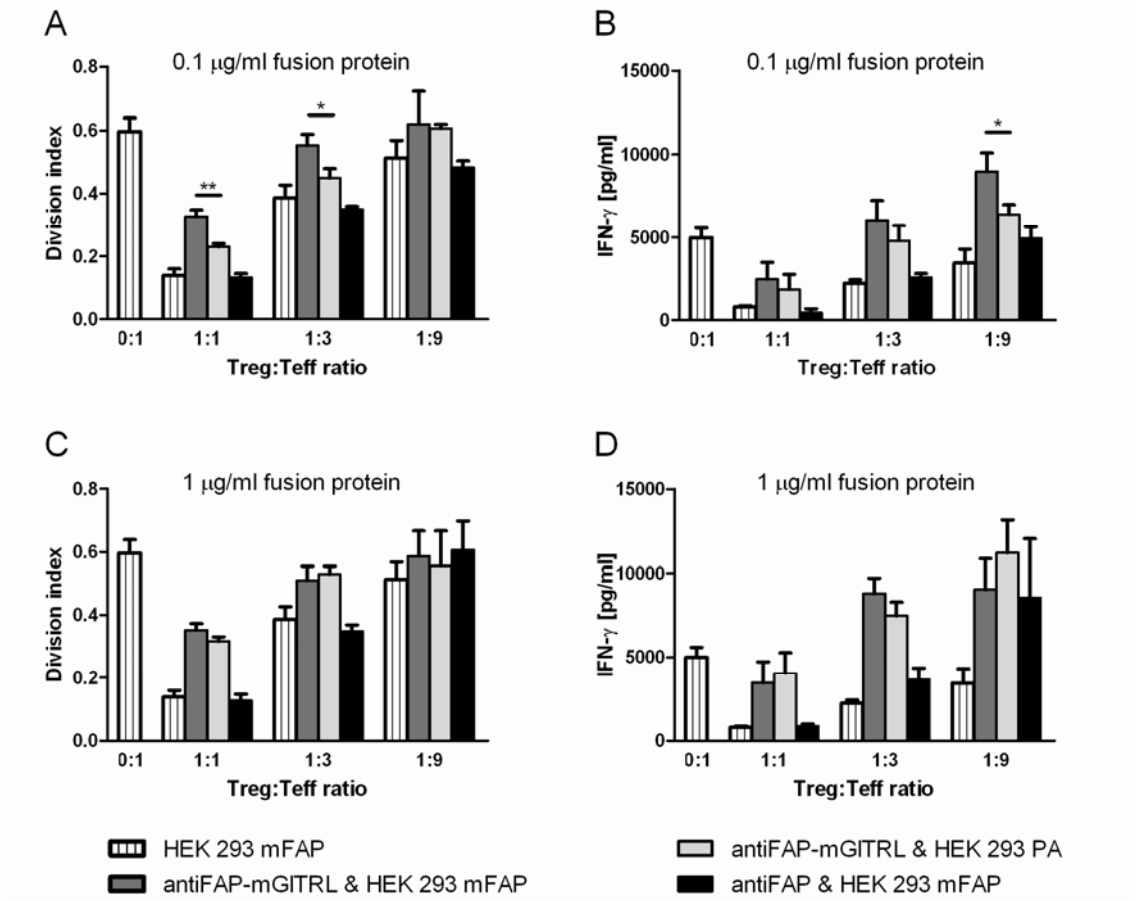

Figure 13. antiFAP-mGITRL presented by FAP-positive cells reduces suppression by BALB/c Treg cells. 1 x 10^5 BALB/c $CD8^+$ T cells were cocultivated with various ratios of $CD4^+25^+$ Treg cells in the presence of 2 x 10^4 anti-CD3/CD28 microbeads and antiFAP-mGITRL or antiFAP for 3 days. HEK 293 mFAP or parental cells were added for presentation of the fusion protein. Treg:Teff ratios were titrated at 0.1 µg/ml (A, B) and 1 µg/ml (C, D) fusion protein and proliferation (A, C) and IFN-γ production (B, D) was measured. *:p<0.05.

3.3.5 Therapy of CT26 tumors

Since antiFAP-mGITRL showed significant costimulatory properties *in vitro*, we further tested the fusion proteins in a murine cancer model. We first investigated if the fusion proteins influence the growth of a stroma-inducing tumor. BALB/c mice were inoculated with the syngeneic colorectal carcinoma line CT26. This tumor line has been reported to induce FAP-positive stroma (Loeffler et al., 2006; Santos et al., 2009). Preliminary experiments showed that tumor growth was heterogeneous, therefore the treatment start with the fusion proteins was adapted individually to each mouse to the time when the tumors had reached 2 to 3 mm in diameter. Five daily doses of 100 µg fusion protein were injected i.v. in the tail vein and tumor growth was monitored for 60 days. Treatment with antiFAP-mGITRL, antiCD33-mGITRL or control PBS resulted in similar tumor progression whereas administration of mGITRL-Fc fusion protein significantly delayed tumor growth (Figure 14A, p=0.0476 compared to PBS group). One mouse of the mGITRL-Fc group completely rejected the tumor and remained tumor-free until the end of the experiment when it was euthanized. To follow the tumor-specific T cell response in the mice, we measured the MHC class I-restricted peptide-specific cytotoxic T lymphocyte response toward the AH-1 peptide. Immunization of mice with CT26 cells had revealed the existence of an immunodominant H-2L^d-restricted, gp70-derived epitope termed AH-1 (Huang et al., 1996). On day 3 after tumor inoculation, blood lymphocytes were stained with H-2L^d/AH-1$_{138-147}$ tetramer. The tumor-bearing mice had no AH-1 specific CD8$^+$ T cells compared to naïve mice (Figure 14B). Tetramer staining of blood lymphocytes 8 or 9 days after therapy start showed no significant increase in AH-1 specific cells among CD8$^+$ T cells for the groups treated with antiFAP-mGITRL, antiCD33-mGITRL and PBS (Figure 14C-E). However, mGITRL-Fc treated mice had increased numbers of AH-1 specific T cells in the blood. Four mice still had low numbers of specific T cells whereas in two mice a dramatic increase was observed (3% and 6% of CD8$^+$ T cells). The mouse showing 6% AH-1$^+$ of CD8$^+$ T cells on day 8 after beginning of treatment (Figure 14F) showed tumor regression and was tumor-free 16 days after start of treatment with 13% AH-1 specific CTLs (Figure 14G).

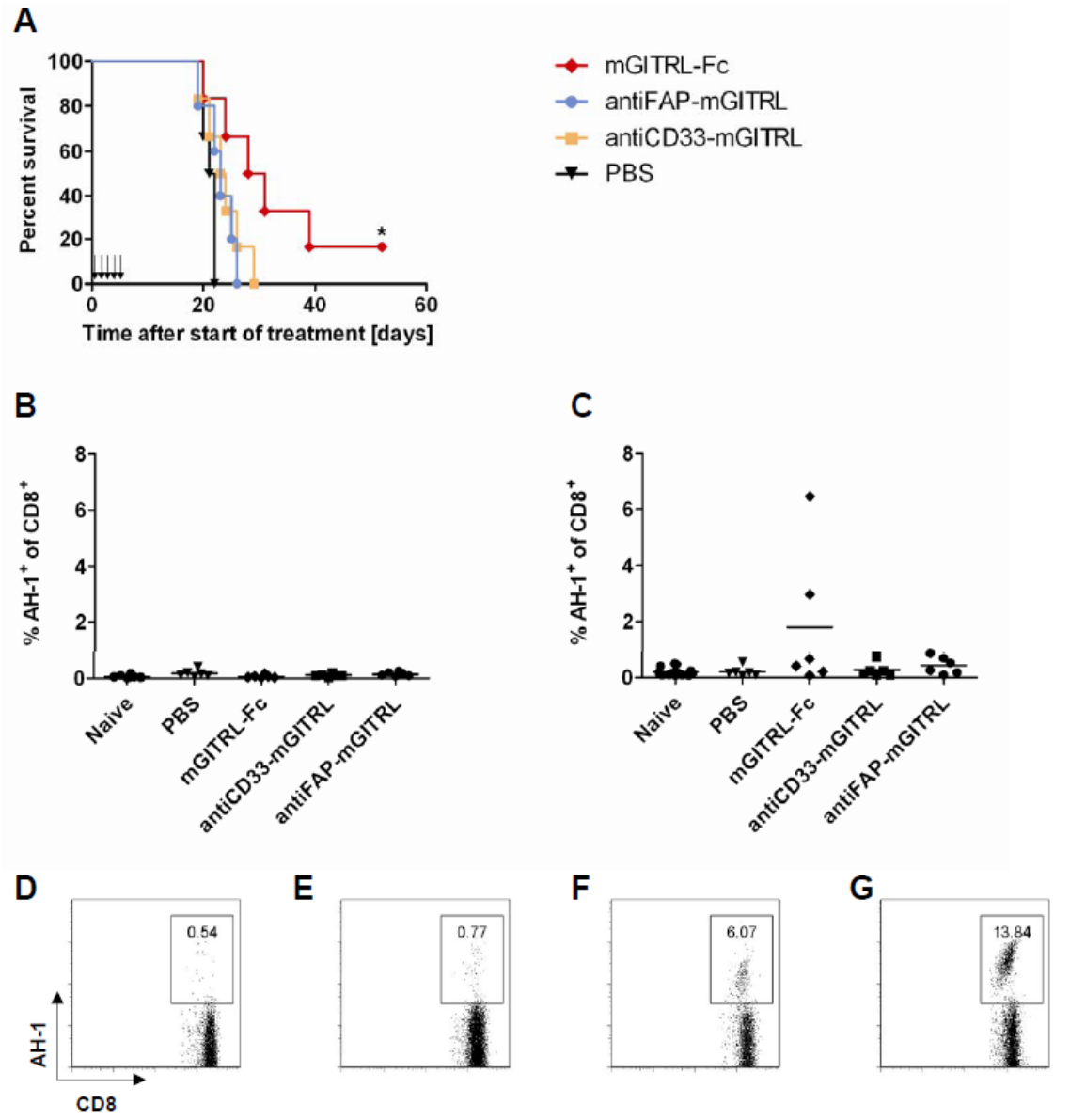

Figure 14. mGITRL-Fc delays growth of CT26 tumors. BALB/c mice (n=6 per group) were injected s.c. in the left flank with 1 x 10^5 CT26 tumor cells and tumor progression was monitored. When tumors had reached 2-3 mm in diameter, mice were treated daily with i.v. injections of 100 µg fusion protein on 5 consecutive days (A, arrows). Kaplan-Meier survival curves of the treated and control groups are shown (A). For detection of a CD8 response against H-2L^d-restricted AH-1 epitope, blood samples from day 3 after tumor inoculation (B) and day 8 or 9 after treatment start (C) were taken from the tail vein and stained with for CD8 and with AH-1 tetramer. Naïve mice without a tumor are shown as control. Percentage of tetramer-positive cells for each mouse and mean of each group are represented in the graphs. Representative AH-1 tetramer staining on day 8 or 9 is shown for antiFAP (D), antiFAP-mGITRL (E) and mGITRL-Fc (F). Tetramer staining of T cells from mouse shown in F was performed again on day 16 (G). *: $p<0.05$ as determined by log-rank analysis between mGITRL-Fc and PBS group.

3.4 Targeting of sarcomas

3.4.1 Costimulation of T cells

We further wanted to test if the fusion proteins influence the growth of a FAP^+ tumor. The murine osteosarcoma cell line LM8 is FAP^+ but is syngeneic to C3H mice and not BALB/c mice. Therefore, we first assessed the influence of the fusion proteins on purified T cell populations from that mouse strain. Isolation of T cell subsets from C3H splenocytes was performed as for BALB/c mice and yielded the same range of purity. Splenocytes of C3H mice show similar GITR expression pattern than BALB/c mice both before and after *in vitro* activation (Shimizu et al., 2002).

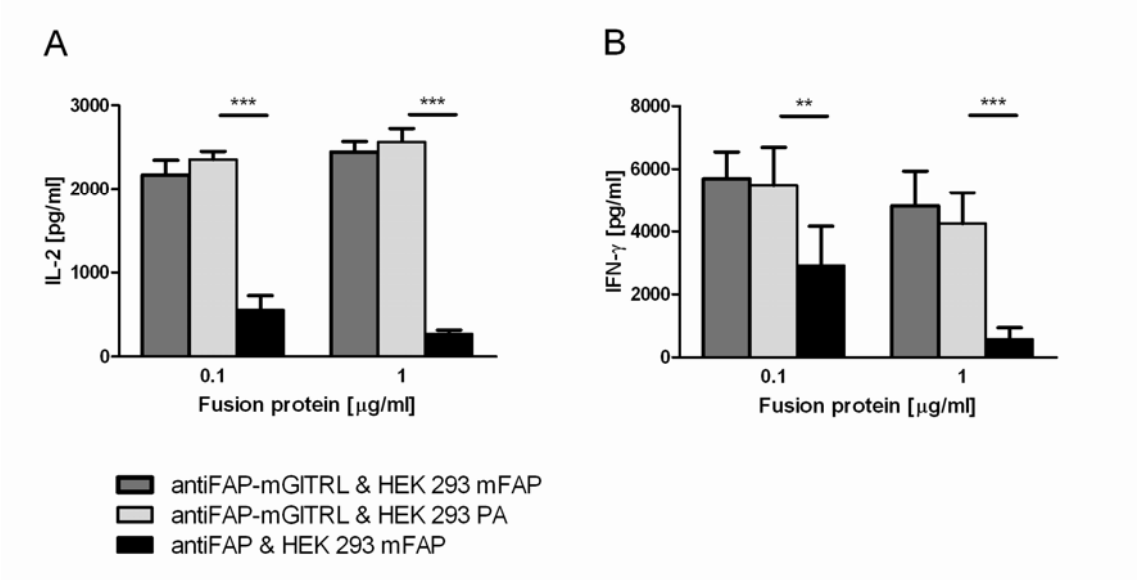

Figure 15. antiFAP-mGITRL presented by FAP-positive cells enhances production of IL-2 and IFN-γ by $CD4^+$ T cells. 1 x 10^5 freshly isolated C3H $CD4^+25^-$ T cells were stimulated with 1 µg/ml soluble anti-CD3 antibody and various concentrations of antiFAP-mGITRL or control construct. 2 x 10^4 mFAP-positive (HEK 293 mFAP) or parental cells (HEK 293 PA) were added for presentation of the fusion protein. After 3 days, IL-2 (A) and IFN-γ (B) production was quantified by ELISA from the supernatant of the culture. **:p<0.01, ***:p<0.001

The costimulatory activity of the fusion protein on C3H $CD4^+25^-$ T cells was analyzed by measuring proliferation, IL-2 production and secretion of IFN-γ upon suboptimal TCR stimulation with 1 µg/ml soluble anti-CD3 antibody. Monitoring of CFSE staining in $CD4^+25^-$ cells after 3 days revealed a main peak of undivided T cells together with very few divided cells for all tested concentrations of fusion protein (data not shown). Proliferation of $CD4^+$ T cells was very low but production of cytokines by $CD4^+$ T cells could be induced in our system. Secretion of IL-2 was enhanced 4-fold upon

costimulation with unbound or FAP-presented antiFAP-mGITRL compared to anti-CD3 stimulus alone (Figure 15A, $p<0.0001$). Production of IFN-γ was also enhanced upon stimulation with antiFAP-mGITRL in the presence of parental HEK 293 cells but could not be further increased by using the mFAP HEK 293 cells (Figure 15B). In both cases, increased cytokine production was only dependent on presence of antiFAP-mGITRL construct but it was neither dose-dependent at the tested concentrations nor was it influenced by presentation by FAP-positive cells.

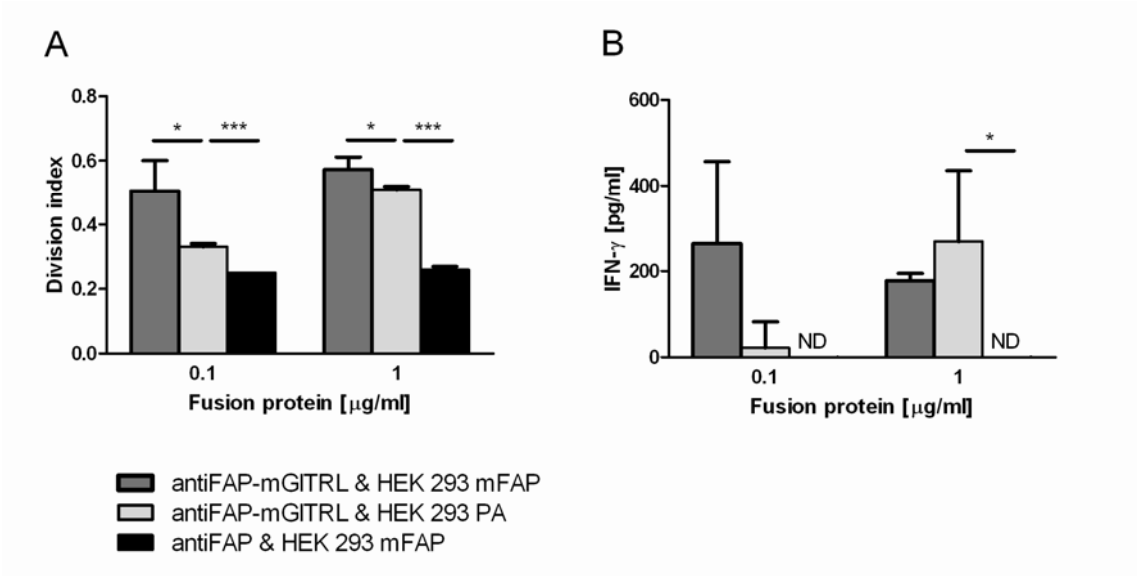

Figure 16. antiFAP-mGITRL presented by FAP-positive cells costimulates $CD8^+$ T cells. 1 x 10^5 purified C3H $CD8^+$ T cells were incubated with 0.01 µg/ml soluble anti-CD3 antibody, various concentrations of antiFAP-mGITRL or control construct and 2 x 10^4 HEK 293 mFAP or HEK 293 PA cells. Costimulatory effect of the fusion protein was measured by CFSE-dilution (A) and IFN-γ production (B) on day 3. *:$p<0.05$, ***:$p<0.001$

The costimulatory properties of antiFAP-mGITRL on $CD8^+$ T cells were further determined by measuring proliferation and IFN-γ production after exposure to suboptimal TCR and fusion protein stimulation. Proliferation of $CD8^+$ T cells was enhanced by soluble antiFAP-mGITRL in a concentration-dependent manner as shown by the proliferation indexes of 0.33 at 0.1 µg/ml and 0.51 at 1 µg/ml ($p<0.0001$, Figure 16A). Presentation of the fusion protein by FAP-positive cells led to further increase in proliferation but maximal proliferation was not dose-dependent. Although $CD8^+$ T cells proliferated upon TCR stimulation, no IFN-γ secretion was detected (Figure 16B). Costimulation with soluble antiFAP-mGITRL in the presence of parental HEK 293 cells triggered IFN-γ production in a dose-dependant fashion. Stimulation in the presence of mFAP HEK 293 cells further increased secretion at 0.1 µg/ml antiFAP-mGITRL. At 1 µg/ml antiFAP-mGITRL, IFN-γ levels were comparable after stimulation in the presence of mFAP HEK 293 cells or parental HEK 293 cells.

3.4.2 Inhibition of Treg-mediated suppression

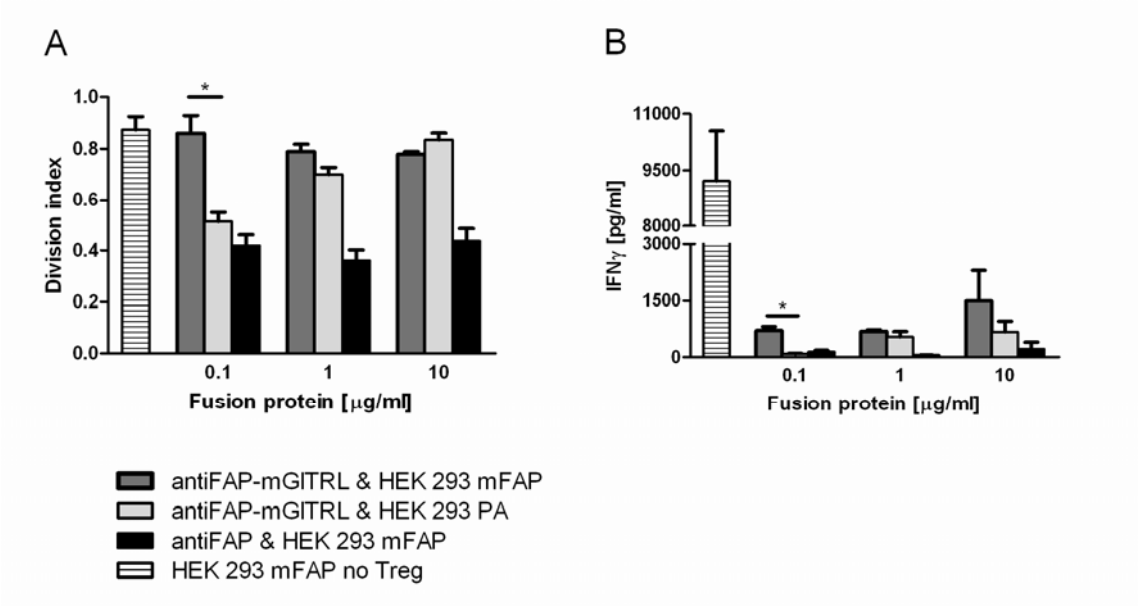

Figure 17. antiFAP-mGITRL presented by FAP-positive cells reduces suppression by C3H Treg cells. 1 x 10^5 C3H $CD8^+$ T cells were cocultivated with $CD4^+25^+$ Treg cells in the presence of 0.1 µg/ml soluble anti-CD3 antibody and antiFAP-mGITRL or antiFAP for 3 days. HEK 293 mFAP or parental cells were added for presentation of the fusion protein. In a dose-response assay, Treg and Teff cells were cultivated at a 1:1 ratio at different concentrations of fusion protein and proliferation of Teff cells was measured by CFSE-dilution (A). Secretion of IFN-γ was quantified in the supernatant by ELISA (B). *:p<0.05

To determine if antiFAP-mGITRL could also abrogate Treg-mediated suppression of C3H T cells, we performed cocultivation assays with $CD8^+$ T cells and $CD4^+25^+$ Treg cells at a 1:1 ratio. Stimulation with a suboptimal dose of anti-CD3 antibody (0.01 µg/ml) lead to weak proliferation of the $CD8^+$ T cells, therefore we used a dose of 0.1 µg/ml anti-CD3 for the suppression assays which allowed to better monitor the effect of the regulatory T cells. For TCR-stimulated $CD8^+$ T cells we calculated a division index of 0.87 (Figure 17A). This was lowered to 0.44 in the presence of Treg cells (p=0.0019), thus resulting in a standard suppression of proliferation of 50%. Addition of soluble antiFAP-mGITRL to the coculture inhibited Treg-mediated suppression in a dose-dependent manner. At 10 µg/ml soluble fusion protein in the presence of parental HEK 293, proliferation of $CD8^+$ T cells was completely restored (division index of 0.84). Presentation of FAP-presented antiFAP-mGITRL to the coculture already cancelled out the effect of Treg cells at 0.1 µg/ml fusion protein (division index of 0.86). The supernatant from these coculture assays were analyzed by ELISA to quantify IFN-γ secretion by $CD8^+$ T cells. Parental or mFAP-transfected HEK 293 cells as well as Treg cells alone did not produce IFN-γ (data not shown). TCR stimulation of $CD8^+$ T cells induced very strong IFN-γ secretion of 9217 pg/ml that was almost completely abolished in the presence Treg cells where 50 to 215 pg/ml were detected (Figure

17B). Both, soluble and membrane-bound antiFAP-mGITRL increased IFN-γ production in a dose-dependent manner, with FAP-presented antiFAP-mGITRL always being more efficient. However, the overall rescue of IFN-γ secretion was very low with FAP-presented antiFAP-mGITRL where a maximum of 1490 pg/ml could be reached, corresponding to 16% of the unsuppressed amount.

3.4.3 Characterization of the sarcoma LM8

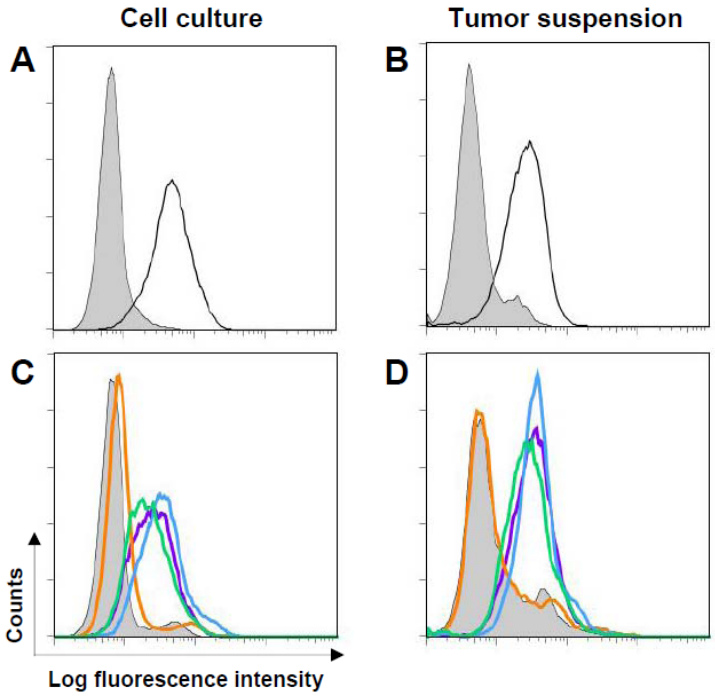

Figure 18. LM8 cells from cell culture and from tumor suspension are FAP-positive. LM8 cells cultivated in T-flasks were analyzed for FAP expression by flow cytometry using ESC11 antiFAP antibody (A) and the fusion proteins (C). LM8 tumor of 5 mm diameter was enzymatically digested and the single cell suspension was stained with ESC11 antiFAP antibody (B) and the fusion proteins (D). Samples were stained with antiFAP-mGITRL (blue), antiCD33-mGITRL (orange), antiFAP (green), antiFAP-hGITRL (purple) and isotype control/secondary antibody (grey area).

Since FAP expression on osteosarcoma cells has been reported (Dolznig et al., 2005), we measured FAP expression on LM8 osteosarcoma cells. This highly aggressive osteosarcoma cell line is a subclone from Dunn osteosarcoma and has high metastatic potential to the lung (Asai et al., 1998). It had been obtained by 8 rounds of i.v. injections of Dunn cells into C3H mice, isolation of pulmonary metastasis and reinjection of these cells into naïve mice. We first assessed the FAP status of the LM8 cell line by staining with our fusion proteins and the anti-FAP antibody ESC11. The ESC11 antibody detected FAP on LM8 cells and the isotype control remained negative (Figure 18B). Binding of antiFAP, antiFAP-mGITRL and antiFAP-hGITRL to LM8 cells

confirmed the expression of FAP on this tumor cell line (Figure 18A). The antiCD33-mGITRL fusion protein did not bind. Parental Dunn cells were subjected to the same staining and showed very weak FAP expression, thereby revealing the different phenotype of these two cell lines (data not shown). To analyze whether LM8 cells maintain expression of FAP in the tumor microenvironment, we removed a s.c. LM8 tumor from one mouse. After enzymatic digestion, the single cell suspension was subjected to staining for FAP and measured by flow cytometry. The dissociated cells stained positively with antiFAP, antiFAP-mGITRL, antiFAP-hGITRL (Figure 18C) and ESC11 (Figure 18D). No binding was detected with antiCD33-mGITRL or isotype control. Furthermore, immunohistochemical analysis of frozen sections of LM8 tumors confirmed the expression of FAP on tumor cells, as determined by positive staining with ESC11 and ESC14 anti-FAP antibodies (Figure 19C-F). H&E staining of the LM8 tumor section revealed densely packed tumor cells (Figure 19A, B).

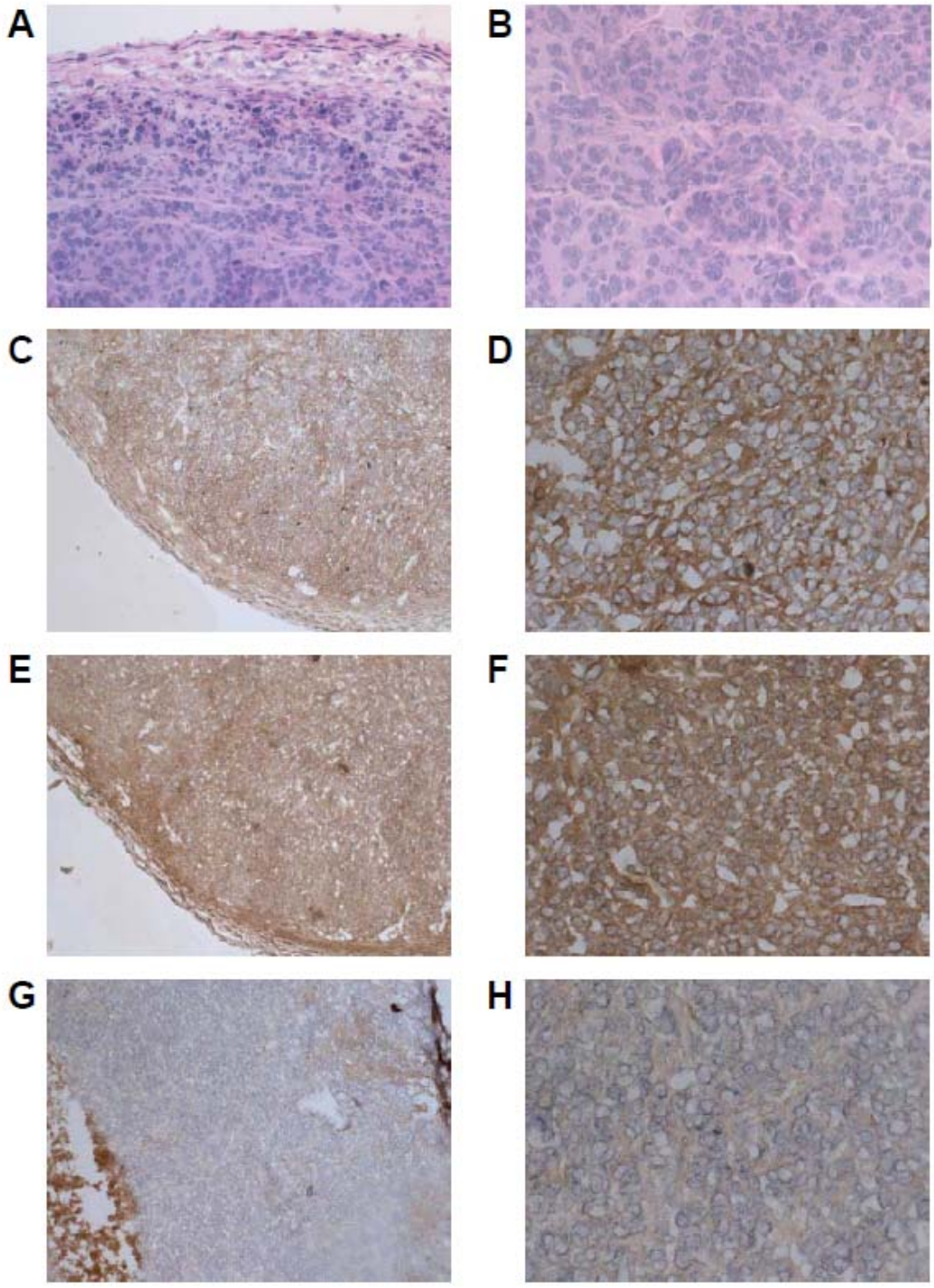

Figure 19. Detection of FAP on frozen sections of LM8 tumors. Immunohistochemical microscopy of 6 µm thick sections of LM8 tumors 5 mm in diameter stained with H&E (A, B), ESC11 (C, D), ESC14 (E, F) and isotype control (G, H) is shown. Tumor sections were analyzed with a Polyvar 2 microscope with 10x (A, C, E, G) and 40x (B, D, F, H) magnification objectives.

3.4.4 Therapy of LM8 tumors

After having identified a FAP^+ sarcoma cell line, we tested the potency of the fusion proteins to inhibit growth of the corresponding FAP-expressing tumor in a syngeneic mouse model. We injected 2 x 10^6 LM8 cells s.c. into the right flank of C3H mice. On day 3 when treatment was started, all mice had developed tumors with 2 to 3 mm in diameter. Fusion protein was administered on 5 consecutive days and tumor growth was monitored. Animals treated with antiCD33-mGITRL, antiFAP and PBS exhibited similar tumor progression and survival (Figure 20). Mice treated with antiFAP-mGITRL showed delayed tumor growth and enhanced survival in comparison to the other group. However, this effect was not statistically significant as determined by log-rank test between antiFAP-mGITRL and PBS treated groups (p=0.0606).

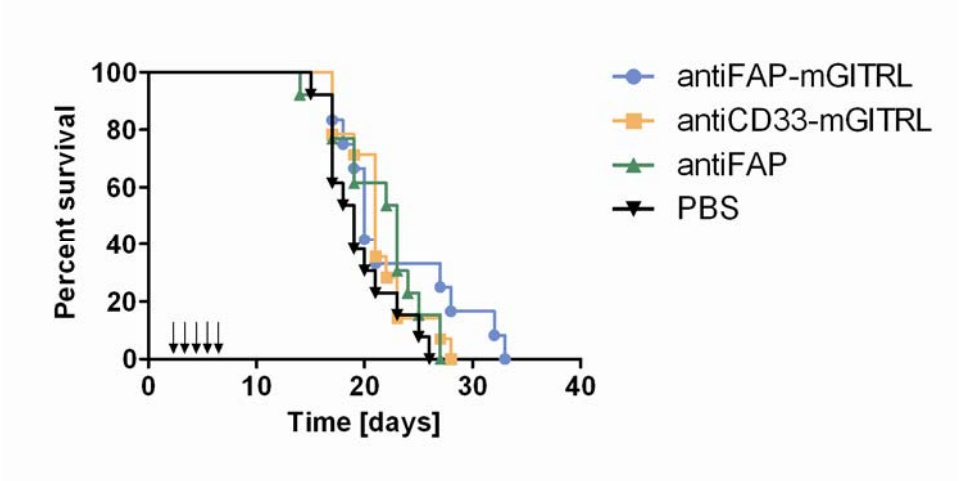

Figure 20. antiFAP-mGITRL slightly delays tumor growth of LM8 osteosarcoma. C3H mice were injected s.c. in the right flank with 2 x 10^6 LM8 tumor cells. Mice received daily i.v. injections of 100 µg fusion protein from day 3 to 7 (marked by arrows, n=12-14 mice per group). Kaplan-Meier survival curve of the different therapy groups is shown.

4 Discussion

The here presented antiFAP-mGITRL bispecific fusion protein aims at modulating the T cell response in the tumor microenvironment. We show that FAP-specific crosslinking of GITR is significantly more efficient in costimulating T cells and overcoming Treg-mediated suppression than untargeted GITR stimulation. Therefore, the use of antiFAP-mGITRL is very attractive for immunotherapeutic applications where a site-specific immune response is to be induced while avoiding systemic toxicity.

Among the TNF receptor superfamily members available as costimulatory receptors, GITR has the valuable characteristic to be expressed not only on activated but also on naïve T cells (Kanamaru et al., 2004; McHugh et al., 2002; Nocentini et al., 1997). Costimulation of T cells through triggering of GITR with its natural ligand or agonistic antibodies has been shown to stimulate antiviral (Dittmer et al., 2004), antiparasitic (Haque et al., 2010) and antitumoral responses (Calmels et al., 2005; Cho et al., 2009; Cohen et al., 2006; Hu et al., 2008; Ko et al., 2005; Liu et al., 2009; Nishikawa et al., 2008; Nishioka et al., 2008; Piao et al., 2009; Zhou et al., 2007). Soluble mGITRL abrogates Treg-mediated suppression (Ji et al., 2004) and tumor growth can be delayed through therapy with Fc-mGITRL fusion protein (Hu et al., 2008), immunization with plasmids encoding a tumor rejection antigen and mGITRL (Nishikawa et al., 2008) or tumor cells transfected with mGITRL (Calmels et al., 2005; Cho et al., 2009; Piao et al., 2009). To improve the therapeutic efficacy and biochemical properties of mGITRL, we added the FAP-targeting component to recombinant mGITRL.

The molecular weight of a fusion protein is of major importance for serum half-life of the construct. Small antibody constructs rapidly undergo systemic clearance through renal excretion as their molecular weight is below the renal retention limit of ~55 kDa. Through increasing the molecular weight of the construct, *in vivo* half-life can be extended by avoiding rapid kidney elimination. Like most TNF receptor superfamily (TNFRSF) ligands that have been described as trimers (Bossen et al., 2006), human GITRL shows loose trimeric assembly in dynamic equilibrium with either monomers (Chattopadhyay et al., 2007) or dimers (Zhou et al., 2008). N-terminal fusion of antiFAP scFv to hGITRL did impact on the hGITRL ectodomain by hampering trimer formation which, in turn, resulted in predominant monomeric antiFAP-hGITRL. In contrast, crystal structure as well as ultracentrifugation and gelfiltration data have shown dimer formation of mGITRL at 40 µM (Chattopadhyay et al., 2008) and a concentration-

dependent equilibrium of monomers and dimers below 10 µM (Zhou et al., 2008). Like mGITRL, our antiFAP-mGITRL fusion protein consists of dimers and low amounts of monomer at 4.4 µM. Thus, the N-terminal fusion of antiFAP scFv to mGITRL did not impair dimerization of the fusion protein. Our dimeric antiFAP-mGITRL fusion protein displayed a molecular weight of 85 kDa, thereby corresponding approximately to the size of a minibody (80 kDa) and being above the threshold of renal excretion. Comparative biodistribution studies have shown that this minibodies display better tumor penetration and *in vivo* half-life than smaller scFvs or diabodies and faster blood clearance than IgGs, thereby offering the best compromise of molecular stability, clearance rate and tumor accumulation. We expect that the serum half-life of the antiFAP-mGITRL fusion protein *in vivo* is longer than for the monomeric form of soluble mGITRL (Ji et al., 2004) but similar to that of Fc-mGITRL (Hu et al., 2008). AntiFAP-mGITRL and Fc-mGITRL constructs both show dimeric assembly, thus being present in the natural format of mGITRL. We determined a KD value of 1.2 µM of antiFAP-mGITRL to mGITR, similar to the reported range of 4 to 15 µM for mGITRL (Chattopadhyay et al., 2008) and to the 1.8 µM as determined for mGITRL-Fc. With 1.7 µM, the antiCD33-mGITRL fusion protein displayed a KD similar to that of antiFAP-mGITRL, thereby being in the expected range since we assumed that the mGITRL domain of this construct would also induce dimer formation and that the antiCD33 scFv domain would not impair the biochemical characteristics in a different way than antiFAP scFv.

The apparent affinities of our constructs for murine FAP are in the low nanomolar range like the reported KDapp of antiFAP scFv of 8 nM to recombinant mFAP in sandwich ELISA and 1.5 nM on mFAP-transfected cells (Brocks et al., 2001). In our study, the overall slightly lower apparent affinities of 4.5 nM for dimeric antiFAP-mGITRL and 29-35 nM for antiFAP and antiFAP-hGITRL can be due to experimental setup as well as differences in the production system (*E. coli* versus NS0). The dimerization of the antiFAP-mGITRL fusion protein correlates with a 6-fold better KDapp on murine FAP-expressing cells compared to monomeric constructs antiFAP-hGITRL and antiFAP. This avidity effect of the dimer together with the expected increased serum half-life due to its molecular weight, should not only enhance accumulation of antiFAP-mGITRL in the tumor but also increase retention time and, therefore, might prolong T cell costimulation in the tumor. The high affinity of our fusion protein for FAP and the low affinity to the costimulatory target are optimal to allow accumulation of the construct in the tumor without being quenched by receptor molecules on the surface of circulating T cells in the blood.

AntiFAP-mGITRL, but not antiFAP-hGITRL or antiFAP, bound to GITR on murine splenocytes, these results being a prerequisite for further costimulatory effects on murine T cells. Unexpectedly, on transfected CMS5a cells, murine and human GITRL domains each bound to both murine and human GITR. However, in line with published data (Bossen et al., 2006; Chattopadhyay et al., 2008; Chattopadhyay et al., 2007; Zhou et al., 2008), our surface plasmon resonance experiments did not show any crossreactivity between the murine and human GITR/GITRL system. Thus, we presume that the high receptor density on the transfected cells led to apparent interspecies crossreactivity of the fusion proteins since ectodomains of murine and human GITRL have 55% sequence identity at protein level and display considerable overall structural similarity as monomers (Chattopadhyay et al., 2008) and the murine and human GITR ectodomain orthologs are 57% homologous (Gurney et al., 1999).

Low affinity interaction of mGITRL with GITR is sufficient for costimulation of T cells (Hu et al., 2008; Kanamaru et al., 2004; Ronchetti et al., 2004; Tone et al., 2003), thus our fusion protein efficiently costimulated $CD4^+$ and $CD8^+$ effector T cells resulting in enhanced proliferation, augmented production of IFN-γ by $CD4^+$ and $CD8^+$ and secretion of IL-2 by $CD4^+$ T cells. Furthermore, in the presence of FAP-expressing cells, antiFAP-mGITRL is presented on the surface of these cells, resulting in an increase in costimulatory activity compared to unbound fusion protein. Interaction of the cell surface bound antiFAP-mGITRL with GITR on the T cell results in aggregation and crosslinking of GITR which enhances GITR signaling (Ji et al., 2004) and thus explains the increased activity if FAP-expressing cells are present. Anti-GITR antibody (Kanamaru et al., 2004; Ronchetti et al., 2004) or soluble GITRL (Ji et al., 2004) treatment has been reported to not only stimulate proliferation of $CD4^+25^-$ T cells but also to enhance anti-CD3-induced secretion of IL-2, IFN-γ, IL-4 and IL-10. Whereas costimulation by antiFAP-mGITRL only slightly enhanced proliferation of $CD4^+$ T cells in our study, the therapeutically more important secretion of IFN-γ or IL-2 was enhanced even 3-fold through presentation of the construct by FAP-expressing cells compared to only TCR-stimulated cells. Triggering of GITR with antiFAP-mGITRL induced stronger proliferation of $CD8^+$ T cells than $CD4^+$ T cells, consistent with data from stimulation with Fc-mGITRL (Hu et al., 2008). The overall lower induction of proliferation of $CD4^+$ and $CD8^+$ T cells compared to other reports (Cho et al., 2009; Hu et al., 2008; Ji et al., 2004; Kanamaru et al., 2004; Liao et al., 2010; Stephens et al., 2004) is due to the use of soluble anti-CD3 antibody in our assays instead of support-bound antibody. Most importantly, we show that antiFAP-mGITRL markedly reduces Treg-mediated suppression of proliferation and function of $CD8^+$ T cells. Most studies analyzing the influence of GITR activation in suppression assays use $CD4^+25^-$ effector

T cells and the few that investigate suppression of $CD8^+$ T cells only quantified proliferation and not cytokine production (Hu et al., 2008; Shimizu et al., 2002). GITR triggering has been shown to restore the secretion of IL-2 by $CD4^+$ T cells in suppression assays (Ji et al., 2004; Valzasina et al., 2005) with one exception stating that Fc-mGITRL failed to restore IL-2 production but restored proliferation to some extent (Liao et al., 2010). We focused on the less well characterized suppression of $CD8^+$ T cells. At ratio 1:1 of BALB/c Treg:$CD8^+$ Teff, suppression could be lowered to 35% at highest concentration of antiFAP-mGITRL presented by FAP-expressing cells. The suppression of T cell proliferation mediated by Treg cells is a powerful effect and the extent to which this effect can be abrogated greatly depends on the experimental setup *in vitro* (Hu et al., 2008; Ji et al., 2004; Liao et al., 2010; McHugh et al., 2002; Nishioka et al., 2008; Shimizu et al., 2002; Stephens et al., 2004). A 1:1 ratio of Treg:$CD8^+$ Teff does not reflect the physiological setting since it is around 1:4 in the tumor of a BALB/c CT26 model (Cho et al., 2009). Proliferation of BALB/c $CD8^+$ T cells could be restored completely at 1:3 ratio in the presence of construct-presenting cells. IFN-γ production of $CD8^+$ T cells could be increased beyond the level of control proliferation, thereby not only cancelling the effect of Treg cells but also activating the T cells even further. Most importantly, we demonstrate that presentation of antiFAP-mGITRL by FAP-expressing cells is 100-fold more effective in overcoming Treg-mediated suppression than unbound fusion protein, presumably due to clustering and crosslinking of GITR molecules on the surface of the $CD8^+$ T cells.

Agonistic anti-GITR treatment by DTA-1 antibody eradicates Meth A tumors and induces a long-lasting protective immune response (Ko et al., 2005). However, this DTA-1-mediated antitumor response is accompanied by some degree of autoimmune reaction (Cohen et al., 2006; Ko et al., 2005; Shimizu et al., 2002). Systemic administration leads to higher autoantibody titers than local injection of DTA-1 directly into the tumor. Ectopic expression of mGITRL on CT26 tumor cells delays tumor growth and enhances infiltration of $CD8^+$ in the tumor (Cho et al., 2009) thus showing that local immune modulation through targeted anti-GITR treatment could lead to tumor immunity without systemic activation. Presentation of our antiFAP-mGITRL fusion protein through FAP-positive cells, i.e. tumor cells or activated fibroblasts, is a particularly efficient method not only to provide a site-specific and long lasting stimulus but also to enhance signaling through crosslinking of receptors on the target cell. To test this model *in vivo*, we studied the efficacy of antiFAP-mGITRL fusion protein in two different syngeneic murine tumor models.

In the first mouse model we investigated the efficacy of antiFAP-mGITRL in the treatment of an epithelial cancer that has been reported to induce formation of FAP^+ stroma. First, determination of an optimal treatment schedule for tumor therapy was required. Since dimeric antiFAP-mGITRL displays approximately the same molecular weight as a minibody, we assumed similar biodistribution patterns. Minibodies show rapid tumor uptake, i.e. within a few hours, and minimal residual blood activity is reached after 24 h (Borsi et al., 2002; Wu and Senter, 2005; Yazaki et al., 2001). We therefore hypothesized that the antiFAP-mGITRL level in the blood should have reached very low levels after 24 h. Thus we decided to administrate our fusion protein i.v. on a daily schedule on five consecutive days. With repeated injections we aimed at further increasing the concentration of antiFAP-mGITRL in the tumor.

We injected the colon carcinoma cell line CT26 subcutaneously into BALB/c mice. This cell line shows intermediate growth rate with tumors reaching 1.5 cm in diameter after 1 month. We aimed at accumulating antiFAP-mGITRL in the tumor microenvironment through binding to the FAP^+ fibroblasts in the stroma (Loeffler et al., 2006; Santos et al., 2009). Tumor progression could not be retarded with antiFAP-mGITRL or antiCD33-mGITRL but administration of mGITRL-Fc delayed tumor growth and even led to tumor rejection in one animal. In line with our results for mGITRL-Fc, another Fc-mGITRL fusion protein had previously been reported to delay tumor growth of CT26 and RENCA tumors (Hu et al., 2008). Even though we injected low amounts of only 1 x 10^5 cells for tumor induction, the growth rate of the tumors was too fast to induce significant stroma formation. Histological analysis of the CT26 tumors showed densely packed tumor cells and very little stroma and thus no FAP^+ activated fibroblasts. Furthermore, mGITRL-Fc fusion protein might be more stable *in vivo* due to the disulfide bridge stabilizing the dimer. The dimeric form of antiFAP-mGITRL, however, may be disrupted under certain physiological conditions *in vivo*. The resulting monomers would have the characteristics of a smaller immunoprotein such as a diabody and be more easily eliminated leading to lower tumor uptake than the dimer, thus hampering an efficient antitumor effect.

Furthermore, we investigated the induction of a tumor-specific T cell response. In our study, the mGITRL-Fc treated mice developed AH-1 specific T cells in the blood. Strikingly, the mouse with the highest tumor-specific $CD8^+$ T cell response was the one that rejected the tumor. Indeed, anti-GITR treatment has previously been reported to promote infiltration of T cells in the tumor (Cho et al., 2009; Ko et al., 2005) or induce and support tumor-specific T cells (Cohen et al., 2006; Nishikawa et al., 2008; Ramirez-Montagut et al., 2006), thereby suggesting a crucial role of $CD8^+$ T cells in the

antitumor response. Moreover, depletion of $CD8^+$ T cells abolishes the antitumor effect of anti-GITR treatment (Cho et al., 2009; Hu et al., 2008; Nishikawa et al., 2008; Piao et al., 2009; Ramirez-Montagut et al., 2006; Zhou et al., 2007). Therefore, either the direct effect of GITRL on $CD8^+$ T cells or the indirect effect through inhibition of suppressive mechanisms is responsible for the enhanced survival of mGITRL-Fc treated mice.

The second mouse model uses the highly aggressive osteosarcoma LM8 that develops tumors reaching 1.5 cm in diameter after 2 to 3 weeks. We showed that this cell line is FAP^+ in culture, in contrast to its FAP^- parental Dunn cell line. LM8 cells maintained their FAP expression *in vivo*, as confirmed by flow cytometry and IHC, thus being an adequate model for FAP-targeted immunotherapy of osteosarcomas. Furthermore, through the *in vitro* cell-based assays with splenocytes from C3H mice, we showed that antiFAP-mGITRL is able to costimulate T cells from that mouse strain. T cells from BALB/c and C3H mice showed the same trend of costimulatory effect in response to TCR and GITR activation but the magnitude of proliferation and cytokine production varied depending on the mouse strain. The antiFAP-mGITRL fusion protein enhanced IL-2 and IFN-γ production by C3H $CD4^+$ T cells and increased proliferation and IFN-γ secretion by C3H $CD8^+$ T cells. C3H $CD8^+$ T cells showed approximately the same proliferation at 0.01 µg/ml anti-CD3 stimulus as BALB/c $CD8^+$ T cells at a 100-fold higher dose of anti-CD3 (1 µg/ml). This difference is due to the fact that T cells from mice of different background have different activation thresholds. At ratio 1:1 of C3H Treg:$CD8^+$, suppression of proliferation could be completely restored through membrane-bound antiFAP-mGITRL even at very low fusion protein concentrations. As in the suppression assays with BALB/c splenocytes, membrane-bound antiFAP-mGITRL was 100-fold more effective in abolishing Treg-mediated suppression than unbound antiFAP-mGITRL. However, in the BALB/c costimulation assays, proliferation of $CD8^+$ T cells could never be completely restored (at ratio 1:1 of Treg: $CD8^+$). This is either due to the different sensitivity of the mouse strains to the anti-GITR costimulus or to the additional stimulation of BALB/c splenocytes with anti-CD28 antibody, which might positively act on Treg cells besides costimulating $CD8^+$ effector T cells. Restoration of IFN-γ production by C3H $CD8^+$ T cells was very weak, probably due to the missing anti-CD28 costimulus compared to BALB/c assays. To translate these *in vitro* results in a preclinical model, we injected C3H mice with LM8 cells and treated them with our fusion proteins. To our knowledge, only one study investigated the effect of GITR stimulation in a C3H tumor model. mGITRL-transfected squamous cell carcinoma cells (SCCVII) injected s.c. completely regressed after transient growth (Piao et al., 2009), thereby showing an antitumoral effect of GITR activation in C3H

mice. In our experiments, therapy of LM8 tumors with antiCD33-mGITRL did not delay tumor growth, whereas administration of antiFAP-mGITRL led to enhanced survival. Since neither the untargeted group treated with antiCD33-mGITRL nor the control group without GITRL (antiFAP treatment) showed a beneficial effect, we conclude that the antitumoral effect of antiFAP-mGITRL effect is due to the specific accumulation of the construct in the FAP^+ tumor and to thereby mediated local GITR activation. To further enhance the antitumoral efficacy of antiFAP-mGITRL, the treatment schedule could be optimized or antiFAP-mGITRL may be used in combination with other molecules.

Since antiFAP-mGITRL costimulated murine T cells and induced an antitumor response in a murine cancer model, the effects of GITR triggering in the human system are of great interest. For potential use of a GITRL fusion protein for human therapy, we cloned the antiFAP-hGITRL fusion protein. It displayed an affinity of 14 nM to hGITR in surface plasmon resonance experiments, which was in the range of the human GITR/GITRL system (Chattopadhyay et al., 2007). This 100-fold better affinity of the human system in comparison to the murine system is due to the different multimerization properties of hGITRL compared to mGITRL, together with the suspected formation of superclusters consisting of several hGITRL molecules (Zhou et al., 2008). These observations point to possible physiological differences between the murine and human GITR/GITRL system. The role of human GITR and its ligand is less well characterized than of the murine system and research results remain inconclusive. GITR is highly expressed on human NK cells but the effects of its triggering through GITRL are still controversial (Baessler et al., 2009; Baltz et al., 2007; Hanabuchi et al., 2006). hGITRL costimulates human $CD4^+$ and $CD8^+$ T cells leading to proliferation and cytokine production (Levings et al., 2002; Tuyaerts et al., 2007). Although no inhibition of Treg-mediated suppression by GITRL treatment has been reported in human *in vitro* coculture assays so far (Levings et al., 2002; Tuyaerts et al., 2007), the overexpression of hGITRL on human monocyte-derived DCs enhances their capacity to prime tumor antigen-specific $CD8^+$ T cells (Tuyaerts et al., 2007) and may therefore enhance a tumor-specific $CD8^+$ T cell response. The outcome of a potential anti-GITR treatment in humans remains unclear and the interplay between tumor cells, T cells, NK cells and DCs in the setting of human GITR stimulation need to be further elucidated. Although some effects of GITR signaling might differ in human and mice, human T cells can be costimulated by activation of GITR, thereby representing a potential target for therapeutic interventions. A promising approach in human antitumor therapy would be to combine anti-GITR treatment with further approaches such as vaccines or mAb against other targets. CTLA-blockade, e.g., showed synergistic activity when combined

with anti-GITR treatment, leading to very potent antitumor effects in mice (Ko et al., 2005; Mitsui et al., 2010). Therefore a combination therapy may generate effective tumor immunity in a clinical setting.

Overall, tumor-specific GITR ligation through antiFAP-mGITRL has the potential to control tumor growth due to its unique characteristics of dimeric assembly, high affinity binding to mFAP and low affinity binding to mGITRL and its costimulatory properties. Therefore, at a low dose of fusion protein localizing to the tumor, crosslinking of GITR molecules by antiFAP-mGITRL can induce an antitumor effect in FAP^+ sarcomas. Anti-GITR therapy could be supported by vaccination, activation of APCs or other costimulatory signals in order to further enhance tumor immunity.

5 Appendix

5.1 Amino acid sequence of antiFAP-hGITRL

M G Q V Q L K Q S G A E L V K P G A S V K L S C K T S G Y T F T
E N I I H W V K Q R S G Q G L E W I G W F H P G S G S I K Y N E
K F K D K A T L T A D K S S S T V Y M E L S R L T S E D S A V Y
F C A R H G G T G R G A M D Y W G Q G T S V T V S S A K T T P P
K L E E G E F S E A R V D I L M T Q S P A S S V V S L G Q R A T
I S C R A S K S V S T S A Y S Y M H W Y Q Q K P G Q P P K L L I
Y L A S N L E S G V P P R F S G S G S G T D F T L N I H P V E E
E D A A T Y Y C Q H S R E L P Y T F G G G T K L E I K R A G S G
G G G S M G L Q L E T A K E P C M A K F G P L P S K W Q M A S S
E P P C V N K V S D W K L E I L Q N G L Y L I Y G Q V A P N A N
Y N D V A P F E V R L Y K N K D M I Q T L T N K S K I Q N V G G
T Y E L H V G D T I D L I F N S E H Q V L K N N T Y W G I I L L
A N P Q F I S G S E Q K L I S E E D L N S H H H H H H

5.2 Amino acid sequence of antiCD33-mGITRL

M K V Q L Q Q S G P E L V K P G A S V K I S C K A S G Y T F T D
Y N M H W V K Q S H G K S L E W I G Y I Y P Y N G G T G Y N Q K
F K S K A T L T V D N S S S T A Y M E L R S L T S E D S A V Y Y
C A R G R P A M D Y W G Q G T S V T V S S A K T T P K L E E G E
F S E A R V D I V L T Q S P A S L A V S L G Q R A T I S C R A S
E S V D N Y G I S F M N W F Q Q K P G Q P P K L L I Y A A S N Q
R S G V P A R F S G S G S G T D F S L N I H P M E E D D T A M Y
F C Q Q S K E V P W T F G G G T K L E I K R A D T A P T G S G G
G G S M G P W S L K P T A I E S C M V K F E L S S S K W H M T S
P K P H C V N T T S D G K L K I L Q S G T Y L I Y G Q V I P V D
K K Y I K D N A P F V V Q I Y K K N D V L Q T L M N D F Q I L P
I G G V Y E L H A G D N I Y L K F N S K D H I Q K N N T Y W G I
I L M P D L P F I S G S E Q K L I S E E D L N S H H H H H H

5.3 Amino acid sequence of antiFAP-mGITRL

M G Q V Q L K Q S G A E L V K P G A S V K L S C K T S G Y T F T
E N I I H W V K Q R S G Q G L E W I G W F H P G S G S I K Y N E
K F K D K A T L T A D K S S S T V Y M E L S R L T S E D S A V Y
F C A R H G G T G R G A M D Y W G Q G T S V T V S S A K T T P P
K L E E G E F S E A R V D I L M T Q S P A S S V V S L G Q R A T
I S C R A S K S V S T S A Y S Y M H W Y Q Q K P G Q P P K L L I
Y L A S N L E S G V P P R F S G S G S G T D F T L N I H P V E E
E D A A T Y Y C Q H S R E L P Y T F G G G T K L E I K R A G S G
G G G S M G P W S L K P T A I E S C M V K F E L S S S K W H M T
S P K P H C V N T T S D G K L K I L Q S G T Y L I Y G Q V I P V
D K K Y I K D N A P F V V Q I Y K K N D V L Q T L M N D F Q I L
P I G G V Y E L H A G D N I Y L K F N S K D H I Q K N N T Y W G
I I L M P D L P F I S G S E Q K L I S E E D L N S H H H H H H

5.4 Amino acid sequence of antiFAP

M G Q V Q L K Q S G A E L V K P G A S V K L S C K T S G Y T F T
E N I I H W V K Q R S G Q G L E W I G W F H P G S G S I K Y N E
K F K D K A T L T A D K S S S T V Y M E L S R L T S E D S A V Y
F C A R H G G T G R G A M D Y W G Q G T S V T V S S A K T T P P
K L E E G E F S E A R V D I L M T Q S P A S S V V S L G Q R A T
I S C R A S K S V S T S A Y S Y M H W Y Q Q K P G Q P P K L L I
Y L A S N L E S G V P P R F S G S G S G T D F T L N I H P V E E
E D A A T Y Y C Q H S R E L P Y T F G G G T K L E I K R A G S E
Q K L I S E E D L N S H H H H H H

6 References

Adams S., Miller G. T., Jesson M. I., Watanabe T., Jones B. and Wallner B. P. (2004) PT-100, a small molecule dipeptidyl peptidase inhibitor, has potent antitumor effects and augments antibody-mediated cytotoxicity via a novel immune mechanism. *Cancer Res* **64**, 5471-80.

Agostini M., Cenci E., Pericolini E., Nocentini G., Bistoni G., Vecchiarelli A. and Riccardi C. (2005) The glucocorticoid-induced tumor necrosis factor receptor-related gene modulates the response to Candida albicans infection. *Infect Immun* **73**, 7502-8.

Asai T., Ueda T., Itoh K., Yoshioka K., Aoki Y., Mori S. and Yoshikawa H. (1998) Establishment and characterization of a murine osteosarcoma cell line (LM8) with high metastatic potential to the lung. *Int J Cancer* **76**, 418-22.

Bach J. F. (2003) Regulatory T cells under scrutiny. *Nat Rev Immunol* **3**, 189-98.

Baessler T., Krusch M., Schmiedel B. J., Kloss M., Baltz K. M., Wacker A., Schmetzer H. M. and Salih H. R. (2009) Glucocorticoid-induced tumor necrosis factor receptor-related protein ligand subverts immunosurveillance of acute myeloid leukemia in humans. *Cancer Res* **69**, 1037-45.

Bagshawe K. D., Sharma S. K. and Begent R. H. (2004) Antibody-directed enzyme prodrug therapy (ADEPT) for cancer. *Expert Opin Biol Ther* **4**, 1777-89.

Baltz K. M., Krusch M., Bringmann A., Brossart P., Mayer F., Kloss M., Baessler T., Kumbier I., Peterfi A., Kupka S., Kroeber S., Menzel D., Radsak M. P., Rammensee H. G. and Salih H. R. (2007) Cancer immunoediting by GITR (glucocorticoid-induced TNF-related protein) ligand in humans: NK cell/tumor cell interactions. *FASEB J* **21**, 2442-54.

Bauer S., Adrian N., Williamson B., Panousis C., Fadle N., Smerd J., Fettah I., Scott A. M., Pfreundschuh M. and Renner C. (2004) Targeted bioactivity of membrane-anchored TNF by an antibody-derived TNF fusion protein. *J Immunol* **172**, 3930-9.

Bauer S., Jendro M. C., Wadle A., Kleber S., Stenner F., Dinser R., Reich A., Faccin E., Godde S., Dinges H., Muller-Ladner U. and Renner C. (2006) Fibroblast activation protein is expressed by rheumatoid myofibroblast-like synoviocytes. *Arthritis Res Ther* **8**, R171.

Bettelli E., Dastrange M. and Oukka M. (2005) Foxp3 interacts with nuclear factor of activated T cells and NF-kappa B to repress cytokine gene expression and effector functions of T helper cells. *Proc Natl Acad Sci U S A* **102**, 5138-43.

Bettini M. and Vignali D. A. (2009) Regulatory T cells and inhibitory cytokines in autoimmunity. *Curr Opin Immunol* **21**, 612-8.

Borghaei H. and Schilder R. J. (2004) Safety and efficacy of radioimmunotherapy with yttrium 90 ibritumomab tiuxetan (Zevalin). *Semin Nucl Med* **34**, 4-9.

Borsi L., Balza E., Bestagno M., Castellani P., Carnemolla B., Biro A., Leprini A., Sepulveda J., Burrone O., Neri D. and Zardi L. (2002) Selective targeting of tumoral vasculature: comparison of different formats of an antibody (L19) to the ED-B domain of fibronectin. *Int J Cancer* **102**, 75-85.

Borsi L., Balza E., Carnemolla B., Sassi F., Castellani P., Berndt A., Kosmehl H., Biro A., Siri A., Orecchia P., Grassi J., Neri D. and Zardi L. (2003) Selective targeted delivery of TNFalpha to tumor blood vessels. *Blood* **102**, 4384-92.

Bossen C., Ingold K., Tardivel A., Bodmer J. L., Gaide O., Hertig S., Ambrose C., Tschopp J. and Schneider P. (2006) Interactions of tumor necrosis factor (TNF) and TNF receptor family members in the mouse and human. *J Biol Chem* **281**, 13964-71.

Brocks B., Garin-Chesa P., Behrle E., Park J. E., Rettig W. J., Pfizenmaier K. and Moosmayer D. (2001) Species-crossreactive scFv against the tumor stroma marker "fibroblast activation protein" selected by phage display from an immunized FAP-/- knock-out mouse. *Mol Med* **7**, 461-9.

Bross P. F., Beitz J., Chen G., Chen X. H., Duffy E., Kieffer L., Roy S., Sridhara R., Rahman A., Williams G. and Pazdur R. (2001) Approval summary: gemtuzumab ozogamicin in relapsed acute myeloid leukemia. *Clin Cancer Res* **7**, 1490-6.

Burnet F. M. (1970) Concept of Immunological Surveillance. *Progress in Experimental Tumor Research* **13**, 1-&.

Calmels B., Paul S., Futin N., Ledoux C., Stoeckel F. and Acres B. (2005) Bypassing tumor-associated immune suppression with recombinant adenovirus constructs expressing membrane bound or secreted GITR-L. *Cancer Gene Ther* **12**, 198-205.

Carnemolla B., Borsi L., Balza E., Castellani P., Meazza R., Berndt A., Ferrini S., Kosmehl H., Neri D. and Zardi L. (2002) Enhancement of the antitumor properties of interleukin-2 by its targeted delivery to the tumor blood vessel extracellular matrix. *Blood* **99**, 1659-65.

Chattopadhyay K., Ramagopal U. A., Brenowitz M., Nathenson S. G. and Almo S. C. (2008) Evolution of GITRL immune function: murine GITRL exhibits unique structural and biochemical properties within the TNF superfamily. *Proc Natl Acad Sci U S A* **105**, 635-40.

Chattopadhyay K., Ramagopal U. A., Mukhopadhaya A., Malashkevich V. N., Dilorenzo T. P., Brenowitz M., Nathenson S. G. and Almo S. C. (2007) Assembly and structural properties of glucocorticoid-induced TNF receptor ligand: Implications for function. *Proc Natl Acad Sci U S A* **104**, 19452-7.

Cheng J. D., Dunbrack R. L., Jr., Valianou M., Rogatko A., Alpaugh R. K. and Weiner L. M. (2002) Promotion of tumor growth by murine fibroblast activation protein, a serine protease, in an animal model. *Cancer Res* **62**, 4767-72.

Cheng J. D., Valianou M., Canutescu A. A., Jaffe E. K., Lee H. O., Wang H., Lai J. H., Bachovchin W. W. and Weiner L. M. (2005) Abrogation of fibroblast activation protein enzymatic activity attenuates tumor growth. *Mol Cancer Ther* **4**, 351-60.

Cho J. S., Hsu J. V. and Morrison S. L. (2009) Localized expression of GITR-L in the tumor microenvironment promotes CD8+ T cell dependent anti-tumor immunity. *Cancer Immunol Immunother* **58**, 1057-69.

Cohen A. D., Diab A., Perales M. A., Wolchok J. D., Rizzuto G., Merghoub T., Huggins D., Liu C., Turk M. J., Restifo N. P., Sakaguchi S. and Houghton A. N. (2006) Agonist anti-GITR antibody enhances vaccine-induced CD8(+) T-cell responses and tumor immunity. *Cancer Res* **66**, 4904-12.

Cohen S. J., Alpaugh R. K., Palazzo I., Meropol N. J., Rogatko A., Xu Z., Hoffman J. P., Weiner L. M. and Cheng J. D. (2008) Fibroblast activation protein and its relationship to clinical outcome in pancreatic adenocarcinoma. *Pancreas* **37**, 154-8.

Colombo M. P. and Piconese S. (2007) Regulatory-T-cell inhibition versus depletion: the right choice in cancer immunotherapy. *Nat Rev Cancer* **7**, 880-7.

Cortez-Retamozo V., Backmann N., Senter P. D., Wernery U., De Baetselier P., Muyldermans S. and Revets H. (2004) Efficient cancer therapy with a nanobody-based conjugate. *Cancer Res* **64**, 2853-7.

Curiel T. J., Coukos G., Zou L., Alvarez X., Cheng P., Mottram P., Evdemon-Hogan M., Conejo-Garcia J. R., Zhang L., Burow M., Zhu Y., Wei S., Kryczek I., Daniel B., Gordon A., Myers L., Lackner A., Disis M. L., Knutson K. L., Chen L. and Zou W. (2004) Specific recruitment of regulatory T cells in ovarian carcinoma fosters immune privilege and predicts reduced survival. *Nat Med* **10**, 942-9.

Dancey G., Begent R. H. and Meyer T. (2009) Imaging in targeted delivery of therapy to cancer. *Target Oncol* **4**, 201-17.

Dean-Colomb W. and Esteva F. J. (2008) Her2-positive breast cancer: herceptin and beyond. *Eur J Cancer* **44**, 2806-12.

Dittmer U., He H., Messer R. J., Schimmer S., Olbrich A. R., Ohlen C., Greenberg P. D., Stromnes I. M., Iwashiro M., Sakaguchi S., Evans L. H., Peterson K. E., Yang G. and Hasenkrug K. J. (2004) Functional impairment of CD8(+) T cells by regulatory T cells during persistent retroviral infection. *Immunity* **20**, 293-303.

Dolznig H., Schweifer N., Puri C., Kraut N., Rettig W. J., Kerjaschki D. and Garin-Chesa P. (2005) Characterization of cancer stroma markers: in silico analysis of an mRNA expression database for fibroblast activation protein and endosialin. *Cancer Immun* **5**, 10.

Dunn G. P., Old L. J. and Schreiber R. D. (2004) The three Es of cancer immunoediting. *Annu Rev Immunol* **22**, 329-60.

Eggermont A. M., Schraffordt Koops H., Lienard D., Kroon B. B., van Geel A. N., Hoekstra H. J. and Lejeune F. J. (1996) Isolated limb perfusion with high-dose tumor necrosis factor-alpha in combination with interferon-gamma and melphalan for nonresectable extremity soft tissue sarcomas: a multicenter trial. *J Clin Oncol* **14**, 2653-65.

Ehrlich P. (1900) Croonian lecture: on immunity with special reference to cell life. *Proceedings of the Royal Society of London* **66**, 424-448.

Esparza E. M. and Arch R. H. (2005) Glucocorticoid-induced TNF receptor functions as a costimulatory receptor that promotes survival in early phases of T cell activation. *J Immunol* **174**, 7869-74.

Fishman M. and Seigne J. (2002) Immunotherapy of metastatic renal cell cancer. *Cancer Control* **9**, 293-304.

Fontenot J. D., Gavin M. A. and Rudensky A. Y. (2003) Foxp3 programs the development and function of CD4+CD25+ regulatory T cells. *Nat Immunol* **4**, 330-6.

Gao Q., Qiu S. J., Fan J., Zhou J., Wang X. Y., Xiao Y. S., Xu Y., Li Y. W. and Tang Z. Y. (2007) Intratumoral balance of regulatory and cytotoxic T cells is associated with prognosis of hepatocellular carcinoma after resection. *J Clin Oncol* **25**, 2586-93.

Garin-Chesa P., Old L. J. and Rettig W. J. (1990) Cell surface glycoprotein of reactive stromal fibroblasts as a potential antibody target in human epithelial cancers. *Proc Natl Acad Sci U S A* **87**, 7235-9.

Gerstmayer B., Hoffmann M., Altenschmidt U. and Wels W. (1997) Costimulation of T-cell proliferation by a chimeric B7-antibody fusion protein. *Cancer Immunol Immunother* **45**, 156-8.

Gotter J., Brors B., Hergenhahn M. and Kyewski B. (2004) Medullary epithelial cells of the human thymus express a highly diverse selection of tissue-specific genes colocalized in chromosomal clusters. *J Exp Med* **199**, 155-66.

Grohmann U., Volpi C., Fallarino F., Bozza S., Bianchi R., Vacca C., Orabona C., Belladonna M. L., Ayroldi E., Nocentini G., Boon L., Bistoni F., Fioretti M. C., Romani L., Riccardi C. and Puccetti P. (2007) Reverse signaling through GITR ligand enables dexamethasone to activate IDO in allergy. *Nat Med* **13**, 579-86.

Gurney A. L., Marsters S. A., Huang R. M., Pitti R. M., Mark D. T., Baldwin D. T., Gray A. M., Dowd A. D., Brush A. D., Heldens A. D., Schow A. D., Goddard A. D., Wood W. I., Baker K. P., Godowski P. J. and Ashkenazi A. (1999) Identification of a new member of the tumor necrosis factor family and its receptor, a human ortholog of mouse GITR. *Curr Biol* **9**, 215-8.

Halin C., Gafner V., Villani M. E., Borsi L., Berndt A., Kosmehl H., Zardi L. and Neri D. (2003) Synergistic therapeutic effects of a tumor targeting antibody fragment, fused to interleukin 12 and to tumor necrosis factor alpha. *Cancer Res* **63**, 3202-10.

Hanabuchi S., Watanabe N., Wang Y. H., Ito T., Shaw J., Cao W., Qin F. X. and Liu Y. J. (2006) Human plasmacytoid predendritic cells activate NK cells through

glucocorticoid-induced tumor necrosis factor receptor-ligand (GITRL). *Blood* **107**, 3617-23.

Haque A., Stanley A. C., Amante F. H., Rivera Fde L., Zhou Y., Kuns R. D., Yardley V., Sakaguchi S., Hill G. R. and Engwerda C. R. (2010) Therapeutic glucocorticoid-induced TNF receptor-mediated amplification of CD4+ T cell responses enhances antiparasitic immunity. *J Immunol* **184**, 2583-92.

Hauptrock B. and Hess G. (2008) Rituximab in the treatment of non-Hodgkin's lymphoma. *Biologics* **2**, 619-33.

Henry L. R., Lee H. O., Lee J. S., Klein-Szanto A., Watts P., Ross E. A., Chen W. T. and Cheng J. D. (2007) Clinical implications of fibroblast activation protein in patients with colon cancer. *Clin Cancer Res* **13**, 1736-41.

Hirsch B., Brauer J., Fischdick M., Loddenkemper C., Bulfone-Paus S., Stein H. and Durkop H. (2009) Anti-CD30 human IL-2 fusion proteins display strong and specific cytotoxicity in vivo. *Curr Drug Targets* **10**, 110-7.

Hofheinz R. D., al-Batran S. E., Hartmann F., Hartung G., Jager D., Renner C., Tanswell P., Kunz U., Amelsberg A., Kuthan H. and Stehle G. (2003) Stromal antigen targeting by a humanised monoclonal antibody: an early phase II trial of sibrotuzumab in patients with metastatic colorectal cancer. *Onkologie* **26**, 44-8.

Hoogenboom H. R. (2005) Selecting and screening recombinant antibody libraries. *Nat Biotechnol* **23**, 1105-16.

Hori S., Nomura T. and Sakaguchi S. (2003) Control of regulatory T cell development by the transcription factor Foxp3. *Science* **299**, 1057-61.

Hu P., Arias R. S., Sadun R. E., Nien Y. C., Zhang N., Sabzevari H., Lutsiak M. E., Khawli L. A. and Epstein A. L. (2008) Construction and preclinical characterization of Fc-mGITRL for the immunotherapy of cancer. *Clin Cancer Res* **14**, 579-88.

Huang A. Y., Gulden P. H., Woods A. S., Thomas M. C., Tong C. D., Wang W., Engelhard V. H., Pasternack G., Cotter R., Hunt D., Pardoll D. M. and Jaffee E. M. (1996) The immunodominant major histocompatibility complex class I-restricted antigen of a murine colon tumor derives from an endogenous retroviral gene product. *Proc Natl Acad Sci U S A* **93**, 9730-5.

Huang Y., Wang S. and Kelly T. (2004) Seprase promotes rapid tumor growth and increased microvessel density in a mouse model of human breast cancer. *Cancer Res* **64**, 2712-6.

Huber M. A., Kraut N., Park J. E., Schubert R. D., Rettig W. J., Peter R. U. and Garin-Chesa P. (2003) Fibroblast activation protein: differential expression and serine protease activity in reactive stromal fibroblasts of melanocytic skin tumors. *J Invest Dermatol* **120**, 182-8.

Ji H. B., Liao G., Faubion W. A., Abadia-Molina A. C., Cozzo C., Laroux F. S., Caton A. and Terhorst C. (2004) Cutting edge: the natural ligand for glucocorticoid-induced TNF receptor-related protein abrogates regulatory T cell suppression. *J Immunol* **172**, 5823-7.

Kanamaru F., Youngnak P., Hashiguchi M., Nishioka T., Takahashi T., Sakaguchi S., Ishikawa I. and Azuma M. (2004) Costimulation via glucocorticoid-induced TNF receptor in both conventional and CD25+ regulatory CD4+ T cells. *J Immunol* **172**, 7306-14.

Khattri R., Cox T., Yasayko S. A. and Ramsdell F. (2003) An essential role for Scurfin in CD4+CD25+ T regulatory cells. *Nat Immunol* **4**, 337-42.

Kim J. D., Choi B. K., Bae J. S., Lee U. H., Han I. S., Lee H. W., Youn B. S., Vinay D. S. and Kwon B. S. (2003) Cloning and characterization of GITR ligand. *Genes Immun* **4**, 564-9.

Ko K., Yamazaki S., Nakamura K., Nishioka T., Hirota K., Yamaguchi T., Shimizu J., Nomura T., Chiba T. and Sakaguchi S. (2005) Treatment of advanced tumors with agonistic anti-GITR mAb and its effects on tumor-infiltrating Foxp3+CD25+CD4+ regulatory T cells. *J Exp Med* **202**, 885-91.

Kreitman R. J., Stetler-Stevenson M., Margulies I., Noel P., Fitzgerald D. J., Wilson W. H. and Pastan I. (2009) Phase II trial of recombinant immunotoxin RFB4(dsFv)-PE38 (BL22) in patients with hairy cell leukemia. *J Clin Oncol* **27**, 2983-90.

Leach D. R., Krummel M. F. and Allison J. P. (1996) Enhancement of antitumor immunity by CTLA-4 blockade. *Science* **271**, 1734-6.

Lee J., Fassnacht M., Nair S., Boczkowski D. and Gilboa E. (2005) Tumor immunotherapy targeting fibroblast activation protein, a product expressed in tumor-associated fibroblasts. *Cancer Res* **65**, 11156-63.

Levings M. K., Sangregorio R., Sartirana C., Moschin A. L., Battaglia M., Orban P. C. and Roncarolo M. G. (2002) Human CD25+CD4+ T suppressor cell clones produce transforming growth factor beta, but not interleukin 10, and are distinct from type 1 T regulatory cells. *J Exp Med* **196**, 1335-46.

Levy M. T., McCaughan G. W., Abbott C. A., Park J. E., Cunningham A. M., Muller E., Rettig W. J. and Gorrell M. D. (1999) Fibroblast activation protein: a cell surface dipeptidyl peptidase and gelatinase expressed by stellate cells at the tissue remodelling interface in human cirrhosis. *Hepatology* **29**, 1768-78.

Liao D., Luo Y., Markowitz D., Xiang R. and Reisfeld R. A. (2009) Cancer associated fibroblasts promote tumor growth and metastasis by modulating the tumor immune microenvironment in a 4T1 murine breast cancer model. *PLoS One* **4**, e7965.

Liao G., Nayak S., Regueiro J. R., Berger S. B., Detre C., Romero X., de Waal Malefyt R., Chatila T. A., Herzog R. W. and Terhorst C. (2010) GITR engagement preferentially enhances proliferation of functionally competent CD4+CD25+FoxP3+ regulatory T cells. *Int Immunol* **22**, 259-70.

Linenberger M. L. (2005) CD33-directed therapy with gemtuzumab ozogamicin in acute myeloid leukemia: progress in understanding cytotoxicity and potential mechanisms of drug resistance. *Leukemia* **19**, 176-82.

Liu A., Hu P., Khawli L. A. and Epstein A. L. (2005) Combination B7-Fc fusion protein treatment and Treg cell depletion therapy. *Clin Cancer Res* **11**, 8492-502.

Liu Z., Tian S., Falo L. D., Jr., Sakaguchi S. and You Z. (2009) Therapeutic immunity by adoptive tumor-primed CD4(+) T-cell transfer in combination with in vivo GITR ligation. *Mol Ther* **17**, 1274-81.

Loeffler M., Kruger J. A., Niethammer A. G. and Reisfeld R. A. (2006) Targeting tumor-associated fibroblasts improves cancer chemotherapy by increasing intratumoral drug uptake. *J Clin Invest* **116**, 1955-62.

Maker A. V., Phan G. Q., Attia P., Yang J. C., Sherry R. M., Topalian S. L., Kammula U. S., Royal R. E., Haworth L. R., Levy C., Kleiner D., Mavroukakis S. A., Yellin M. and Rosenberg S. A. (2005) Tumor regression and autoimmunity in patients treated with cytotoxic T lymphocyte-associated antigen 4 blockade and interleukin 2: a phase I/II study. *Ann Surg Oncol* **12**, 1005-16.

Marcus R. (2005) Use of 90Y-ibritumomab tiuxetan in non-Hodgkin's lymphoma. *Semin Oncol* **32**, S36-43.

McHugh R. S., Whitters M. J., Piccirillo C. A., Young D. A., Shevach E. M., Collins M. and Byrne M. C. (2002) CD4(+)CD25(+) immunoregulatory T cells: gene expression analysis reveals a functional role for the glucocorticoid-induced TNF receptor. *Immunity* **16**, 311-23.

Melero I., Hervas-Stubbs S., Glennie M., Pardoll D. M. and Chen L. (2007) Immunostimulatory monoclonal antibodies for cancer therapy. *Nat Rev Cancer* **7**, 95-106.

Milenic D. E., Brady E. D. and Brechbiel M. W. (2004) Antibody-targeted radiation cancer therapy. *Nat Rev Drug Discov* **3**, 488-99.

Mitsui J., Nishikawa H., Muraoka D., Wang L., Noguchi T., Sato E., Kondo S., Allison J. P., Sakaguchi S., Old L. J., Kato T. and Shiku H. (2010) Two distinct mechanisms of augmented antitumor activity by modulation of immunostimulatory/inhibitory signals. *Clin Cancer Res* **16**, 2781-91.

Muller D., Frey K. and Kontermann R. E. (2008) A novel antibody-4-1BBL fusion protein for targeted costimulation in cancer immunotherapy. *J Immunother* **31**, 714-22.

Nahta R. and Esteva F. J. (2006) Herceptin: mechanisms of action and resistance. *Cancer Lett* **232**, 123-38.

Napier M. P., Sharma S. K., Springer C. J., Bagshawe K. D., Green A. J., Martin J., Stribbling S. M., Cushen N., O'Malley D. and Begent R. H. (2000) Antibody-directed enzyme prodrug therapy: efficacy and mechanism of action in colorectal carcinoma. *Clin Cancer Res* **6**, 765-72.

Niedermeyer J., Kriz M., Hilberg F., Garin-Chesa P., Bamberger U., Lenter M. C., Park J., Viertel B., Puschner H., Mauz M., Rettig W. J. and Schnapp A. (2000) Targeted disruption of mouse fibroblast activation protein. *Mol Cell Biol* **20**, 1089-94.

Nishikawa H., Kato T., Hirayama M., Orito Y., Sato E., Harada N., Gnjatic S., Old L. J. and Shiku H. (2008) Regulatory T cell-resistant CD8+ T cells induced by glucocorticoid-induced tumor necrosis factor receptor signaling. *Cancer Res* **68**, 5948-54.

Nishioka T., Nishida E., Iida R., Morita A. and Shimizu J. (2008) In vivo expansion of CD4+Foxp3+ regulatory T cells mediated by GITR molecules. *Immunol Lett* **121**, 97-104.

Nocentini G., Giunchi L., Ronchetti S., Krausz L. T., Bartoli A., Moraca R., Migliorati G. and Riccardi C. (1997) A new member of the tumor necrosis factor/nerve growth factor receptor family inhibits T cell receptor-induced apoptosis. *Proc Natl Acad Sci U S A* **94**, 6216-21.

O'Day S. J., Hamid O. and Urba W. J. (2007) Targeting cytotoxic T-lymphocyte antigen-4 (CTLA-4): a novel strategy for the treatment of melanoma and other malignancies. *Cancer* **110**, 2614-27.

Onizuka S., Tawara I., Shimizu J., Sakaguchi S., Fujita T. and Nakayama E. (1999) Tumor rejection by in vivo administration of anti-CD25 (interleukin-2 receptor alpha) monoclonal antibody. *Cancer Res* **59**, 3128-33.

Orimo A., Gupta P. B., Sgroi D. C., Arenzana-Seisdedos F., Delaunay T., Naeem R., Carey V. J., Richardson A. L. and Weinberg R. A. (2005) Stromal fibroblasts present in invasive human breast carcinomas promote tumor growth and angiogenesis through elevated SDF-1/CXCL12 secretion. *Cell* **121**, 335-48.

Ostermann E., Garin-Chesa P., Heider K. H., Kalat M., Lamche H., Puri C., Kerjaschki D., Rettig W. J. and Adolf G. R. (2008) Effective immunoconjugate therapy in cancer models targeting a serine protease of tumor fibroblasts. *Clin Cancer Res* **14**, 4584-92.

Park J. E., Lenter M. C., Zimmermann R. N., Garin-Chesa P., Old L. J. and Rettig W. J. (1999) Fibroblast activation protein, a dual specificity serine protease expressed in reactive human tumor stromal fibroblasts. *J Biol Chem* **274**, 36505-12.

Peggs K. S., Quezada S. A. and Allison J. P. (2009) Cancer immunotherapy: co-stimulatory agonists and co-inhibitory antagonists. *Clin Exp Immunol* **157**, 9-19.

Peng G., Guo Z., Kiniwa Y., Voo K. S., Peng W., Fu T., Wang D. Y., Li Y., Wang H. Y. and Wang R. F. (2005) Toll-like receptor 8-mediated reversal of CD4+ regulatory T cell function. *Science* **309**, 1380-4.

Phan G. Q., Yang J. C., Sherry R. M., Hwu P., Topalian S. L., Schwartzentruber D. J., Restifo N. P., Haworth L. R., Seipp C. A., Freezer L. J., Morton K. E., Mavroukakis S. A., Duray P. H., Steinberg S. M., Allison J. P., Davis T. A. and Rosenberg S. A. (2003) Cancer regression and autoimmunity induced by cytotoxic T lymphocyte-associated antigen 4 blockade in patients with metastatic melanoma. *Proc Natl Acad Sci U S A* **100**, 8372-7.

Piao J., Kamimura Y., Iwai H., Cao Y., Kikuchi K., Hashiguchi M., Masunaga T., Jiang H., Tamura K., Sakaguchi S. and Azuma M. (2009) Enhancement of T-cell-mediated anti-tumour immunity via the ectopically expressed glucocorticoid-

induced tumour necrosis factor receptor-related receptor ligand (GITRL) on tumours. *Immunology* **127**, 489-99.

Ramirez-Montagut T., Chow A., Hirschhorn-Cymerman D., Terwey T. H., Kochman A. A., Lu S., Miles R. C., Sakaguchi S., Houghton A. N. and van den Brink M. R. (2006) Glucocorticoid-induced TNF receptor family related gene activation overcomes tolerance/ignorance to melanoma differentiation antigens and enhances antitumor immunity. *J Immunol* **176**, 6434-42.

Read S., Malmstrom V. and Powrie F. (2000) Cytotoxic T lymphocyte-associated antigen 4 plays an essential role in the function of CD25(+)CD4(+) regulatory cells that control intestinal inflammation. *J Exp Med* **192**, 295-302.

Rettig W. J., Chesa P. G., Beresford H. R., Feickert H. J., Jennings M. T., Cohen J., Oettgen H. F. and Old L. J. (1986) Differential expression of cell surface antigens and glial fibrillary acidic protein in human astrocytoma subsets. *Cancer Res* **46**, 6406-12.

Rettig W. J., Garin-Chesa P., Healey J. H., Su S. L., Ozer H. L., Schwab M., Albino A. P. and Old L. J. (1993) Regulation and heteromeric structure of the fibroblast activation protein in normal and transformed cells of mesenchymal and neuroectodermal origin. *Cancer Res* **53**, 3327-35.

Ribas A., Hanson D. C., Noe D. A., Millham R., Guyot D. J., Bernstein S. H., Canniff P. C., Sharma A. and Gomez-Navarro J. (2007) Tremelimumab (CP-675,206), a cytotoxic T lymphocyte associated antigen 4 blocking monoclonal antibody in clinical development for patients with cancer. *Oncologist* **12**, 873-83.

Rivera F., Vega-Villegas M. E. and Lopez-Brea M. F. (2008) Cetuximab, its clinical use and future perspectives. *Anticancer Drugs* **19**, 99-113.

Roncarolo M. G. and Levings M. K. (2000) The role of different subsets of T regulatory cells in controlling autoimmunity. *Curr Opin Immunol* **12**, 676-83.

Ronchetti S., Zollo O., Bruscoli S., Agostini M., Bianchini R., Nocentini G., Ayroldi E. and Riccardi C. (2004) GITR, a member of the TNF receptor superfamily, is costimulatory to mouse T lymphocyte subpopulations. *Eur J Immunol* **34**, 613-22.

Rudensky A. Y. and Campbell D. J. (2006) In vivo sites and cellular mechanisms of T reg cell-mediated suppression. *J Exp Med* **203**, 489-92.

Rybak J. N., Trachsel E., Scheuermann J. and Neri D. (2007) Ligand-based vascular targeting of disease. *ChemMedChem* **2**, 22-40.

Sakaguchi S., Wing K., Onishi Y., Prieto-Martin P. and Yamaguchi T. (2009) Regulatory T cells: how do they suppress immune responses? *Int Immunol* **21**, 1105-11.

Sakaguchi S., Yamaguchi T., Nomura T. and Ono M. (2008) Regulatory T cells and immune tolerance. *Cell* **133**, 775-87.

Santos A. M., Jung J., Aziz N., Kissil J. L. and Pure E. (2009) Targeting fibroblast activation protein inhibits tumor stromagenesis and growth in mice. *J Clin Invest* **119**, 3613-25.

Sato E., Olson S. H., Ahn J., Bundy B., Nishikawa H., Qian F., Jungbluth A. A., Frosina D., Gnjatic S., Ambrosone C., Kepner J., Odunsi T., Ritter G., Lele S., Chen Y. T., Ohtani H., Old L. J. and Odunsi K. (2005) Intraepithelial CD8+ tumor-infiltrating lymphocytes and a high CD8+/regulatory T cell ratio are associated with favorable prognosis in ovarian cancer. *Proc Natl Acad Sci U S A* **102**, 18538-43.

Scanlan M. J., Raj B. K., Calvo B., Garin-Chesa P., Sanz-Moncasi M. P., Healey J. H., Old L. J. and Rettig W. J. (1994) Molecular cloning of fibroblast activation protein alpha, a member of the serine protease family selectively expressed in stromal fibroblasts of epithelial cancers. *Proc Natl Acad Sci U S A* **91**, 5657-61.

Scott A. M., Wiseman G., Welt S., Adjei A., Lee F. T., Hopkins W., Divgi C. R., Hanson L. H., Mitchell P., Gansen D. N., Larson S. M., Ingle J. N., Hoffman E. W., Tanswell P., Ritter G., Cohen L. S., Bette P., Arvay L., Amelsberg A., Vlock D., Rettig W. J. and Old L. J. (2003) A Phase I dose-escalation study of

sibrotuzumab in patients with advanced or metastatic fibroblast activation protein-positive cancer. *Clin Cancer Res* **9**, 1639-47.

Shankaran V., Ikeda H., Bruce A. T., White J. M., Swanson P. E., Old L. J. and Schreiber R. D. (2001) IFNgamma and lymphocytes prevent primary tumour development and shape tumour immunogenicity. *Nature* **410**, 1107-11.

Shevach E. M. (2009) Mechanisms of foxp3+ T regulatory cell-mediated suppression. *Immunity* **30**, 636-45.

Shimizu J., Yamazaki S. and Sakaguchi S. (1999) Induction of tumor immunity by removing CD25+CD4+ T cells: a common basis between tumor immunity and autoimmunity. *J Immunol* **163**, 5211-8.

Shimizu J., Yamazaki S., Takahashi T., Ishida Y. and Sakaguchi S. (2002) Stimulation of CD25(+)CD4(+) regulatory T cells through GITR breaks immunological self-tolerance. *Nat Immunol* **3**, 135-42.

Shin H. H., Kim S. J., Lee H. S. and Choi H. S. (2004) The soluble glucocorticoid-induced tumor necrosis factor receptor causes cell cycle arrest and apoptosis in murine macrophages. *Biochem Biophys Res Commun* **316**, 24-32.

Shin H. H., Lee M. H., Kim S. G., Lee Y. H., Kwon B. S. and Choi H. S. (2002) Recombinant glucocorticoid induced tumor necrosis factor receptor (rGITR) induces NOS in murine macrophage. *FEBS Lett* **514**, 275-80.

Siemers N. O., Kerr D. E., Yarnold S., Stebbins M. R., Vrudhula V. M., Hellstrom I., Hellstrom K. E. and Senter P. D. (1997) Construction, expression, and activities of L49-sFv-beta-lactamase, a single-chain antibody fusion protein for anticancer prodrug activation. *Bioconjug Chem* **8**, 510-9.

Sievers E. L. and Linenberger M. (2001) Mylotarg: antibody-targeted chemotherapy comes of age. *Curr Opin Oncol* **13**, 522-7.

Smyth M. J., Godfrey D. I. and Trapani J. A. (2001) A fresh look at tumor immunosurveillance and immunotherapy. *Nat Immunol* **2**, 293-9.

Stephens G. L., McHugh R. S., Whitters M. J., Young D. A., Luxenberg D., Carreno B. M., Collins M. and Shevach E. M. (2004) Engagement of glucocorticoid-induced TNFR family-related receptor on effector T cells by its ligand mediates resistance to suppression by CD4+CD25+ T cells. *J Immunol* **173**, 5008-20.

Sutmuller R. P., van Duivenvoorde L. M., van Elsas A., Schumacher T. N., Wildenberg M. E., Allison J. P., Toes R. E., Offringa R. and Melief C. J. (2001) Synergism of cytotoxic T lymphocyte-associated antigen 4 blockade and depletion of CD25(+) regulatory T cells in antitumor therapy reveals alternative pathways for suppression of autoreactive cytotoxic T lymphocyte responses. *J Exp Med* **194**, 823-32.

Suvas S., Kim B., Sarangi P. P., Tone M., Waldmann H. and Rouse B. T. (2005) In vivo kinetics of GITR and GITR ligand expression and their functional significance in regulating viral immunopathology. *J Virol* **79**, 11935-42.

Takahashi T., Tagami T., Yamazaki S., Uede T., Shimizu J., Sakaguchi N., Mak T. W. and Sakaguchi S. (2000) Immunologic self-tolerance maintained by CD25(+)CD4(+) regulatory T cells constitutively expressing cytotoxic T lymphocyte-associated antigen 4. *J Exp Med* **192**, 303-10.

Tan M. C., Goedegebuure P. S., Belt B. A., Flaherty B., Sankpal N., Gillanders W. E., Eberlein T. J., Hsieh C. S. and Linehan D. C. (2009) Disruption of CCR5-dependent homing of regulatory T cells inhibits tumor growth in a murine model of pancreatic cancer. *J Immunol* **182**, 1746-55.

Thiel M., Wolfs M. J., Bauer S., Wenning A. S., Burckhart T., Schwarz E. C., Scott A. M., Renner C. and Hoth M. (2010) Efficiency of T-cell costimulation by CD80 and CD86 cross-linking correlates with calcium entry. *Immunology* **129**, 28-40.

Thomas L. (1959) Discussion. In *Cellular and Humoral Aspects of the Hypersensitive States* (Edited by Lawrence H.). Hoeber-Harper, New York.

Tone M., Tone Y., Adams E., Yates S. F., Frewin M. R., Cobbold S. P. and Waldmann H. (2003) Mouse glucocorticoid-induced tumor necrosis factor receptor ligand is costimulatory for T cells. *Proc Natl Acad Sci U S A* **100**, 15059-64.

Tuyaerts S., Van Meirvenne S., Bonehill A., Heirman C., Corthals J., Waldmann H., Breckpot K., Thielemans K. and Aerts J. L. (2007) Expression of human GITRL on myeloid dendritic cells enhances their immunostimulatory function but does not abrogate the suppressive effect of CD4+CD25+ regulatory T cells. *J Leukoc Biol* **82**, 93-105.

Valzasina B., Guiducci C., Dislich H., Killeen N., Weinberg A. D. and Colombo M. P. (2005) Triggering of OX40 (CD134) on CD4(+)CD25+ T cells blocks their inhibitory activity: a novel regulatory role for OX40 and its comparison with GITR. *Blood* **105**, 2845-51.

van Elsas A., Hurwitz A. A. and Allison J. P. (1999) Combination immunotherapy of B16 melanoma using anti-cytotoxic T lymphocyte-associated antigen 4 (CTLA-4) and granulocyte/macrophage colony-stimulating factor (GM-CSF)-producing vaccines induces rejection of subcutaneous and metastatic tumors accompanied by autoimmune depigmentation. *J Exp Med* **190**, 355-66.

Vose J. M. (2004) Bexxar: novel radioimmunotherapy for the treatment of low-grade and transformed low-grade non-Hodgkin's lymphoma. *Oncologist* **9**, 160-72.

Wahl R. L. (2005) Tositumomab and (131)I therapy in non-Hodgkin's lymphoma. *J Nucl Med* **46 Suppl 1**, 128S-40S.

Weiner H. L. (2001) Induction and mechanism of action of transforming growth factor-beta-secreting Th3 regulatory cells. *Immunol Rev* **182**, 207-14.

Welt S., Divgi C. R., Scott A. M., Garin-Chesa P., Finn R. D., Graham M., Carswell E. A., Cohen A., Larson S. M., Old L. J. and et al. (1994) Antibody targeting in metastatic colon cancer: a phase I study of monoclonal antibody F19 against a cell-surface protein of reactive tumor stromal fibroblasts. *J Clin Oncol* **12**, 1193-203.

Wu A. M. and Senter P. D. (2005) Arming antibodies: prospects and challenges for immunoconjugates. *Nat Biotechnol* **23**, 1137-46.

Wu Y., Borde M., Heissmeyer V., Feuerer M., Lapan A. D., Stroud J. C., Bates D. L., Guo L., Han A., Ziegler S. F., Mathis D., Benoist C., Chen L. and Rao A. (2006) FOXP3 controls regulatory T cell function through cooperation with NFAT. *Cell* **126**, 375-87.

Wyzgol A., Muller N., Fick A., Munkel S., Grigoleit G. U., Pfizenmaier K. and Wajant H. (2009) Trimer stabilization, oligomerization, and antibody-mediated cell surface immobilization improve the activity of soluble trimers of CD27L, CD40L, 41BBL, and glucocorticoid-induced TNF receptor ligand. *J Immunol* **183**, 1851-61.

Yazaki P. J., Wu A. M., Tsai S. W., Williams L. E., Ikler D. N., Wong J. Y., Shively J. E. and Raubitschek A. A. (2001) Tumor targeting of radiometal labeled anti-CEA recombinant T84.66 diabody and t84.66 minibody: comparison to radioiodinated fragments. *Bioconjug Chem* **12**, 220-8.

Zardi L., Carnemolla B., Siri A., Petersen T. E., Paolella G., Sebastio G. and Baralle F. E. (1987) Transformed human cells produce a new fibronectin isoform by preferential alternative splicing of a previously unobserved exon. *EMBO J* **6**, 2337-42.

Zhou P., L'Italien L., Hodges D. and Schebye X. M. (2007) Pivotal roles of CD4+ effector T cells in mediating agonistic anti-GITR mAb-induced-immune activation and tumor immunity in CT26 tumors. *J Immunol* **179**, 7365-75.

Zhou Z., Song X., Berezov A., Zhang G., Li Y., Zhang H., Murali R., Li B. and Greene M. I. (2008) Human glucocorticoid-induced TNF receptor ligand regulates its signaling activity through multiple oligomerization states. *Proc Natl Acad Sci U S A* **105**, 5465-70.

7 Acknowledgements

First of all, I would like to thank my supervisor Christoph Renner for the opportunity he offered me with this project and for his support, guidance and teaching throughout these years.

My appreciation goes to my PhD committee Josef Jiricny, Alfred Zippelius and Maries van den Broek for their valuable input to the project. I am sincerely thankful to Maries for sharing her knowledge with me and for the help with planning my experiments.

I am indebted to Hiroyoshi Nishikawa, Hiroshi Shiku and the whole Mie lab for their warm welcome and for their cooperation in setting up the cell assays. Thanks also for introducing me to the Japanese culture.

I would like to acknowledge the support of Alexander Knuth from the department of Oncology in Zürich and the collaboration with Gerd Ritter and Lloyd Old from the Ludwig Institute for Cancer Research New York.

I thank Stefan Schauer from the Functional Genomics Center Zurich for introducing me to surface plasmon resonance and his valuable advice and Peter Hunziker for assistance with gel filtration analysis.

I am grateful to Klaus Pfizenmaier, Philippe Guillaume, Immanuel Luescher and Bruno Fuchs for providing reagents for the project.

I thank Oncosuisse for financial support of this project.

Special thanks go to all former and current members of the lab for their help as well as for the fun we had in and out of the lab. I am especially grateful to Markus for introducing me to the topic and for his kindness and enthusiasm. Furthermore, I thank Thomas for the discussions and for sharing his scientific experience. I am most thankful to Petra, Nadia and Margarita for their friendship.

Most importantly, I would like to thank my family for their loving support and confidence, my new friends in Zürich for meeting them and having such a great time, the team from Studenten Wasserball Zürich for the fun and action, my friends out of Zürich for their great friendship and for still being around and Jörg for his encouragement and the amazing years in Zürich.

8 Curriculum Vitae

Last Name	BURCKHART
First Name	Tanja Susanna
Nationality	German
Date of birth	July 10th 1982 in Meyrin, Switzerland

EDUCATION AND EXPERIENCE

Sep 2006 – present	**PhD student at University Hospital Zürich, Zürich, Switzerland** Department of Oncology, Prof. Dr. C. Renner Tumor targeting with bispecific constructs
Feb – Jul 2006	**Internship at Capgemini, Stuttgart, Germany** Work with the Biotechnology Team of the Life Science Consulting Sector
Feb – Aug 2005	**Master Thesis at McGill University, Montreal, Canada** Department of Bioresource Engineering, Prof. J. Sheppard Development of the production process of soy kefir
Oct 2002 – Sep 2005	**Ecole Supérieure de Biotechnologie de Strasbourg (ESBS), Strasbourg, France** Diplome d'ingénieur en biotechnologie/ Diplom-Biotechnologe Diplôme d'Etudes Approfondies (DEA) de Biologie Moléculaire et Cellulaire, option Biotechnologie
July 2004	**Internship at Albert-Ludwigs-Universität, Freiburg, Germany** Plant Biotechnology Research Group, Prof. R. Reski
July 2003	**Internship at the Austin Research Institute, Melbourne, Australia** Molecular Immunogenetics Laboratory, Dr. D. Christiansen
Oct 2000 – Oct 2002	**Albert-Ludwigs-Universität, Freiburg im Breisgau, Germany** **Studies in Biology** Biologie-Vordiplom
1993 – 2000	**Collège et Lycée International de Ferney-Voltaire, France** French Scientific Baccalauréat and German Abitur

PUBLICATIONS

Burckhart, Thiel, Nishikawa, Wüest, Müller, Zippelius, Ritter, Old, Shiku and Renner. Tumor-specific crosslinking of GITR as costimulation for immunotherapy. *Journal of Immunotherapy*, 2010 (accepted)

Thiel, Wolfs, Bauer, Wenning, Burckhart, Schwarz, Scott, Renner and Hoth. Efficiency of T-cell co-stimulation by CD80 or CD86 cross-linking correlates with store-independent Ca^{2+} entry. *Immunology*, 2009

PRESENTATIONS

9th Day of Clinical Research, Zürich, Switzerland, 2010 (talk)

4th Cancer Research Retreat, Ascona, Switzerland, 2009 (talk)

2nd European Congress of Immunology, Berlin, Germany, 2009 (poster)

2nd Cancer Research Student Retreat, Bogis-Bossey, Switzerland, 2009 (talk)

20th Meeting of the Swiss immunology PhD students at Schloss Wolfsberg, Switzerland, 2008 (talk)

3rd Cancer Research Retreat, Fiesch, Switzerland, 2008 (poster)

Kolloquium in angewandter Krebsforschung, UniversitätsSpital Zürich, Switzerland, 2007 (talk)